Elsevier Editorial System(tm) for Geochimica et Cosmochimica Acta

Manuscript Draft

Manuscript Number: GCA-D-17-00867R1

Title: Radiocarbon dating reveals the timing of formation and development of pedogenic calcium carbonate concretions in Central Sudan during the Holocene

Article Type: Article

Corresponding Author: Dr. Gregorio Dal Sasso, Ph.D.

Corresponding Author's Institution: Università degli Studi di Padova

First Author: Gregorio Dal Sasso, Ph.D.

Order of Authors: Gregorio Dal Sasso, Ph.D.; Andrea Zerboni, Ph.D.; Lara Maritan, Ph.D.; Ivana Angelini, Ph.D.; Chiara Compostella; Donatella Usai, Ph.D.; Gilberto Artioli, Ph.D.

Abstract: Calcitic soil horizons are common in arid and semi-arid lands and represent the result of the progressive accumulation of calcium carbonate in the soil profile over time. This process leads to the occurrence of several pedogenetic phases of calcium carbonate dissolution/precipitation. For this reason, timing the formation and development of calcic horizons through radiometric dating is not straightforward as time-averaging effects, due to the superimposition of the same process over time, occur. On this basis, this study aims to define the timing and dynamics of formation and development of pedogenic calcitic concretions from semi-arid Central Sudan, highlighting the relevance of a multi-disciplinary approach and the effectiveness of radiocarbon dating (coupled to an accurate sampling strategy) applied to pedogenic carbonates. Calcium carbonate-rich soil horizons (Bk) were sampled during the archaeological excavation of site 16-D-4 at Al Khiday (Central Sudan) and studied by optical, cathodoluminescence and scanning electron microscopy, as well as by chemical-physical and stable isotopes (C and O) analyses. Radiocarbon ages are obtained for distinctive calcitic pedofeatures and mostly refer to the Early Holocene for calcitic-cemented nodules (11.5, 9.9 and 9.6 cal. ka) and to the Middle Holocene for powdery calcitic-rich matrix (7.9, 7.7, 6.3 and 6.1 cal. ka) samples. Our data are also compared with the available information from detailed physiographic and palaeoenvironmental studies carried out in the region and from the study of the tight interaction between soil horizons and evidence of anthropic activities at Al Khiday site, as the archaeological record provides informative chronological constrains to interpret the 14C ages obtained on selected calcitic pedofeatures. Pedogenic calcitic features dated to the Early Holocene can be related to short arid phases during general wetter climate conditions, whereas those dated to the Middle Holocene can be related to short humid phases. Results show that Bk horizons were characterized by alternate periods of calcite accumulation (precipitation) and dissolution, and periods of quiescence or extremely slow growth rates. Thus, the formation and development of Bk horizons has been a long-lasting process significantly influenced by climatic fluctuations. This study represents a further step in the comprehension of the development of calcium carbonate concretions

and (at a wider perspective) calcrete; the paper also contributes to the definition of a reliable method to radiometrically date the formation of calcitic pedofeatures. In a broader perspective, this work may offer a significant tool for archaeometric studies, where the interaction between secondary calcite and archaeological material is significant (e.g., radiocarbon dating of bioapatite in bones), and palaeoenvironmental studies in arid lands, where Bk horizon development is a function of past rainfall.

Padova, 07/05/2018

Dear Editor,

We accepted all the observations made by the Associate Editor and by two Reviewers to the manuscript:

GCA-D-17-00867
Title: Radiocarbon dating reveals the timing of formation and development of pedogenic calcium carbonate concretions in Central Sudan during the Holocene
Authors: Gregorio Dal Sasso, Andrea Zerboni, Lara Maritan, Ivana Angelini, Chiara Compostella, Donatella Usai, Gilberto Artioli

The useful comments and suggestions helped us to improve the quality of this manuscript; a detailed description of the changes made to the previous submission is reported in the "Response to Reviewers". I hope that it could be suitable for publication in Geochimica et Cosmochimica Acta.

Sincerely,

Gregorio Dal Sasso

Response to Reviewers

Comments from Frank McDermott, Associate Editor

Dear Dr Dal Sasso,

I have now received two reviews of your manuscript 'Radiocarbon dating of calcrete development records the steps of pedogenesis in arid lands'. Whilst one review is broadly positive, both reviewers have expressed fairly substantial concerns with various aspects of the current manuscript. Having read the manuscript and considered the reviews, I have come to the conclusion that substantial revisions will be required before the manuscript can be re-considered. After that, any revised version will have to be sent out for further reviews. An important point is that both reviewers are concerned that the scope of the paper is in fact much narrower than implied by the current rather 'all encompasing' title, a sentiment with which I concur.
- We modified the title

It is also clear that the current abstract is not adequate; it is far too general (and uninformative), and it does not contain any specific results (e.g. dates) that summarise the main conclusions.
- The abstract has been replaced with a more informative one.

There is also a concern that while the term 'calcrete' is useful, it may not be strictly applicable for the range of calcareous soil deposits described in the manuscript.
- Accordingly, we avoid this term, replaced by calcitic horizon. In any case, we noticed that Adamson et al. 1982 (suggested by Rev. #1) occasionally used the term ‘calcrete’ to define similar soil horizons found in a region of central Sudan adjoining to Al Khiday.

Given the geochemistry-focus of Geochimica et Cosmochimica Acta, some basic geochemical data seem to be lacking in the current manuscript. Examples of missing information include the CaCO3 content, pH and organic content of the soils and how these change as a function of depth in the profile.
- As suggested by Rev. #2, we added the results of geochemical analyses on soil samples. We discuss in the revised version of the manuscript the significance of CaCO3 content, pH, organic matter, total carbon, and total nitrogen (sections 3, 4.3, 5, new figure 3).

Linked to this is (a) the absence of a detailed field description and (b) interpretation of the soil profile, e.g. the reasons for the occurrence of two calcic horizons. Is the lower calcic horizon a buried soil for example? The question as to whether the depth of the calcic horizon is linked to annual rainfall in the region should also be addressed.
- We added field description of the sequences of horizons here considered (Tab. 1) and we proposed a genetic interpretation for the occurrence of two calcic horizons (section 4.1). Then we also try to correlate this evidence with the annual amount of rainfall, as suggested by Rev. #2.

On reading the manuscript I particularly missed detailed descriptions and preferably several photographs or photomicrographs showing the exact stratigraphic or micro-stratigraphic relationships between the exact dated material in the context of the profile. For example, the current sentence 'Therefore, three samples of cemented nodules (A3a-cn, 299 A3c-cn and A3d-cn) and three samples of calcitic-rich matrix (A3a-mt, A3c-mt and A3d300mt) from blocks A3a, A3c, and A3d, respectively, were selected and dated' does not convey a sense of the spatial relationships between the dated materials that I would have expected to see in such a manuscript. This absence of detailed documentation of the dated material (e.g. nodule size, internal structure and microfabrics, mineralogy, micro-stratigraphical context) with respect to the profile as a whole, *is frustrating for the reader, and makes the 14C results difficult to evaluate. I would expect to see greatly improved documentation of the precise context of the dated materials in any revised manuscript.*

- Accordingly, we improved sections 3 and 4.1 by adding more detailed information on the sampling points as well as in table 1 and in figure 3. In sections 4.4, 4.5, after showing the results of micromorphological analyses, we clarified the sample strategy for radiocarbon dating and stable isotopes analysis. Additionally, the new figure 7 was added to clarify the relationship between the analysed materials and the graphical representation of results was improved in the new figure 9.

Please consider these comments and those of both reviewers carefully. I hope that the reviews will be helpful in improving the manuscript. If you decide to revise your manuscript and re-submit to GCA, please be aware that the level of revision sought will require further additional reviews. You should also include a separate file documenting in detail how you addressed all of the points above, as well as those of the reviewers. Thank you for submitting your work to Geochimica et Cosmochimica Acta.

Comments from Reviewer #1

Review of Radiocarbon dating of calcrete development records the steps of pedogenesis in arid lands by Gregorio Dal Sasso, Andrea Zerboni, Lara Maritan, Ivana Angelini, Donatella Usai and Gilberto Artioli, submitted to Geochimica et Cosmochimica Acta.

General comments

Using radiocarbon dating to determine the ages of pedogenic calcium carbonate nodules and concretions in arid and semi-arid soils has always been something of a problem, and has been the subject of sustained debate by soil scientists, Quaternary geologists, geomorphologists and geochemists in North America, Australia, India and Africa for over fifty years. There are several reasons why this is so. The carbonate concretions often consist of concentric layers, precipitated at different times. The internal fabric of the concretion sometimes reveals one or more phases of partial carbonate dissolution and ensuing carbonate precipitation. Certain very hard calcareous nodules embedded in a softer calcareous matrix may have been transported by runoff or fluvial action from much older soils or sediments.

Background to the present study

The work described in this paper arose from sustained archaeological excavation at the site of El Khiday immediately west of the lower White Nile, which contains a sequence of pre-Mesolithic, Mesolithic, Neolithic and Meroitic human burials and associated cultural remains, for which there is an independent and credible chronology based on both AMS 14C and OSL ages. This means that the AMS ages obtained on the carbonate nodules can be compared to the ages already obtained for the prehistoric cultural phases, and use can be made of cross-cutting stratigraphic relationships (i.e, whether or not the burials and cultural remains of different ages pre-date or post-date phases of carbonate precipitation) to determine maximum and minimum ages of calcite precipitation.

Achievements

The authors of this manuscript have carried out geochemical, petrographic, micro-morphological and isotopic analyses (carbon, oxygen) from samples of soil carbonate and soil matrix in a test trench dug at archaeological site 16-D-4 near the village of El Khiday, located 3.5 km from the left bank of the lower White Nile and 22 km south of the Blue and White Nile confluence at Khartoum, Sudan. They also obtained 7 AMS 14C ages for authigenic carbonate exposed in the trench wall, and one AMS 14C age on a transported late Pleistocene carbonate nodule contained within a softer calcareous matrix.

The results showed several episodes of carbonate precipitation interspersed with phases of quiescence and phases of carbonate dissolution and re-precipitation, all of Holocene age. The oldest phase of carbonate precipitation pre-dated the Mesolithic burials recovered from this site and dating back to 8.5-8.0 ka. The pre-Mesolithic burials were coated in carbonate; the youngest burials (Meroitic) showed no sign of any secondary carbonate precipitation. The oldest 14C ages from cemented nodules in the lower of two calcareous horizons are 11.5, 9.9 and 9.6 ka, coeval with short arid intervals within a time of high White Nile flood levels and wetter regional climate. The youngest ages are 7.9, 7.7, 6.3 and 6.1 ka, coeval with two short humid phases. (For simplicity and clarity, I have rounded off the ages). The authors point out, correctly, that there have no doubt been multiple episodes of carbonate precipitation and carbonate recycling during the Quaternary in this region (and, indeed, in other arid regions of the world). They also note that in their study area at least six possible sources of carbonate need to be considered. The result of their work is a nuanced interpretation of the scope and limitations of using AMS 14C dating of pedogenic carbonate to help reconstruct past environmental changes.

Title

The focus of the present paper concerns a single carbonate unit at a single Holocene archaeological site

close to the left bank of the lower White Nile in central Sudan. The title is therefore somewhat misleading, because it makes no mention of geographical location, and purports to generalise for soil development in arid lands.
- As suggested we changed the title removing the term calcrete and adding chronological and geographical indications.

Some relevant previous work
In regard to central Sudan, Adamson, Williams and Gillespie (1982) discussed these same issues and the associated dating problems in a detailed chapter written nearly forty years ago, which the authors may wish to consider.
Adamson, D.A., Gillespie, R. and Williams, M.A.J. (1982). 'Palaeogeography of the Gezira and of the lower Blue and White Nile valleys.' In: A Land between Two Niles: Quaternary Geology and Biology of the Central Sudan, M.A.J. Williams & D.A. Adamson (eds.), Balkema, Rotterdam, pp. 165-219.
An additional and earlier paper, dealing with different modes of soil carbonate formation in this area, is: Williams, M.A.J. (1968). 'A dune catena on the clay plains of the west central Gezira, Republic of the Sudan'. Journal of Soil Science, 19(2), 367-378.
- We considered the papers suggested by Rev. #1 and we added specific references in the background section and in the discussion. Especially, we use soil carbonate ages published in Adamson et al. (1982) as comparison to ours (see new figure 8).

Specific comments
I am not convinced that the two calcareous horizons discussed in this work do indeed represent a single calcrete unit, as claimed, nor do I consider the term calcrete to be an appropriate one to use for what are carbonate nodules and a soft calcareous matrix. Perhaps the authors should reconsider their use of the term calcrete.
- As suggested here and by Rev. #2, we revised our hypothesis discussing the existence of two superimposed soil sequence, including two distinct calcitic horizons (Bk and 2Bk), as well as the use of the term calcrete.

References

The reference to Gatto and Zerboni (2015) is incomplete. Please specify the journal and editor of the Special Issue in which this paper appears, together with volume and page numbers.
- We added full reference of this paper.

Clarity, local importance, and wider international appeal
The paper is in general clearly written, logically structured, and well illustrated. The conclusions relating to phases of carbonate precipitation and non-precipitation are supported by the local site evidence presented, and are consistent with independent evidence of high and low White Nile levels and wetter or drier regional climatic phases. Other possible interpretations are weighed judiciously before being discounted.
This paper is a very useful contribution to the study of the geochemistry, mineralogy and stable isotopic composition of carbonate concretions within Holocene soils in the now arid lower White Nile valley. It will also be of interest to soil scientists working in the arid zones of the world.

Comments from Reviewer #2:

This paper presents interesting and important dataset on the characteristics and age estimation of a calcic soil in an archaeological site in Sudan. The findings of the paper stress several periods of pedogenesis, all within the Holocene. The paper is an important addition to our knowledge in this remote, relatively un-explored area of the world. However, it is not focused and suffers from several problems that should be accounted for before it can be accepted.

1. Abstract - The abstract needs to be re-written. As it is now, it is very general. Although the title of the paper deals with radiocarbon dating, the abstract does not include even a single age! (Beside "Holocene"). Also, do not use sentences that say nothing, like "radiocarbon ages are critically discussed….", instead, explicitly write the main results and their implications.

- The abstract has been replaced with a more informative one

2. Lack of laboratory analyses - When studying calcic soils, CaCO3 content is of major importance and I am surprised it lacks from the paper. pH and organic matter are also important, see for example Zerboni et al 2011, Geomorphology. Add these important soil characteristics and discuss them.

- As suggested, we performed and discussed in the revised manuscript the results of several geochemical analyses: $CaCO_3$ content, pH, organic matter content, total carbon, total nitrogen. Methods and results are reported in the manuscript (sections 3, 4.3, 5)., in table 1 and figure 3.

3. Lack of field description - I am sure that the soil profile was fully described but the full description is not included. As the entire paper lean on a single soil profile, a full description of the profile is a must. See for example Zerboni et al 2011, Geomorphology.

- As suggested by the reviewer, we added field description of soil horizons in table 1.

4. Discussion - the discussion is not focused and it was hard for me to follow it. Below are several important points that do not appear in the current version of the discussion:

** The authors found a B horizon (not defined as a calcic horizon) in between two Calcic horizons (Bk). This is not a usual scenario and deserves an explanation. In most cases we find a single Bk horizon that represents the common depth of the wetting front over large time periods. Usually, separated Bk horizons represent buried soils. Does the lower horizon (2Bk) represents a buried soil? If not, how the two separated horizons can be explained?*

- We improved the discussion section and we reconsidered our first interpretation by introducing the existence of a buried 2Bk horizon superimposed by a Bk horizon.

**In addition, the depth of the calcic horizon is known to be related to the average rainfall of the site, see Yaalon 1983; Retellack 2005, Geology; and many others. Thus, the depth of the calcic horizon according to the 130 mm average rainfall should be around 10-30 cm. How the findings of this study are related to this common relationship between rainfall and depth to calcic horizon? Can it be that the upper horizon (Bk) was eroded after it was formed?*

- In this case study the relationship between rainfall and depth of calcic horizon is not easily definable for two main reasons: the first is that the rainfall amount significantly changed over the large span of time here considered (and for which few data are available), the second is that erosional process occurred at the site. Therefore we chose to rely on $\delta^{18}O$ analysis to retrieve information on palaeoenvironmental conditions and suggest a model for calcium carbonate accumulation in the soil profile. We added few remarks on this issue in the discussion and conclusion sections.

** Related to the above mentioned points, the authors should discuss in much detail their findings in relationship to the general scheme calcic soil development (Machette 1985), considering the ages, stages, morphology, and climate.*

- We add in many parts of the manuscript references to the papers by Machete and his ideas on the development of calcitic horizons.

Minor issues:

1. Introduction - *There are almost no citations of classic calcic soil studies (Machette, Gile, etc.).*

- References were added.

2. Table 1 - *Add two more columns: Depth and horizon.*

- Data was added

3. Figure 2 - *Add the exact location of the soil pit in both figure 2a and figure 2b.*

- The location of the soil profile was added to new figure 1b

4. Figure 3 - *Add the depths to the schematic soil section on the left.*

- Data was added

5. Figure 8 - *Add another figure of the stable isotopes with depth.*

- We added a figure (new figure 9) and table 2 with this information.

*Manuscript

Radiocarbon dating reveals the timing of formation and development of pedogenic calcium carbonate concretions in Central Sudan during the Holocene

Gregorio Dal Sasso[1*], Andrea Zerboni[2], Lara Maritan[1], Ivana Angelini[3], Chiara Compostella[2], Donatella Usai[4,5], Gilberto Artioli[1]

[1]Dipartimento di Geoscienze, Università degli Studi di Padova, Via G. Gradenigo 6, 35131 Padova, Italy.

[2]Dipartimento di Scienze della Terra "A. Desio", Università degli Studi di Milano, Via L. Mangiagalli 34, I-20133 Milano, Italy.

[3]Dipartimento dei Beni Culturali: archeologia, storia dell'arte, del cinema e della musica, Università degli Studi di Padova, Piazza Capitaniato 7, 35139 Padova, Italy.

[4]Centro Studi Sudanesi e Sub-Sahariani (CSSeS), Strada Canizzano 128/d, 31100 Treviso, Italy.

[5]Dipartimento di Scienze dell'Antichità, Sapienza Università di Roma, Via dei Volsci 122, I-00185 Roma, Italy

[*]corresponding author: gregorio.dalsasso@unipd.it

Abstract

Calcitic soil horizons are common in arid and semi-arid lands and represent the result of the progressive accumulation of calcium carbonate in the soil profile over time. This process leads to the occurrence of several pedogenetic phases of calcium carbonate dissolution/precipitation. For this reason, timing the formation and development of calcic horizons through radiometric dating is not straightforward as time-averaging effects, due to the superimposition of the same process over time, occur. On this basis, this study aims to define the timing and dynamics of formation and development of pedogenic calcitic concretions from semi-arid Central Sudan, highlighting the relevance of a multi-disciplinary approach and the effectiveness of radiocarbon dating (coupled to an accurate sampling strategy) applied to pedogenic carbonates. Calcium carbonate-rich soil horizons (Bk) were sampled during the archaeological excavation of site 16-D-4 at Al Khiday (Central Sudan) and studied by optical, cathodoluminescence and scanning electron microscopy, as well as by chemical-physical and stable isotopes (C and O) analyses. Radiocarbon ages are obtained for distinctive calcitic pedofeatures and mostly refer to the Early Holocene for calcitic-cemented nodules (11.5, 9.9 and 9.6 cal. ka) and to the Middle Holocene for powdery calcitic-rich matrix (7.9, 7.7, 6.3 and 6.1 cal. ka) samples. Our data are also compared with the available information from detailed physiographic and palaeoenvironmental studies carried out in the region and from the study of the tight interaction between soil horizons and evidence of anthropic activities at Al Khiday site, as the archaeological record provides informative chronological constrains to interpret the ^{14}C ages obtained on selected calcitic pedofeatures. Pedogenic calcitic features dated to the Early Holocene can be related to short arid phases during general wetter climate conditions, whereas those dated to the Middle Holocene can be related to short humid phases. Results show that Bk horizons were characterized by alternate periods of calcite accumulation (precipitation) and dissolution, and periods of quiescence or extremely slow growth rates. Thus, the formation and development of Bk horizons has been a long-lasting process significantly influenced by climatic fluctuations. This study represents a further step in the comprehension of the development of calcium carbonate

concretions and (at a wider perspective) calcrete; the paper also contributes to the definition of a reliable method to radiometrically date the formation of calcitic pedofeatures. In a broader perspective, this work may offer a significant tool for archaeometric studies, where the interaction between secondary calcite and archaeological material is significant (e.g., radiocarbon dating of bioapatite in bones), and palaeoenvironmental studies in arid lands, where Bk horizon development is a function of past rainfall.

Keywords

Holocene; Calcic concretions; North Africa; Cathodoluminescence microscopy; Radiocarbon dating; Pedogenesis.

1 Introduction

Calcic and petrocalcic soil horizons, and pedogenic calcretes are the results of a near-surface terrestrial accumulation of predominantly calcium carbonate, resulting from the introduction and cementation of calcium carbonate into a soil profile in different forms, i.e. powdery, nodular, laminar, or massive (Gile et al., 1965; Machette, 1985; Wright and Tucker, 1991; Wright, 2007; Durand et al., 2010); they are present in present-day soils (WRB, 2006) as much as in paleosols (Mack et al., 1993; Retallack et al., 1993; Nettleton et al., 2000). These pedogenic bodies often occur in areas, where vadose and shallow phreatic groundwater is saturated with respect of calcium carbonate. This general definition is applied to a large variety of calcitic horizons at different stages of development, abundantly occurring worldwide, at different latitudes, within different geological contexts, and under different pedoclimate settings (Gile et al., 1966; Machette, 1985; McFadden and Tinsley, 1985; Alonso-Zarza and Wright, 2010). However, the most evident examples of calcitic soil horizons (Bk) developed in arid and semi-arid regions (Gile et al., 1966; Adamson et al., 1982; Machette, 1985). General assumption is that calcrete develops in soils, characterized by a net moisture deficit, in which the circulating fluids (vadose and shallow phreatic groundwater) are saturated in calcium carbonate. Calcite accumulation is promoted by several physical-chemical processes as well as by biological-mediated processes (Wright et al., 1988; Verrecchia and Verrecchia, 1994; Cailleau et al., 2011), which, in turn, are influenced by climatic conditions, in particular rainfall amount. As a consequence, calcrete is not generally the result of a single pedogenetic phase, but it corresponds to subsequent events, eventually separated by a long time span, during which previously precipitated carbonates undergo a partial or complete new dissolution and then re-precipitation. Calcic horizon and calcrete development, therefore, consists of several, superimposed generations of micritic and/or sparitic calcium carbonate crystals. For this reason, and considering also that a continuous opening of the system hampers the possibility to date calcite with U/Th and ^{14}C, it is hard to define accurately the time and steps of calcrete pedogenesis.

Almost thirty-five years ago, Adamson et al. (1982) have carried out a huge campaign of radiocarbon dating of calcitic nodules in soils from Central Sudan, highlighting the occurrence of reworked carbonates and subsequent recrystallizations. For that reason and for the the large occurrence of carbonate pedofeatures, soils/paleosoils of arid Sudan are an exceptional case study to investigate the chronological development of carbonatic concretions. Therefore, in this research a multi-analytical approach, consisting in mineralogical, micromorphological, geochemical, and geochronological analyses, is applied to the study of calcitic pedogenic features from Central Sudan, in order to contribute towards the understanding of dynamics and timing of their formation and development. Carbonate-bearing soil horizons analysed in this study formed in a localised area along the left bank of the White Nile, few km south of the Khartoum-Omdurman urban system (Fig. 1), where a large, multiphase archaeological site (Al-Khiday, currently under excavation) is in tight relation with the carbonate concretions. In fact, part of the vestiges of the site is embedded in the calcitic crust (Fig. 2a), whereas other features are clearly cut in the pre-existing carbonate-bearing horizon (Fig. 2b and 2c). Detailed studies on the local physiographic and palaeoenvironmental aspects (Zerboni, 2011; Williams et al., 2015), as well as on the anthropic activities, considering the wide span of time covered by the archaeological evidence (almost the whole Holocene) (Usai and Salvatori, 2002; Usai, 2003; Usai and Salvatori, 2005; Salvatori and Usai, 2009; Usai et al., 2010; Salvatori et al., 2011; Salvatori, 2012; Dal Sasso et al., 2014a; Jakob, 2014; Salvatori et al., 2014; Dal Sasso et al., 2014b; Usai et al., 2014; Dal Sasso et al., 2016; Iacumin et al., 2016; Usai et al., 2017; Maritan et al., 2018), supply important information to reconstruct the timing and steps of calcrete formation. In our study, results from the minero-petrographic and pedogenetic study of soil samples, coupled with additional archaeological and palaeoenvironmental information, allowed a more complete understanding of the processes involved in calcitic horizons and calcrete formation, recycling, and development. Moreover, since these processes are strongly dependent on water availability, which, in turn, depends on climatic conditions, our results are discussed taking into account the regional Holocene variations in water availability, as reconstructed by several palaeoenvironmental studies.

2 Study area, palaeoenvironmental settings, and archaeological background

A complex calcrete horizon has been found during the archaeological survey and excavation of several archaeological sites (16-D-3, 16-D-4, 16-D-4b, 16-D-5, 16-D-6) and the geomorphological survey of the region carried out since 2006 within the “El Salha Archaeological Project” (Usai and Salvatori, 2002; Usai, 2003; Usai and Salvatori, 2005; Salvatori and Usai, 2009; Usai et al., 2010; Salvatori et al., 2011; Salvatori, 2012). The archaeological sites are located on the western bank of the White Nile, near the Al Khiday village (Central Sudan), at 3.5 km from the present-day river course and about 22 Km south of its confluence with the Blue Nile (Fig. 1a). They are set on fluvial sandy ridges, corresponding to the remnants of late Pleistocene longitudinal river bars, at the limit of alluvial sediments deposited during the very late Quaternary flooding of the White Nile (Zerboni, 2011; Williams et al., 2015). These fluvial ridges and the surrounding flat areas are weakly weathered by Holocene pedogenesis, despite the intense accumulation of pedogenic calcium carbonate (Zerboni, 2011), thus the poorly developed local soils can be defined as aridisols (Buursink, 1971).

The archaeological excavation and geomorphological investigation (Usai et al., 2010; Salvatori et al., 2011; Zerboni, 2011) revealed a complex stratigraphy at these archaeological sites, resulting from anthropic activities, sedimentary, erosional, and pedogenic processes occurring along a wide span of time. The area had been inhabited several times along almost the entire Holocene. Focusing on the 16-D-4 site (Fig. 1b), a Mesolithic specialised use of the area was defined by the numerous pits (more than 100) that have been excavated, characterized by different types of filling material and presumably with different functions (Zerboni, 2011), and radiocarbon dated to 8650-8250 cal. BP (Salvatori et al., 2011). In addition, the site was used several times as a burial ground: at least three different burial phases have been identified. The most ancient one, named pre-Mesolithic, is characterized by individuals (at least 90) buried in a prone and elongated position. The chronology of this burial phase is uncertain but constrained by the Mesolithic use of the area, as a number of skeletons (16) were found to be cut by radiocarbon-dated Mesolithic pits (Salvatori et al., 2011), which indicate that the pre-Mesolithic burial phase is unambiguously older than 8650 cal. BP. The site was subsequently used as a cemetery during the Neolithic period (38 graves; 6500-6200 cal. BP), and later on during the Meroitic period (43 graves, 2100-1800 cal. BP) (Usai et al., 2010; Salvatori et al., 2011).

Soils in Central Sudan can be classified as Vertisols, Entisols, Aridisols, and Alfisols (Buursink, 1971) in the study region, the first three categories are the most represented and Aridisols are those most recurrent at Al Khiday. In the whole region, pedogenic processes lead to the accumulation of calcic pedofeatures, which have been described previously by several authors (Blokhius et al., 1968; Williams, 1968; Buursink, 1971; Adamson et al., 1982). Buursink (1971) in his classification of soil of Central Sudan describes several petrocalcic horizons, rich in $CaCO_3$ nodules and/or concretions, similar to the K horizons defined by Gile et al. (1966). The same pedofeatures have been reported by Blokhius et al., (1964) and Blokhius et al.(1968), who also described the properties and distribution of pedogenic carbonate in Vertisols. Soils and paleosoils with common to abundant $CaCO_3$ concretions have been reported also by Williams (1968) along the White Nile.

Today, the climate of the region is arid, with mean annual temperature ranging from 22°C to 33°C and average rainfall of ca. 130 mm (El-Tom, 1975; Elagib and Mansell, 2000). However, climatic conditions were significantly different in the past and substantial climatic changes occurred at local and regional levels (Williams and Adamson, 1980; Gasse, 2000; Nicoll, 2001; Nicoll, 2004; Williams, 2009; Williams and Jacobsen, 2011; Zerboni, 2013; Gatto and Zerboni, 2015) during the wide time span of the site use (from the early Holocene to the beginning of the 1st millennium AD). In the early Holocene (11500-8000 cal. BP) the precipitation rate, and consequently also the environmental humidity, were substantially higher, as well as the flooding level of the White Nile, due to a northward expansion of the Indian monsoon domain (Gasse, 2000; Williams, 2009). The formation of seasonal swamps in the surrounding area of the Al Khiday sites during the Mesolithic occupation of the area is attested by geoarchaeological and geomorphological evidence (Williams and Jacobsen, 2011; Zerboni, 2011). Since the middle Holocene (8000-3600 cal. BP), the progressive weakening of monsoon intensity led to rainfall decrease and overall reduction of water availability. In the late Holocene (since ca. 3600 cal. BP), since the Meroitic period and later on, progressively drier environmental conditions occurred, up to the arid climate that now characterizes central Sudan; only short-timed wetter events have been occasionally recorded (Mawson and Williams, 1984). In addition to this general trend, palaeoenvironmental records identified several periods of rapid climatic changes during the early Holocene wet phase, when several short arid periods occurred (Williams, 2009).

3 Materials and methods

The samples considered in this research come from a test trench, exposed in the sandy deposit at Al Khiday and representing the local substrate, brought to light during the excavation of a Mesolithic pit (pit number 151A). The section shows a soil profile with at least 0.7 m of fine to coarse sand (occasionally lenses of pebbles are present), deeply cemented by calcium carbonate. Horizons description is in Tab. 1. Six sampling points, namely A1, A2, A3a, A3b, A3c, and A3d, were selected at different depths from the top to the bottom of the section (see Tab. 1 and Fig. 3 for details). At each sampling point, samples were collected and prepared as required for the analytical techniques applied in this study. Samples were embedded under vacuum in epoxy resin (Araldite 2020) and prepared in petrographic thin sections (3x5 cm). Micromorphological analyses were carried out by petrographic optical microscopy (OM), cathodoluminescence microscopy (CL), and scanning electron microscopy (SEM).

OM analysis was performed with a petrographic microscope (Nikon Eclipse E660) under plane-polarized (PPL) and cross-polarized light (XPL). CL analysis was performed with a petrographic microscope (NIKON Labophot2-POL) equipped with a cold cathode stage (CL8200 MK3, Cambridge Image Technology Ltd) and operating at 15 kV and 200 mA. SEM analysis was carried out with a CamScan MX 2500 coupled to a detector for Energy dispersive X-ray spectroscopy (EDS), equipped with a LaB6 cathode and operating at 20 kV and 160 nA. Thin-sections were described following the terminology proposed by Bullock et al. (1985) and Stoops (2003), and the interpretation mostly followed the concepts discussed in Stoops et al. (2010).

Samples adjoining those prepared in thin sections were selected for chemical and stable isotopes analyses and radiocarbon dating. The chemical characterization of samples was performed measuring $CaCO_3$ equivalents, pH, humified carbon content, total organic carbon, total carbon content (TC) and nitrogen content (TN). Calcium carbonate equivalents were chemically performed using a Dietrich–Frühling calcimeter, which measures the volume of CO_2 developed by acid reacting with the bulk sample, which is proportional to the carbonate concentration. Humified organic carbon was identified by means of the Walkley and Black (1934) method, using chromic acid to measure the oxidizable organic carbon (titration). Total organic carbon was estimated by loss on ignition - LOI - (Heiri et al., 2001); samples were air-dried (at 105°C) and organic matter was oxidized at 500–550°C to carbon dioxide and ash, then the weight lost during the reaction was measured by weighing the samples before and after heating. The analysis of total carbon and total nitrogen were performed on dried soil samples with a Thermo Fisher Scientific Organic Elemental Analyzer (OEA-Flash 2000). Samples were weighed out into tin containers to the nearest 0.001mg on a Gibertini MICRO1000 electronic microbalance. Each sample was then flash-combusted at 1800°C in the OEA.

After a gentle disaggregation in an agate mortar, distinctive calcitic pedofeatures, described by thin section micromorphological analyses, were identified on massive samples and accurately separated by hand-picking under the stereoscopic microscope. Each pedofeature was then analysed for stable carbon and oxygen isotopes and radiocarbon dated.

Stable isotopes analyses were carried out with a Thermo Scientific Delta V Advantage Isotope Ratio Mass Spectrometer. CO_2 was developed at 70 °C by complete reaction with >99% crystalline

H_3PO_4 in a Gasbench II device connected to the spectrometer. Results were calibrated with two internal standards (sieved Carrara marble and Millipore Suprapur carbonate), periodically calibrated against the international reference carbonates NBS 19, NBS 18 and L-SVEC. A control standard (sieved Monzoni marble) was also measured and reproduced with external errors of better than 0.1‰ (1σ) for both carbon and oxygen.

Radiocarbon dating by accelerated mass spectrometry (AMS-^{14}C) was carried out at the Center for Isotopic Research on the Cultural and Environmental heritage (CIRCE) laboratory (Terrasi et al., 2008) of the Second University of Naples. All AMS-^{14}C ages were calibrated according to the INTCAL13 dataset (Reimer et al., 2013) using the CalPal software (Weninger and Jöris, 2008). The method of multiple-group calibration was used to graphically represent and compare calibrated AMS-^{14}C ages (Weninger, 1986).

4 Results

4.1 Field description

The soil profile, here studied, corresponds to the section of the wall of the pit 151A, an archaeological feature related to the Mesolithic use of the site (8650-8250 cal. BP (Salvatori et al., 2011; Salvatori, 2012)), excavated on top of a fluvial sand ridge. In the area of Al Khiday, pedosedimentary sequences generally correspond to poorly weathered soils interlayered to sandy to silty sediments, eventually disturbed by anthropic activities (Buursink, 1971); the sequences are interpreted as fluvial deposits related to an Upper Pleistocene higher level of the White Nile (Zerboni, 2011). The general aspect of a typical soil profile consists of a sandy to silty top horizon, enriched of calcium carbonate in form of nodules (Bk) horizon, lying on a BC horizon. An abrupt limit (possibly erosional) marks the transition to the following 2Bk horizon , which consists of medium to coarse sand, sometimes including lenses of coarser grains (very coarse sand to small pebbles), deeply cemented by calcium carbonate; this buried petrocalcic horizon can be interpreted as a former calcrete. Beneath, there is a sequence of fluvial to lacustrine fine sediments (silt and sand), with few $CaCO_3$ nodules in the upper part (for a complete description see Williams et al., 2015).

At the sampling point, the pedostratigraphy is very clear (Fig. 3): two distinct calcium carbonate-rich horizons, separated by a sandy layer, can be observed. The uppermost Bk horizon (sampling point A1) is constituted by quartz sand slightly cemented by calcium carbonate; calcite concentration within the sediments is detected as coalescent irregular calcitic nodules of few centimetres in diameter. A weakly cemented sandy BC horizon (sampling point A2) is interposed between the first Bk horizon and a second concentration of calcium carbonate, corresponding to the lower part of the section (sampling points A3a, A3b, A3c and A3d). This deepest calcitic horizon (2Bk), up to 0.7 m thick, is nodular and can be interpreted as an early stage of calcrete development in soil profile (Machette, 1985; Wright, 2007), resulting from the illuvial concentration of calcium carbonate in a siliciclastic host material (quartz sand and silt). It is formed by cemented quartz sand and carbonate concretions, where calcitic nodules can be distinguished. Abundance of carbonate concretions as well as cementation increases with depth. From the pedological point of view, this evidence represents a sequence of distinct calcitic horizons on distinct parent materials, probably resulting from a discontinuous pedogenetic process and alternated sedimentary events.

The Bk horizon, as observed in the archaeological area and in naturally exposed sections is at about 20-50 cm depth from the current surface level. In correspondence of site 16-D-4 the close relationship between calcitic pedofeatures and archaeological features of different ages can provide further evidence on the timing of calcium carbonate development. Calcitic concretions partially embed human bones belonging to the pre-Mesolithic burial phase, the most ancient attested at the site (Fig. 2a), whereas Mesolithic pits (Fig. 2b) and Meroitic graves (Fig. 2c) are cut into it. Nevertheless, pre-Mesolithic and Neolithic bones were found to be permeated by secondary calcite, whereas the Meroitic bones, belonging to the most recent burial phase were not affected by pedogenetic precipitation of calcite (Dal Sasso et al., 2014b; Dal Sasso et al., 2016; Dal Sasso et al., 2018). In addition, the lower part of most of the Mesolithic pits is characterized by filling material cemented by calcium carbonate; in particular, some pits, used as fireplaces, present a significant amount of whitish and hard calcitic concretion encrusting the archaeological materials. The same evidence of calcitic concretions embedding human and animal remains in archaeological contexts has been described elsewhere in Sudan, as on the Singa calvaria (McDermott et al., 1996), at Abu Hugar (Whiteman, 1971), and elsewhere in the Gezira (Adamson et al., 1982). The origin of this calcitic cement can be associated to the processes involved in calcrete development; however, the rather high level of cementation must imply a contribution to the total amount of calcite coming from the recrystallization of the abundant remains of Ca-rich wood ash (Canti, 2003) originally constituting the upper part of the pit infilling (Zerboni, 2011).

4.2 Micromorphology of thin sections

Thin sections from the upper part of the soil profile (A1 and A2 samples) show a groundmass with abundant sand- and silt-sized quartz grains, sub-rounded to sub-angular in shape, with a bimodal grain-size distribution. The authigenic calcite is heterogeneously distributed (in shape of nodules, coatings, and infillings) among the sections giving to the slides a single- to double-spaced porphyric c/f (coarse/fine) related distribution, locally open porphyric or gefuric. In the uppermost Bk horizon, areas corresponding to typical calcitic nodules, macroscopically identified, show a micromass mainly constituted by micrite and microsparite (Fig. 4a), much more abundant with respect to that observed for other portions of the poorly cemented samples (Fig. 4c). Allochthonous, well-rounded calcitic pedorelicts (Fig. 4b, 5c, 5d), comparable in size with sandy quartz grains, are frequent. They are constituted by a micritic matrix stained by Mn and Fe oxides/hydroxides, and contain veins of sparitic to micro-sparitic calcite, generally occurring within this kind of pedofeatures (Fig. 5c, 5d).
Samples from the upper units also evidenced the occasional occurrence of wood ash (calcite pseudomorphs after calcium oxalate crystals (Canti, 2003)), fish bone fragments and small charcoals (Fig. 4d). Anthropogenic features were observed in small localised areas of the thin section (Fig. 4d), and possibly migrated from the infilling of the nearby Mesolithic pit, due to

intense bioturbation (Zerboni, 2011). SEM analysis on calcitic nodules from the Bk horizon revealed that the microsparitic groundmass is heterogeneous in terms of compositions and cementation degree: some areas are characterized by densely packed calcite crystals (Fig. 6a) with respect of other areas, where a loose calcite crystals distribution is observed (Fig. 6c). In other areas, calcite crystals occur within a clayey matrix (Fig. 6b). The great heterogeneity in terms of calcite crystals distribution is detected also by CL, where the microsparitic micromass appears with an orange luminescence, whose intensity is proportional to the density of calcite crystals (Fig. 5a). Poorly cemented areas are characterized by low luminescence due to scarcity or lack of calcite in the matrix (Fig 5b).

Thin sections from the lower 2Bk horizon (samples A3a, A3b, A3c, A3d) show areas characterized by slightly cemented quartz grains, sub-rounded to sub-angular in shape, and sand- and silt-sized, embedded into a micritic micromass (Fig. 4e). The distribution of mineral grains and calcite generally results in a single spaced to open porphyric, occasionally gefuric, c/f related distribution. Conversely, highly carbonated areas (Fig. 4f, 4g), corresponding to older calcitic nodules embedded in the micritic micromass, are predominantly constituted by microsparitic calcite, and quartz sand grains are extremely rare. Different textural pedofeatures were identified within calcitic nodules: some portions are characterized by well-cemented calcite crystals forming hard nodules (hereafter called cemented nodules) of sub-rounded to sub-angular shape, identifiable by OM (Fig. 4f, 4g), CL (Fig. 5e) and SEM (Fig 6e, 6f) analyses. These features (Fig. 7) are embedded in a loose matrix mainly constituted by calcite crystals similar in size, but less packed than in the cemented nodules, sometimes associated to clay minerals. Towards the bottom of the 2Bk horizon, the dimension of calcitic-cemented nodules decrease and their margins, in contact with the surrounding matrix, are less defined (Fig. 5f). CL analysis indicates a significant, but not systematic, luminescence variations of calcite crystals along the section, both dispersed and well packed. In some cases, homogeneously luminescent crystals were observed (Fig. 5g), whereas in others the innermost part of crystals is less luminescent with respect to their margins and inter-grain cement (Fig. 5h). OM, CL, and especially SEM images show an overall increase of calcite crystal size from the upper to the lower Bk horizon. Allochthonous calcitic pedorelicts, sub-rounded in shape and permeated by Fe oxides/hydroxides (different from the Mn and Fe-bearing oxides/hydroxides permeating the rounded grains identified in the upper unit) were observed in unit A3c and, less frequently, in unit A3d. Both the two types of pedorelicts show a high concentration of oxides near their margins and a thin layer of clay minerals coating the outer surface (Fig. 4h, 6d).

4.3 Chemical and physical analyses

Tab. 1 and Fig. 3 illustrate the results of chemical analyses on soil samples. Calcium carbonate equivalent content and pH show similar trends, being the latter generally basic and buffered by the high content of carbonates; the B horizon is the less rich in carbonate. Humified organic carbon contents show trends antithetic of $CaCO_3$ content and the highest peak in organics (B horizon) corresponds to the less basic horizon. LOI result indicates a higher content of organics in the lowermost part, possibly suggesting a lower preservation of organic matter in the uppermost part of the sequence, where in fact humified carbon is more abundant. TC content is mainly ruled by the occurrence of calcium carbonate, whereas TN variations correspond to the variation of the humified carbon, confirming that organic matter is the main source of nitrogen.

4.4 AMS-^{14}C dating

Due to the lack of well identifiable organics in the soil matrix, AMS-^{14}C radiocarbon dating was performed on different calcium carbonate-bearing pedofeatures, identified by micro-morphological analysis, and mechanically selected under the stereoscopic microscope. As for the uppermost Bk horizon (A1 sampling point, Fig. 3), calcitic nodules, constituted by micritic/microsparitic micromass (as shown in Fig. 4a) were identified in the massive sample as powdery aggregates, up to 1 cm in size. A fraction of micritic/microsparitic micromass was selected for radiocarbon dating

(A1-mt samples). Allochthonous pedorelicts (A1-pedorelict) were also selected from the same sampling point (A1) and dated.

In the lower 2Bk horizon, micromorphological analyses of calcitic nodules (up to 2 cm in size) showed the occurrence of different textural pedofeatures, previously addressed as cemented nodules and loose calcitic-rich matrix (as shown in Fig. 4f, 4g and 5e). In Fig. 7, OM photomicrographs and the segmented false-colour image show a representative example of the relationship between these pedofeatures. On the massive samples, cemented nodules were found to be much more lithified than the surrounding loose calcitic-rich matrix, therefore, after a gentle disaggregation of the samples, these two adjoining pedofeatures were effectively separated by hand-picking under a stereoscopic microscope. This sampling strategy was then applied to massive samples collected at A3a, A3c and A3d points (Fig. 3), so that for each of them cemented nodules (labelled as A3a-cn, A3c-cn and A3d-cn) and calcitic-rich matrix (labelled as A3a-mt, A3c-mt and A3d-mt) samples were selected for radiocarbon dating. As expected, an old radiocarbon age, 29540 ± 440 cal. years BP, was obtained for the allochthonous pedorelicts (A1-pedorelict). The cemented nodules from A3a, A3c and A3d sampling points show older ages (9620 ± 100, 9900 ± 580 and 11480 ± 240 cal. years BP for A3a-cn, A3c-cn and A3d-cn, respectively) with respect to the nearby loose calcitic-rich matrix (6340 ± 80, 7920 ± 100 and 7730 ± 80 cal. years BP for A3a-mt, A3c-mt and A3d-mt, respectively) and from the calcitic nodules from A1 sampling point (6080 ± 240 cal. years BP) (Tab. 2, Fig. 8a, 9a).

Apart from a single radiocarbon age dating to the Upper Pleistocene (for the allochthonous pedorelict), the radiocarbon dates are Holocene in age and can be tentatively clustered to the Early and Middle-Holocene. Statistical treatment of dating results can better delineate the distribution of radiocarbon ages on the sampled calcitic horizons. The method of multiple-group calibration (Weninger, 1986; Weninger and Jöris, 2008) was used to represent radiocarbon ages, in order to discern if close radiocarbon ages might refer to the same or different pedogenetic phases as well as to ease the comparison with other regional radiocarbon age datasets. Our AMS-^{14}C ages on carbonates were compared (Fig. 7) with the ^{14}C ages obtained on calcium carbonate deposits in soils from Central Sudan (Adamson et al., 1982), and on fossil shells (Williams, 2009; Williams et al., 2015) The latter ages indicates the late Quaternary high flow levels of the White Nile, representing a proxy for wetter climatic conditions. In Fig. 7 the radiometric chronology of the Holocene human occupation of the Al Khiday archaeological sites (Salvatori et al., 2011) is also reported. A further, indirect piece of the chronological puzzle of calcrete development at Al Khiday is represented by the radiometric dating of the archaeological structures cutting the carbonatic crusts; most of them belong to the Mesolithic phase and date to the 8650-8250 cal years BP.

4.5 Stable isotopes analysis

C and O stable isotope analyses were carried out on an aliquot from the same samples that were radiocarbon dated; moreover, additional samples of calcitic nodules from A1 and cemented nodules (cn) and calcitic-rich matrix (mt) from A3a, A3b, A3c and A3d sampling points (Fig. 3) were separately selected and analysed (Tab. 2). Overall $\delta^{18}O$ ranges between -8.27‰ and -1.85‰ (V-PDB) and $\delta^{13}C$ between -1.48‰ and 1.06‰ (V-PDB). $\delta^{13}C$ values show a narrow range of variation and no significant differences were observed between cemented nodule and matrix samples. Conversely, a wider range of variation was observed for $\delta^{18}O$, with matrix samples showing more negative values with respect to cemented nodules (Tab. 2, Fig. 9b, 9c). A good consistency was observed between results obtained from the same samples double-measured, in particular for those from the matrix samples.

5 Discussion

The authigenic accumulation of calcium carbonate in siliciclastic host sediments, composed of quartz sand lacking in calcite, indicates an external source for calcium carbonate. Conceivable sources may be identified in the geological bedrock of the area, as the limited quantity of calcite, occurring in the local sandstone and shale, is firstly dissolved, then mobilized and finally reprecipitated thanks to circulating pore water. Further significant sources of carbonate may be represented by alkaline atmospheric dust and calcium carbonate precipitated over a long period in the Pleistocene lake sediments identified in the region (Williams et al., 2015). Similar sources of carbonates have been claimed by Cremaschi et al. (2010) to explain the origin of spring calcareous tufa in a sandstone-bearing central Saharan massif. Less important contributions are likely those from the Nile overbank sediments, and from the anthropogenic calcitic ash related to the Mesolithic occupation of the site, the latter being available only after the onset of pedogenetic processes related to the formation of calcrete. Moreover, the dissolution and mobilization of calcium carbonate accumulated in pre-existent Pleistocene Fe-enriched paleosols, which are highly cemented and heavily affected by pedogenesis (Fig. 2d), may have contributed to the formation of the calcrete horizon at 16D4 site. However, the origin of calcium carbonate in these paleosols is not well-defined and its accumulation likely results from long-lasting processes of dissolution/reprecipitation of calcite, possibly mediated by biological activity. Evidence of this type of paleosols, widely outcropping in the region (Zerboni et al., 2016), can be also found few hundred meters west from the 16D4 site. These Pleistocene paleosols are also the most probable source of the pedorelicts identified in the calcrete section (those separated from sample A1 and dated to the 29540 ± 440 cal. years BP). In fact, they probably derive from surface transportation, as suggested by their sub-rounded to rounded shape and by the occurrence of clayey material coating their external surface, which can be interpreted as a rolled pedofeature (Zerboni, 2011). Also Adamson et al. (1982) obtained Upper Pleistocene dating on rolled carbonates, suggesting their single or multistep reworking of older carbonate-impregnated clays and silts from former soils.

Calcitic nodules formed since the accumulation of microcrystalline calcite; the small size of crystals suggests a relatively fast precipitation of calcite, associated with high rates of evapotranspiration. In this case, the contribution of microbially induced calcite precipitation is assumed to be minimal, as micromorphological features characteristic of biological activity (Newman et al., 1997; Richter et al., 2008) are not observed. The upper Bk horizon is characterized by weak cementation and nodules are formed by microcrystalline calcite precipitated in the porosity between sand- and silt-sized quartz grains. The lower 2Bk horizon shows a significant increase in the accumulation of calcium carbonate and the formation of larger concretions. The occurrence of very few quartz grains much more dispersed in the microsparitic groundmass within nodules, with respect to those observed in less cemented portions of the sample, may indicates a displacive calcite crystal growth (Armenteros, 2010). Moreover, higher permeating cementation of sediments was observed in this unit, thus representing subsequent development stages of the calcitic horizon. However, features characteristic of successive stages of calcite precipitation/recrystallization observed in well-developed calcrete profiles (Wright, 2007) are lacking in our case study, thus suggesting an intermediate development stage for calcitic horizons. At Al Khiday, Bk and 2Bk horizons can be described as nodular calcitic horizons as suggested by Alonso-Zarza and Wright (Alonso-Zarza and Wright, 2010), or at least comparable to a Stage III of calcrete development (Machette, 1985).

Cathodoluminescence of carbonates, in terms of colours and intensities, is mainly attributed to the occurrence of Mn^{2+} and Fe^{2+} ions in trace quantity in the calcite crystal structure, which, in turn, is related to geochemical conditions during precipitation. Therefore, even if only qualitatively, luminescence variations of calcite crystals observed in CL images indicates variations in the chemical composition and/or redox conditions during precipitation and subsequent recrystallization (Hiatt and Pufahl, 2014). These data, coupled with information on the diachronic interaction between calcrete horizon and archaeological records, indicate that calcrete formation and subsequent development is a long-lasting and discontinuous multi-step process, acting at least since the Early Holocene. Notwithstanding the evidence of calcite accumulation in Late Pleistocene fluvial sediments, the widespread occurrence of calcium carbonate features in paleosols and sediments of the region, may suggest that environmental conditions suitable for calcite mobilization, redistribution and precipitation in soils may have occurred many times since the Pleistocene, as described also elsewhere in North Africa (Szabo et al., 1995; Brookes, 2010; Zerboni et al., 2011). Yet, Adamson et al. (1982) suggest multiple events of carbonate dissolution and precipitations in soil and sediments of Central Sudan since the Late Pleistocene and probably earlier.

On these bases, timing the formation and development of carbonate concretions in the soil profile by radiometric dating techniques requires an accurate sampling strategy and a careful evaluation of results. Radiocarbon dating of calcrete and recrystallization-prone carbonates is not a routinely performed type of analysis, even if some studies are reported in literature (Wang et al., 1996; Geyh and Eitel, 1998; Deutz et al., 2002; Geyh and Thiedig, 2008; Vogel and Geyh, 2008; Achyuthan et al., 2010). In fact, AMS-^{14}C dating of calcite forming calcrete horizons might not lead to a straightforward interpretation of results. When calcite precipitates, its ^{14}C activity is in equilibrium to that of circulating pore water, which, in turn, may not be in equilibrium with atmospheric CO_2 due to the so defined "reservoir effect" (Geyh and Eitel, 1998). This can cause an overestimation of the actual age of calcium carbonate. Moreover, when dissolution and recrystallization occurs, ^{14}C activity of former calcite is then superimposed to that of the new-generated calcite, in equilibrium with pore water circulating at that time (Geyh and Eitel, 1998). Notwithstanding that, Adamson et al. (1982) conclude that Sudanese soil carbonates are fairly suitable materials for dating. They are also aware of the ineluctability of contamination from some of the older carbonates in some cases; we may confirm this and highlight also the possibility of contamination from younger calcite precipitated after the climate-driven re-opening of the system.

Despite these difficulties, in our case study, the well-defined geomorphological, palaeoenvironmental, and archaeological contexts provide valuable information to estimate the consistency of radiocarbon ages on calcrete samples. Moreover, some of these issues can be overcome by the very low amount (~ 10 mg) of sample required by AMS-^{14}C dating, enabling one to apply an accurate sampling strategy on small portions of the sample, thus separately analysing calcite precipitated in a single pedogenetic event. In this case, the reservoir effect is assumed to be minimal, since circulating pore water is more conceivably provided by the White Nile flooding and, during the Early Holocene, by rainwater rather than fossil groundwater (Dee et al., 2010). In addition to the superficial location of the calcitic horizons, the high values of $\delta^{13}C$, measured both on cemented nodule and matrix samples, suggest the predominant contribution of atmospheric CO_2 as a source of CO_2 to the groundwater, whereas the contribution of plant-sourced CO_2 can be considered minimal, thus suggesting a sparse vegetation cover (Cerling, 1984; Burns and Matter, 1995; Deutz et al., 2001) during the phases of precipitation.

The main issue that has to be taken into account when dealing with radiocarbon dating on pedogenic calcite is the overprinting effect, which is not negligible (Deutz et al., 2002). Calcitic horizons and calcretes form over time as results of subsequent dissolution and reprecipitation processes (e.g., Machette, 1985), thus ^{14}C activity is time averaged and determination of the time of actual onset of calcite precipitation may be hazardous. As a matter of fact, soil carbonates can be reasonably considered an open system, implying environmental conditions that promote loops of calcite dissolution and reprecipitation. However, when changes in environmental conditions (mostly humidity) lead to the interruption of carbonate accumulation, the closed system can be hypothesised. Therefore, radiocarbon ages of calcrete samples reasonably indicate the last stage of calcite recrystallization; this may provide valuable information on the timing of Bk horizons development. For these reasons, radiocarbon ages cannot be used according to sample stratigraphy to determine a linear sequence of depositional events; this is also obvious considering the complexity of this nonlinear and multistep process (Wright, 2007). However, micro-sampling should minimize the artificial homogenization of different generations of calcite, and thus radiocarbon ages may provide reliable information on the long soil carbonates evolution, even if each sample may still be partially affected by time-averaging blurring effect.

The considered sequence consists of superimposed calcitic soil horizons, which distinctly developed in phases of enhanced evapotranspiration; consequently, as suggested by Machete (1985), the development of calcitic horizons is a clue to their dissolution-precipitation history. According to the distribution of radiocarbon ages shown in Fig. 9a, the lower part of the sequence (2Bk horizons) may have been affected by old pedogenetic accumulation of calcium carbonate; then, after the burying of this soil and aggradation of the uppermost part of the pedosequence, a further phase of calcite accumulation took place. Its occurrence is recorded by the accumulation of calcitic pedofeatures in the uppermost Bk horizon and the recrystallization or freshly accumulation of calcite in the 2Bk horizon. The higher concentration of calcitic pedofeatures in the 2Bk horizon can be interpreted as the result of subsequent phases of precipitation and/or of a more intense initial accumulation.

As for authigenic calcite, in order to correlate the radiocarbon ages of different calcrete pedofeatures to the climatic conditions occurring in the area, radiocarbon dating results were compared with radiometric ages obtained by Adamson et al. (1982), Williams (2009), and Williams et al. (2015) in a cumulative graph of calibrated radiocarbon ages (Fig. 8). Williams (2015) identified several Late Quaternary periods characterized by more humid climatic conditions, corresponding to higher flow level of the White Nile, Blue Nile, and main Nile River. These phases occurred at 14700–13100, 9700–9000, 7900–7600, ca. 6300, and 3200–2800 cal. years BP (Fig. 8c). On the bases of published data we may infer several phases of carbonates development at c. >30000, 26000–24200, 18200–13000, and 11000–9100 cal. years BP (Adamson et al., 1982); these ages were obtained on bulk carbonate samples, not separated between matrix and cemented nodules (Fig. 8b).

In this study, the oldest radiocarbon ages were obtained on cemented nodules from lower sampling points A3d, A3c, and A3a (11480 ± 240, 9900 ± 580, and 9620 ± 100 cal. years BP, respectively), corresponding to dry climatic phases (Fig. 8), according to palaeoenvironmental evidence provided by Williams (2009). These older ages have a quite good correspondence (Fig. 8b) with those obtained by Adamson et al. (1982). Younger radiocarbon ages, obtained from powdery calcitic-rich matrix sampled at A3d and A3c points (dated to 7730 ± 80 and 7920 ± 100 cal. years BP, respectively) as well as from calcitic-rich matrix sampled at A3a and from calcitic nodules sampled at A1 (dated to 6340 ± 80 and 6080 ± 240 cal. years BP, respectively), show a good agreement with two short periods characterized by more humid conditions, dated to 7900-7600 and about 6300 cal. BP (Williams, 2009; Williams et al., 2015), respectively (Fig. 8).

Further evidence that cemented nodules and calcitic-rich matrix possibly formed under different conditions is provided by the stable isotope analysis, in particular by the significant variation of $\delta^{18}O$ values observed between cemented nodules and matrix samples (Fig. 9a, 9b). Variation in $\delta^{18}O$ values of calcrete samples generally reflects the variation in isotopic composition of meteoric water; however, the latter may not necessarily reflect a significant variation in $\delta^{18}O$ of rainfall. In fact, considering the available information on palaeoenvironmental conditions in this region, previously discussed, a $\delta^{18}O$ enrichment can also be due to evaporative enrichment due to high evapotranspiration rates (Cerling, 1984; Burns and Matter, 1995; Budd et al., 2002). Therefore, the higher $\delta^{18}O$ values measured on cemented nodules can indicate higher evapotranspiration rates related to drier environmental conditions during calcite precipitation. On the other hand, more negative $\delta^{18}O$ values, as those measured on matrix samples, can reflect the $\delta^{18}O$ signature of rainfall or at least a certain $\delta^{18}O$ depletion, triggered by higher rainfall intensity caused by a short-timed increase of monsoon intensity (Cerling, 1984; Burns and Matter, 1995; Andrews et al., 1998).

The consistency of these results suggests that during the Late Pleistocene and mostly initial Holocene a first onset of calcite precipitation occurred during dry climatic conditions, which is compatible with the formation of a thick calcitic horizon in the lower part of the sequence. The occurrence of a net moisture deficit in the vadose zone, as well as pore water saturated with respect to calcium carbonate, due to decreased precipitation and the reduction of the White Nile flow, possibly promoted the calcite precipitation. Subsequently, more humid climatic conditions in the Early and Middle Holocene led to partial dissolution of calcite, whereas a subsequent shift towards drier conditions caused the reprecipitation of calcite. Therefore, alternation of wet and dry periods triggered the partial dissolution and reprecipitation of calcite, leading to a progressive calcite accumulation. Cemented nodules may be interpreted as remnants of previously precipitated calcium carbonate, partially dissolved during subsequent humid periods and then reprecipitated as looser calcitic matrix. This hypothesis also suggests that carbonate pedogenesis occurred as a series of subsequent events of calcite dissolution and precipitation, discontinuously distributed along the Upper Pleistocene and Holocene, driven by local environmental conditions.

This interpretation is further supported by archaeological evidence. Several burial phases were identified and attributed to different periods along the Holocene (Fig. 8), whereas pits, dated to the Mesolithic period, were established after the pre-Mesolithic burial phase (the oldest one). Mesolithic pits were cut into the deeper calcitic horizon, whereas pre-Mesolithic and Neolithic human bones are permeated by secondary calcite. In the Meroitic bones, belonging to the most recent burial phase (dated to 2000-1700 cal. BP; (Usai et al., 2010)), pedogenetic calcite is absent, despite the fact that graves were cut within the calcrete horizon and placed deeper from the surface with respect to the older ones. On the basis of these evidence, the mobilization of calcite in the last 2000 years, a period characterized by semi-arid to arid climatic conditions (Gasse, 2000) and lower level of the White Nile (Williams, 2009), was negligible, indicating the occurrence of quiescent stages during calcrete development process under arid conditions, when the amount of circulating pore water is extremely limited.

6 Conclusions

In Central Sudan, the formation of calcitic soil horizons was a long-lasting process and their development was significantly influenced by changes from humid to arid environmental conditions. Bk horizons were characterized by alternate periods of growth due to dissolution and precipitation processes, and periods of quiescence or extremely slow growth rates. These events possibly occurred many times along the Quaternary, but the best-preserved evidence is the one related to the Holocene. Despite the fact that radiocarbon dating of calcrete has severe limitations due to the uncertain determination of the contribution of ^{14}C by different sources, accurate sampling method coupled with additional information from a well-defined palaeoenvironmental context may provide a reliable interpretation of the sequence of events. A higher number of carefully selected radiocarbon-dated samples could supply a more statistically significant dataset for radiocarbon ages as well as highlight the variability of AMS-^{14}C determinations on this type of material. However, radiocarbon ages obtained in the present work confirm the general model for accumulation, formation and development of calcium carbonate in sediments/soil horizons established in previous studies (Gile et al., 1966; Machette, 1985; Khormali et al., 2006; Zhou and Chafetz, 2009), suggesting a progressive accumulation of calcium carbonate within sediments/soil horizons.

Specifically for this context, the interest in deciphering the relationship between carbonates pedogenesis and archaeological records concerns the evaluation of the interaction between secondary calcite and archaeological materials. In fact, the occurrence of secondary calcite in archaeological materials may represent a complex issue in all those cases in which calcite may alter conventional radiocarbon dates. An example can be, in the specific case, represented by the radiocarbon dating of archaeological bones performed on bioapatite (the mineral fraction of bone material) (Zazzo, 2014). Calcite is therefore a significant contaminant when measuring ^{14}C activity of bioapatite; despite the chemical removal of secondary calcite, the radiocarbon ages obtained (Dal Sasso, 2015) are in good agreement with those obtained on pedogenic calcite, thus resulting substantially younger than those hypothesized on the basis of archaeological and stratigraphic evidences (Fig. 8d). Since bioapatite is not a closed system with respect to the environment (Cherkinsky, 2009), carbonate exchange between calcite and bioapatite during burial may significantly affect the result when dating the archaeological bones. Therefore, the study of soil sediments and burial environment is fundamental in order to assess the reliability of radiocarbon ages. A further example of the importance of understanding the time and steps of calcrete genesis in archaeological context concerns the applicability of luminescence dating on archaeological material (pottery); in fact, the dose rate of Thermoluminescence (TL) is heavily tuned by environmental humidity and radiation, and the carbonate content of sediments may influence water mobilization and change the natural radiation due to the increase of uranium occasionally substituting calcium in calcite crystals. In TL dating, radiation is generally supposed to be constant over time, but irregular development of calcrete through time may consistently vary the environmental radioactivity after the burial of archaeological material (Wintle and Murray, 2006).

This study highlights the relevance of a multi-analytical approach to the study of carbonates pedogenesis. Specifically for this case, a comprehensive study on the interaction between the archaeological record and the calcrete formation and development supplies valuable information both on the processes and timing of carbonates pedogenesis and on the preservation state of archaeological materials.

Considering a wider perspective, the results of this study may represent a further step in the comprehension of calcitic horizons formation and in the definition of a reliable method to date their formation. This may offer a significant tool in palaeoenvironmental studies in arid lands, where carbonatic concretions may represent the only archive for past climatic changes; in fact, several authors had highlighted the correspondence (climofunction, *sensu* Jenny (1941) between depth of Bk horizons and precipitations (e.g., Yaalon, 1983; Mack and James, 1992; Caudill et al., 1996; Retallack, 2000; Retallack, 2005), being horizon's depth the results of the average amount of rainfall.

Acknowledgments

We are grateful to Sandro Salvatori, co-director of the "El Salha Archaeological Project", for the precious collaboration. We thank the Italian Ministry of Foreign Affairs and Centro Studi Sudanesi e sub-Sahariani (CSSeS) for funding the archaeological research. We thank the "National Corporation for Antiquities and Museums", Khartoum (Sudan), in particular the General Director Abdelrahman Ali Mohamed for authorising the study of archaeological materials. We thank Filippo Terrasi and Fabio Marzaioli (Second University of Naples) for their help for radiocarbon dating, Nereo Preto (University of Padua) for his help for stable isotope analyses, Massimo Tiepolo and Enrico Cannaò (University of Milano) for their help with the OEA. Two anonymous reviewers and

Associate Editor Frank McDermott are acknowledged for insightful comments on a preliminary version of the manuscript.

Conflict of Interest

The authors declare that they have no conflict of interest.

References

Achyuthan H., Flora O., Braida M., Shankar N. and Stenni B. (2010) Radiocarbon ages of pedogenic carbonate nodules from Coimbatore region, Tamil Nadu. *J. Geol. Soc. India* **75**, 791–798.

Adamson D. A., Gillespie R. and Williams M. A. J. (1982) Palaeogeography of the Gezira and of the lower Blue and White Nile valleys. In *A Land between Two Niles: Quaternary Geology and Biology of the Central Sudan* (eds. M. A. J. Williams and D. A. Adamson). Balkema, Rotterdam. pp. 165–219.

Alonso-Zarza A. M. and Wright V. P. (2010) Chapter 5 Calcretes. In *Developments in Sedimentology* (eds. A. M. Alonso-Zarza and L. H. Tanner). Elsevier B.V. pp. 225–267. Available at: http://linkinghub.elsevier.com/retrieve/pii/S0070457109061056.

Andrews J. E., Singhvi A. K., Kailath A. J., Kuhn R., Dennis P. F., Tandon S. K. and Dhir R. P. (1998) Do Stable Isotope Data from Calcrete Record Late Pleistocene Monsoonal Climate Variation in the Thar Desert of India? *Quat. Res.* **50**, 240–251. Available at: http://www.sciencedirect.com/science/article/B6WPN-45M3173-5/1/f846d4a9d1da466792c556c2d9b72dfa%5Cnhttp://linkinghub.elsevier.com/retrieve/pii/S0033589498920026.

Armenteros I. (2010) Diagenesis of Carbonates in Continental Settings. In *Developments in Sedimentology* (eds. A. M. Alonso-Zarza and L. H. Tanner). pp. 61–151. Available at: http://linkinghub.elsevier.com/retrieve/pii/S0070457109062025.

Blokhius W. A., Ochtman L. H. J. and Peters K. H. (1964) Vertisols in the Gezira and the Khashm el Girba clay pan. *Soil Sci.* **5**, 591–603.

Blokhius W. A., Pape T. and Slager S. (1968) Morphology and distribution of pedogenic carbonate in some Vertisols of the Sudan. *Geoderma* **2**, 173–200.

Brookes I. A. (2010) Spatially variable sedimentary responses to orbitally driven pluvial climate during Marine Oxygen Isotope Stage 5.1, Dakhla Oasis region, Egypt. *Quat. Res.* **74**, 252–264.

Available at: http://dx.doi.org/10.1016/j.yqres.2010.05.001.

Budd D. a, Pack S. M. and Fogel M. L. (2002) The destruction of paleoclimatic isotopic signals in Pleistocene carbonate soil nodules of Western Australia. *Palaeogeogr. Palaeoclimatol. Palaeoecol.* **188**, 249–273.

Bullock P., Fedoroff N., Jongerius A., Stoops G., Tursina T. and Babel U. (1985) *Handbook for Soil Thin Section Description*., Waine Research Publication, Albrighton.

Burns S. J. and Matter A. (1995) Geochemistry of Carbonate Cements in Surficial Alluvial Conglomerates and their Paleoclimatic Implications, Sultanate of Oman. *SEPM J. Sediment. Res.* **Vol. 65A**. Available at: http://jsedres.sepmonline.org/cgi/doi/10.1306/D426805E-2B26-11D7-8648000102C1865D.

Buursink J. (1971) Soils of the central Sudan. .

Cailleau G., Braissant O. and Verrecchia E. P. (2011) Turning sunlight into stone: The oxalate-carbonate pathway in a tropical tree ecosystem. *Biogeosciences* **8**, 1755–1767.

Canti M. G. (2003) Aspects of the chemical and microscopic characteristics of plant ashes found in archaeological soils. *Catena* **54**, 339–361.

Caudill M. R., Driese S. G. and Mora C. I. (1996) Preservation of a proto-Vertisol and an estimate of Late Mississippian paleoprecipitation. *J. Sediment. Res.* **A66**, 58–70.

Cerling T. E. (1984) The stable isotopic composition of modern soil carbonate and its relationship to climate. *Earth Planet. Sci. Lett.* **71**, 229–240. Available at: http://linkinghub.elsevier.com/retrieve/pii/0012821X8490089X.

Cherkinsky A. (2009) Can We Get a Good Radiocarbon Age from “Bad Bone”? Determining the Reliability of Radiocarbon Age from Bioapatite. *Radiocarbon* **51**, 647–655. Available at: https://www.cambridge.org/core/product/identifier/S0033822200055995/type/journal_article.

Cremaschi M., Zerboni A., Spötl C. and Felletti F. (2010) The calcareous tufa in the Tadrart Acacus Mt. (SW Fezzan, Libya). *Palaeogeogr. Palaeoclimatol. Palaeoecol.* **287**, 81–94. Available at: http://linkinghub.elsevier.com/retrieve/pii/S0031018210000313.

Dal Sasso G. (2015) Characterization of archaeological bones from the Al Khiday cemetery (Central Sudan): structure and microstructure of diagenetically altered bioapatite. Università degli Studi di Padova.

Dal Sasso G., Angelini I., Maritan L. and Artioli G. (2018) Raman hyperspectral imaging as an effective and highly informative tool to study the diagenetic alteration of fossil bones. *Talanta* **179**, 167–176. Available at: http://dx.doi.org/10.1016/j.talanta.2017.10.059.

Dal Sasso G., Lebon M., Angelini I., Maritan L., Usai D. and Artioli G. (2016) Bone diagenesis variability among multiple burial phases at Al Khiday (Sudan) investigated by ATR-FTIR spectroscopy. *Palaeogeogr. Palaeoclimatol. Palaeoecol.* **463**, 168–179. Available at: http://linkinghub.elsevier.com/retrieve/pii/S0031018216305569.

Dal Sasso G., Maritan L., Salvatori S., Mazzoli C. and Artioli G. (2014a) Discriminating pottery production by image analysis: A case study of Mesolithic and Neolithic pottery from Al Khiday (Khartoum, Sudan). *J. Archaeol. Sci.* **46**, 125–143. Available at: http://dx.doi.org/10.1016/j.jas.2014.03.004.

Dal Sasso G., Maritan L., Usai D., Angelini I. and Artioli G. (2014b) Bone diagenesis at the micro-scale: Bone alteration patterns during multiple burial phases at Al Khiday (Khartoum, Sudan) between the Early Holocene and the II century AD. *Palaeogeogr. Palaeoclimatol. Palaeoecol.* **416**, 30–42. Available at: http://dx.doi.org/10.1016/j.palaeo.2014.06.034.

Dee M. W., Brock F., Harris S. A., Ramsey C. B., Shortland A. J., Higham T. F. G. and Rowland J. M. (2010) Investigating the likelihood of a reservoir offset in the radiocarbon record for ancient Egypt. *J. Archaeol. Sci.* **37**, 687–693. Available at: http://dx.doi.org/10.1016/j.jas.2009.09.003.

Deutz P., Montanez I. P. and Monger H. C. (2002) Morphology and Stable and Radiogenic Isotope Composition of Pedogenic Carbonates in Late Quaternary Relict Soils, New Mexico, U.S.A.: An Integrated Record of Pedogenic Overprinting. *J. Sediment. Res.* **72**, 809–822. Available at: http://jsedres.sepmonline.org/cgi/doi/10.1306/040102720809.

Deutz P., Montañez I. P., Monger H. C. and Morrison J. (2001) Morphology and isotope heterogeneity of Late Quaternary pedogenic carbonates: Implications for paleosol carbonates as paleoenvironmental proxies. *Palaeogeogr. Palaeoclimatol. Palaeoecol.* **166**, 293–317.

Durand N., Monger C. H. and Canti M. G. (2010) Calcium Carbonate Features. In *Interpretation of Micromorphological Features of Soils and Regoliths* (eds. G. Stoops, V. Marcelino, and F. Mees). Elsevier B.V. pp. 149–194. Available at: http://dx.doi.org/10.1016/B978-0-444-53156-8.00009-X.

El-Tom M. A. (1975) *The rains od the Sudan*., Khartoum University Press, Khartoum.

Elagib N. A. and Mansell M. G. (2000) Recent trends and anomalies in mean seasonal and annual temperatures over Sudan. *J. Arid Environ.* **45**, 263–288. Available at: http://www.idealibrary.com.

Gaballo V. (2009) Studio di reperti osteologici provenienti dalla necropoli 16-D-4 (Sudan) attraverso analisi spettroscopiche e spettrochimiche. Università degli Studi di Parma.

Gasse F. (2000) Hydrological changes in the African tropics since the Last Glacial Maximum. *Quat. Sci. Rev.* **19**, 189–211.

Gatto M. C. and Zerboni A. (2015) Holocene Supra-Regional Environmental Changes as Trigger for Major Socio-Cultural Processes in Northeastern Africa and the Sahara. *African Archaeol. Rev.* **32**, 301–333. Available at: http://link.springer.com/10.1007/s10437-015-9191-x.

Geyh M. A. and Eitel B. (1998) Radiometric dating of young and old calcrete. *Radiocarbon* **40**, 795–802.

Geyh M. A. and Thiedig F. (2008) The Middle Pleistocene Al Mahrúqah Formation in the Murzuq Basin, northern Sahara, Libya evidence for orbitally-forced humid episodes during the last 500,000 years. *Palaeogeogr. Palaeoclimatol. Palaeoecol.* **257**, 1–21.

Gile L. H., Peterson F. F. and Grossman R. B. (1966) Morphological and Genetic Sequences of Carbonate Accumulation in Desert Soils. *Soil Sci.* **101**, 347–360.

Gile L. H., Peterson F. F. and Grossman R. B. (1965) The K horizon: a master soil horizon of carbonate accumulation. *Soil Sci.* **99**, 74–82.

Heiri O., Lotter A. F. and Lemcke G. (2001) Loss on ignition as a method for estimating organic and carbonate content in sediments: Reproducibility and comparability of results. *J. Paleolimnol.* **25**, 101–110. Available at: http://link.springer.com/10.1023/A:1008119611481.

Hiatt E. E. and Pufahl P. K. (2014) Cathodoluminescence petrography of carbonate rocks: a review of applications for understanding diagenesis, reservoir quality, and pore system evolution. In *Cathodoluminescence and its application to geoscience* (ed. I. M. Coulson). Mineralogical Association of Canada short course, Fredericton NB. pp. 75–96.

Iacumin P., Di Matteo A., Usai D., Salvatori S. and Venturelli G. (2016) Stable isotope study on ancient populations of central sudan: Insights on their diet and environment. *Am. J. Phys. Anthropol.* **160**, 498–518.

Jakob T. (2014) A Bioarchaeological Appraisal of the Human Skeletal Remains from e l-Khiday 2, Central Sudan. In *The Fourth Cataract and Beyond. Proceedings of the 12th International Conference for Nubian Studies* (eds. J. R. Anderson and D. A. Welsby). Peeters Publishers, Leuven. pp. 271–277.

Jenny H. J. (1941) *Factors of soil formation*., McGraw-Hill, New York.

Khormali F., Abtahi A. and Stoops G. (2006) Micromorphology of calcitic features in highly calcareous soils of Fars Province, Southern Iran. *Geoderma* **132**, 31–46.

Machette M. N. (1985) Calcitic soils of the southwestern United States. *Geol. Soc. Am. Spec. Pap.* **203**, 1–22.

Mack G. H. and James W. C. (1992) Calcic paleosols of the Plio-Pleistocene Camp Rice and Palomas Formations, southern Rio Grande rift, USA. *Sediment. Geol.* **77**, 89–109. Available at: http://linkinghub.elsevier.com/retrieve/pii/003707389290105Z.

Mack G. H., James W. C. and Monger H. C. (1993) Classification of paleosols. *Geol. Soc. Am. Bull.* **105**, 129–136. Available at: https://pubs.geoscienceworld.org/gsabulletin/article/105/2/129-136/182768.

Maritan L., Iacumin P., Zerboni A., Venturelli G., Dal Sasso G., Linseele V., Talamo S., Salvatori S. and Usai D. (2018) Fish and salt: The successful recipe of White Nile Mesolithic hunter-gatherer-fishers. *J. Archaeol. Sci.* **92**, 48–62. Available at: http://linkinghub.elsevier.com/retrieve/pii/S0305440318300426.

Mawson R. and Williams M. A. J. (1984) A wetter climate in eastern Sudan 2,000 years ago? *Nature* **309**, 49–51. Available at: http://www.nature.com/doifinder/10.1038/309049a0.

McDermott F., Stringer C., Grün R., Williams C. T., Din V. K. and Hawkesworth C. J. (1996) New Late-Pleistocene uranium–thorium and ESR dates for the Singa hominid (Sudan). *J. Hum. Evol.* **31**, 507–516. Available at: http://linkinghub.elsevier.com/retrieve/pii/S0047248496900767.

McFadden L. D. and Tinsley J. C. (1985) Rate and depth of pedogenic-carbonate accumulation in soils: Formulation and testing of a compartment model. In pp. 23–42. Available at: https://pubs.geoscienceworld.org/books/book/339/chapter/3796184/.

Nettleton W. ., Olson C. . and Wysocki D. . (2000) Paleosol classification: Problems and solutions. *CATENA* **41**, 61–92. Available at: http://linkinghub.elsevier.com/retrieve/pii/S0341816200001090.

Newman B. D., Campbell A. R., Norman D. I. and Ringelberg D. B. (1997) A model for microbially induced precipitation of vadose-zone calcites in fractures at Los Alamos, New Mexico, USA. *Geochim. Cosmochim. Acta* **61**, 1783–1792. Available at: http://www.sciencedirect.com/science/article/pii/S0016703797000252.

Nicoll K. (2001) Radiocarbon chronologies for prehistoric human occupation and hydroclimatic change in Egypt and Northern Sudan. *Geoarchaeology* **16**, 47–64. Available at: http://doi.wiley.com/10.1002/1520-6548%28200101%2916%3A1%3C47%3A%3AAID-GEA5%3E3.0.CO%3B2-P.

Nicoll K. (2004) Recent environmental change and prehistoric human activity in Egypt and Northern Sudan. *Quat. Sci. Rev.* **23**, 561–580.

Reimer P. J., Bard E., Bayliss A., Beck J. W., Blackwell P. G., Bronk C., Caitlin R., Hai E. B. and Edwards R. L. (2013) Intcal13 and marine13 radiocarbon age calibration curves 0 – 50,000 years cal CP. *Radiocarbon* **55**, 1869–1887.

Retallack G. J. (2000) Depth to pedogenic carbonate horizon as a paleoprecipitation indicator?: Comment and Reply. *Geology* **28**, 572. Available at: https://pubs.geoscienceworld.org/geology/article/28/6/572/185736.

Retallack G. J. (2005) Pedogenic carbonate proxies for amount and seasonality of precipitation in paleosols. *Geology* **33**, 333. Available at: https://pubs.geoscienceworld.org/geology/article/33/4/333-336/29600.

Retallack G. J., James W. C., Mack G. H. and Monger H. C. (1993) Classification of paleosols: Discussion and reply. *Geol. Soc. Am. Bull.* **105**, 1635–1637. Available at: https://pubs.geoscienceworld.org/gsabulletin/article/105/12/1635-1637/182783.

Richter D. K., Immenhauser A. and Neuser R. D. (2008) Electron backscatter diffraction documents randomly orientated c-axes in moonmilk calcite fibres: Evidence for biologically induced precipitation. *Sedimentology* **55**, 487–497.

Salvatori S. (2012) Disclosing Archaeological Complexity of the Khartoum Mesolithic: New Data at the Site and Regional Level. *African Archaeol. Rev.* **29**, 399–472.

Salvatori S. and Usai D. (2009) El Salha Project 2005: New Khartoum Mesolithic sites from central Sudan. *Kush* **19**, 87–96.

Salvatori S., Usai D., Abdelrahman M. F., Di Matteo A., Iacumin P., Linseele V. and Magzoub M. K. (2014) Archaeological evidence at Al Khiday. New insight on the prehistory and History of Central Sudan. In *The Fourth Cataract and Beyond. Proceedings of the 12th International Conference of Nubian Studies* (eds. J. R. Anderson and D. A. Welsby). Peeters Publishers, Leuven. pp. 243–258.

Salvatori S., Usai D. and Zerboni A. (2011) Mesolithic Site Formation and Palaeoenvironment Along the White Nile (Central Sudan). *African Archaeol. Rev.* **28**, 177–211.

Stoops G. (2003) *Guidelines for analysis and description of soil and regolith thin sections*., Soil Science Society of America, Madison, WI.

Stoops G., Marcellino V. and Mees F. (2010) *Interpretation of micromorphological features of soil and regoliths*., Elsevier, Amsterdam.

Szabo B. J., Haynes C. V. and Maxwell T. a. (1995) Ages of Quaternary pluvial episodes determined by uranium-series and radiocarbon dating of lacustrine deposits of Eastern Sahara. *Palaeogeogr. Palaeoclimatol. Palaeoecol.* **113**, 227–242.

Terrasi F., De Cesare N., D'Onofrio A., Lubritto C., Marzaioli F., Passariello I., Rogalla D., Sabbarese C., Borriello G., Casa G. and Palmieri A. (2008) High precision 14C AMS at CIRCE. *Nucl. Instruments Methods Phys. Res. Sect. B Beam Interact. with Mater. Atoms* **266**, 2221–2224.

Usai D. (2003) The Is.I.A.O. El Salha project. *Kush* **18**, 173–182.

Usai D., Maritan L., Dal Sasso G., Artioli G., Salvatori S., Jakob T. and Salviato T. (2017) Late Pleistocene/Early Holocene Evidence of Prostatic Stones at Al Khiday Cemetery, Central Sudan. *PLoS One* **12**, e0169524. Available at: http://dx.plos.org/10.1371/journal.pone.0169524.

Usai D. and Salvatori S. (2002) The Is.I.A.O. El Salha archaeological project. *Sudan & Nubia* **6**, 67–72.

Usai D. and Salvatori S. (2005) The IsIAO archaeological project in the El Salha area (Omdurman South, Sudan): results and perspectives. *Africa (Lond).* **60**, 474–493.

Usai D., Salvatori S., Iacumin P., Di Matteo A., Jakob T. and Zerboni A. (2010) Excavating a unique pre-Mesolithic cemetery in central Sudan. *Antiquity* **84**, 16–18. Available at: http://www.antiquity.ac.uk/projgall/usai323/.

Usai D., Salvatori S., Jakob T. and David R. (2014) The Al Khiday Cemetery in Central Sudan and its "Classic/Late Meroitic" Period Graves. *J. African Archaeol.* **12**, 183–204. Available at: http://booksandjournals.brillonline.com/content/journals/10.3213/2191-5784-10254.

Verrecchia E. P. and Verrecchia K. E. (1994) Needle-fiber Calcite: A Critical Review and a Proposed Classification. *J. Sediment. Res.* **64**, 650–664. Available at: https://pubs.geoscienceworld.org/jsedres/article/64/3a/650-664/98618.

Vogel J. C. and Geyh M. A. (2008) Radiometric dating of hillslope calcrete in the Negev Desert, Israel. *S. Afr. J. Sci.* **104**, 493–495.

Walkley A. and Black I. A. (1934) An examination of Degtjareff method for determining soil organic matter and a proposed modification of the chromic acid titration method. *Soil Sci.* **37**, 29–38.

Wang Y., McDonald E., Amundson R., McFadden L. and Chadwick O. (1996) An isotopic study of soils in chronological sequences of alluvial deposits, Providence Mountains, California. *Bull. Geol. Soc. Am.* **108**, 379–391.

Weninger B. (1986) High-precision calibration of archaeological radiocarbon dates. *Acta Interdiscip. Archaeol.* **4**, 11–53.

Weninger B. and Jöris O. (2008) A 14C age calibration curve for the last 60 ka: the Greenland-Hulu U/Th timescale and its impact on understanding the Middle to Upper Paleolithic transition in Western Eurasia. *J. Hum. Evol.* **55**, 772–781.

Whiteman A. J. (1971) *The Geology of the Sudan Republic*., Oxford University Press, Oxford.

Williams M. A. J. (1968) A DUNE CATENA ON THE CLAY PLAINS OF THE WEST CENTRAL GEZIRA, REPUBLIC OF THE SUDAN. *J. Soil Sci.* **19**, 367–378. Available at: http://doi.wiley.com/10.1111/j.1365-2389.1968.tb01547.x.

Williams M. A. J. (2009) Late Pleistocene and Holocene environments in the Nile basin. *Glob. Planet. Change* **69**, 1–15. Available at: http://dx.doi.org/10.1016/j.gloplacha.2009.07.005.

Williams M. A. J. and Adamson D. (1980) Late Quaternary depositional history of the Blue and White Nile rivers in central Sudan. In *The Sahara and the Nile: Quaternary environments and prehistoric occupation in northern Africa* (eds. M. A. J. Williams and H. Faure). A. A. Balkema, Rotterdam. pp. 281–304.

Williams M. A. J. and Jacobsen G. E. (2011) A wetter climate in the desert of northern Sudan 9900-7600 years ago. *Sahara* **22**, 7–14.

Williams M. A. J., Usai D., Salvatori S., Williams F. M., Zerboni A., Maritan L. and Linseele V. (2015) Late Quaternary environments and prehistoric occupation in the lower White Nile valley, central Sudan. *Quat. Sci. Rev.* **130**, 72–88. Available at: http://dx.doi.org/10.1016/j.quascirev.2015.03.007.

Wintle A. G. and Murray A. S. (2006) A review of quartz optically stimulated luminescence characteristics and their relevance in single-aliquot regeneration dating protocols. *Radiat. Meas.* **41**, 369–391.

WRB (2006) *World reference base for soil resources 2006.* World Soil. ed. FAO, Rome.

Wright V. P. (2007) Calcrete. In *Geochemical Sediments and Landscapes* (eds. D. J. Nash and S. J. McLaren). Wiley-Blackwell. pp. 10–45.

Wright V. P., Platt N. H. and Wimbledon W. A. (1988) Biogenic laminar calcretes: evidence of calcified root-mat horizons in paleosols. *Sedimentology* **35**, 603–620. Available at: http://doi.wiley.com/10.1111/j.1365-3091.1988.tb01239.x.

Wright V. P. and Tucker M. E. (1991) Calcretes: an introduction. In *Calcretes* (eds. V. P. Wright and M. E. Tucker). Blackwell, Oxford. pp. 1–22.

Yaalon D. H. (1983) Climate, time and soil development. In *Pedogenesis and Soil Taxonomy. 1. Concepts and Interactions* (eds. L. P. Wilding, N. E. Smeck, and G. P. Hall). Elsevier, Amsterdam. pp. 233–251.

Zazzo A. (2014) Bone and enamel carbonate diagenesis: A radiocarbon prospective. *Palaeogeogr. Palaeoclimatol. Palaeoecol.* **416**, 168–178. Available at: http://dx.doi.org/10.1016/j.palaeo.2014.05.006.

Zerboni A. (2013) Early Holocene palaeoclimate in North Africa: an overview. In *Neolithisation of Northeastern Africa, Studies in Early Near Eastern Production, Subsistence, and Environment* (ed. N. Shirai). Ex Oriente, Berlin. pp. 65–82.

Zerboni A. (2011) Micromorphology reveals in situ Mesolithic living floors and archaeological features in multiphase sites in central Sudan. *Geoarchaeology* **26**, 365–391.

Zerboni A., Trombino L. and Cremaschi M. (2011) Micromorphological approach to polycyclic pedogenesis on the Messak Settafet plateau (central Sahara): Formative processes and palaeoenvironmental significance. *Geomorphology* **125**, 319–335. Available at: http://dx.doi.org/10.1016/j.geomorph.2010.10.015.

Zerboni A., Usai D. and Meyer M. (2016) The Middle Palaeolithic / Middle Stone Age site of Al Jamrab in central Sudan. *Antiq. Proj. Gall.*, 4–7. Available at: http://antiquity.ac.uk/projgall/zerboni351.

Zhou J. and Chafetz H. S. (2009) The genesis of late Quaternary caliche nodules in Mission Bay, Texas: Stable isotopic compositions and palaeoenvironmental interpretation. *Sedimentology* **56**, 1392–1410.

List of figures

Figure 1. a. Location of archaeological sites at Al Khiday, Khartoum, Sudan (from Google Earth™, version 7.1.8.3036; 15°27'10.37''N, 32°24'25.73''E, alt 112.8 Km, Image Landsat/Copernicus, [12/05/2017]; **b.** Oblique aerial picture of the 16D4 site during the 2015 archaeological campaign (photo by Yves Guichard, CSSeS); a white arrow shows the location of the soil profile analysed in this study (pit 151A).

Figure 2. a. Carbonate concretions partially embed pre-Mesolithic bones (grave 152); **b.** Mesolithic pit cut into the calcium carbonate-rich horizon; **c.** Meroitic grave cut into the calcium carbonate-rich horizon; **d**. Early (?) Pleistocene paleosol, highly cemented by calcium carbonate outcropping in the area surrounding 16D4 site.

Figure 3. Field photograph of exposed calcrete section sampled for this study (pit 151A). A schematic sketch of the studied profile and the location of sampling points and results of physico-chemical analyses (carbonate and humified carbon content, pH, LOI, total carbon and total nitrogen content) are shown. 1: Quartz sand slightly cemented by calcium carbonate, coalescent irregular calcitic nodules occur (Bk); 2: Sandy lens weakly cemented by calcium carbonate (BC); 3: Quartz sand cemented by calcium carbonate and carbonate concretions (2Bk).

Figure 4. Photomicrographs from the Bk, BC (a–d) and 2Bk (e–h) horizons. **a.** Micritic micromass cementing quartz sand grains, corresponding to a calcitic nodule (A1 – XPL); **b.** Well-rounded allochthonous calcitic pedorelict stained by Mn and Fe oxides (A1 - XPL, top-right); **c.** Quartz grains in a porphyric c/f related distribution, poorly cemented by authigenic calcite (A1 - XPL); **d.** calcite recrystallized after wood ash, as confirmed by the occurrence of microcharcoals (arrows); this calcite derives from the infilling material of the Mesolithic pit (A2 - PPL). **e.** Micritic micromass slightly cementing sand- and silt-sized quartz grains (A3a – XPL); **f.**, **g.** High concentration of calcium carbonate, corresponding to calcitic nodules predominantly constituted by microsparitic calcite. Cemented nodules formed by well-cemented calcite crystals with sub-rounded

to sub-angular shape, are shown (A3a – XPL); **h.** Allochthonous calcitic pedorelict sub-rounded in shape and stained by Fe oxides (A3c – PPL).

Figure 5. CL photomicrographs of: **a.** Micritic micromass (orange) cementing quartz sand grains (dark blue) within calcitic nodule from the BK horizon (A1); **b.** Poorly cemented area characterized by low luminescence due to the scarcity of calcite (A1); **c., d.** Well-rounded calcitic pedorelict constituted a by micritic matrix stained by Mn and Fe oxides-hydroxides and containing veins of sparitic and microsparitic calcite (A1, PPL and CL); **e.** Highly carbonated areas corresponding to a calcitic nodule from the 2Bk horizon, predominantly constituted by microsparitic calcite (A3a); cemented nodules formed by well-cemented calcite crystals, sub-rounded to sub-angular in shape, are shown; **f.** Cemented nodules characterized by lower size and less defined margins (A3d). **g., h.** Luminescence variations of calcite crystals forming cemented nodules from A3d and A3a sampling points.

Figure 6. SEM-BSE images of different portions of calcitic nodules from the Bk (a-c) and 2Bk (d-f) horizons showing: **a.** Densely packed calcite crystals (light grey) and part of a quartz sand grain (dark grey); **b.** Calcite crystals associated to a clayey matrix; **c.** Sparse distribution of calcite crystals. SEM-BSE images of calcitic nodules from the lower unit showing: **d.** The outermost part of allochthonous calcitic pedorelict characterized by clay minerals coating its outer surface (A3c); **e.**, **f.** part of a cemented nodule, formed by well-cemented calcite crystals, embedded in a matrix characterized by less packed calcite crystals (A3a).

Figure 7. a., b. Photomicrographs of a calcitic nodule predominantly constituted by microsparitic calcite in which cemented nodules are well-distinguishable from the surrounding calcitic-rich matrix (2Bk horizon, A3a sampling point – PPL, XPL); **c.** Segmented false-colour image obtained from Fig. 7a, 7b highlights the spatial distribution of these two pedofeatures.

Figure 8. Cumulative calibrated dating probability of radiocarbon ages obtained from: **a.** Calcium carbonate samples (8) from the section analysed in this study; **b.** Calcitic nodules from soils sampled in Central Sudan (Adamson et al., 1982) **c.** Freshwater shells (33) indicating higher

flooding level of the White Nile (Williams, 2009; Williams et al., 2015). **d.** Bioapatite fraction of archaeological bones (19) from graves found at 16D4 site (Gaballo, 2009; Zazzo, 2014; Dal Sasso, 2015). More humid periods characterized by higher flow of the White Nile (light-blue bars) and the chronology established for the anthropic use of the site at Al Khiday (Salvatori et al., 2011) (orange bars – Mesolithic, Neolithic and Meroitic periods) are reported.

Figure 9. a. AMS-^{14}C ages obtained for cemented nodules and calcitic-rich matrix at each sampling point. The sketch of the studied profile, shown in Fig. 3, is also reported; **b., c.** C and O stable isotope data for cemented nodules and and calcitic-rich matrix samples.

Manuscript with marked changes

Radiocarbon dating reveals the timing of formation and development of pedogenic calcium carbonate concretions in Central Sudan during the Holocene

~~Radiocarbon dating of calcrete development records the steps of pedogenesis in arid lands~~

Gregorio Dal Sasso[1*], Andrea Zerboni[2], Lara Maritan[1], Ivana Angelini[3], Chiara Compostella[2], Donatella Usai[4,5], Gilberto Artioli[1]

[1]Dipartimento di Geoscienze, Università degli Studi di Padova, Via G. Gradenigo 6, 35131 Padova, Italy.

[2]Dipartimento di Scienze della Terra "A. Desio", Università degli Studi di Milano, Via L. Mangiagalli 34, I-20133 Milano, Italy.

[3]Dipartimento dei Beni Culturali: archeologia, storia dell'arte, del cinema e della musica, Università degli Studi di Padova, Piazza Capitaniato 7, 35139 Padova, Italy.

[4]Centro Studi Sudanesi e Sub-Sahariani (CSSeS), Strada Canizzano 128/d, 31100 Treviso, Italy.

[5]Dipartimento di Scienze dell'Antichità, Sapienza Università di Roma, Via dei Volsci 122, I-00185 Roma, Italy

[*]corresponding author: gregorio.dalsasso@unipd.it

Abstract

~~A calcrete horizon formed in Central Sudan, sampled during the archaeological excavation of the Al Khiday 16-D-4 site, is here analysed by optical, cathodoluminescence and scanning electron microscopy. Distinct calcitic pedofeatures were identified, mechanically separated and analysed for stable carbon and oxygen isotopes and radiocarbon dated. Results are discussed taking into account all the available information from detailed physiographic and palaeoenvironmental studies carried out in this area and from the study of the tight interaction between calcrete and evidence of anthropic activities, as attested in the archaeological record. This allowed a more complete understanding of the processes involved in calcrete formation, recycling, and development in this area during almost the entire Holocene. Calcrete was characterized by alternate periods of growth and quiescence, depending on changes of environmental conditions at local and regional scale. Radiocarbon ages are critically discussed, highlighting advantages and limitations of this approach to timing calcrete development. These results show the effectiveness of a multi-analytical approach to the study of pedogenic calcrete, aiming to define the timing and dynamics of its formation and development.~~

~~Considering a wider perspective, our results may represent a further step in the comprehension of calcrete formation and in the definition of a reliable method to date its formation. This may offer a significant tool for both archaeometric studies, where the interaction between secondary calcite and archaeological material may alter results and hamper their straightforward interpretation, and palaeoenvironmental studies in arid lands, where calcrete may represent the only archive for past climatic changes.~~

Calcitic soil horizons are common in arid and semi-arid lands and represent the result of the progressive accumulation of calcium carbonate in the soil profile over time. This process leads to the occurrence of several pedogenetic phases of calcium carbonate dissolution/precipitation. For this reason, timing the formation and development of calcic horizons through radiometric dating is not straightforward as time-averaging effects, due to the superimposition of the same process over

time, occur. On this basis, this study aims to define the timing and dynamics of formation and development of pedogenic calcitic concretions from semi-arid Central Sudan, highlighting the relevance of a multi-disciplinary approach and the effectiveness of radiocarbon dating (coupled to an accurate sampling strategy) applied to pedogenic carbonates. Calcium carbonate-rich soil horizons (Bk) were sampled during the archaeological excavation of site 16-D-4 at Al Khiday (Central Sudan) and studied by optical, cathodoluminescence and scanning electron microscopy, as well as by chemical-physical and stable isotopes (C and O) analyses. Radiocarbon ages are obtained for distinctive calcitic pedofeatures and mostly refer to the Early Holocene for calcitic-cemented nodules (11.5, 9.9 and 9.6 cal. ka) and to the Middle Holocene for powdery calcitic-rich matrix (7.9, 7.7, 6.3 and 6.1 cal. ka) samples. Our data are also compared with the available information from detailed physiographic and palaeoenvironmental studies carried out in the region and from the study of the tight interaction between soil horizons and evidence of anthropic activities at Al Khiday site, as the archaeological record provides informative chronological constrains to interpret the ^{14}C ages obtained on selected calcitic pedofeatures. Pedogenic calcitic features dated to the Early Holocene can be related to short arid phases during general wetter climate conditions, whereas those dated to the Middle Holocene can be related to short humid phases. Results show that Bk horizons were characterized by alternate periods of calcite accumulation (precipitation) and dissolution, and periods of quiescence or extremely slow growth rates. Thus, the formation and development of Bk horizons has been a long-lasting process significantly influenced by climatic fluctuations. This study represents a further step in the comprehension of the development of calcium carbonate concretions and (at a wider perspective) calcrete; the paper also contributes to the definition of a reliable method to radiometrically date the formation of calcitic pedofeatures. In a broader perspective, this work may offer a significant tool for archaeometric studies, where the interaction between secondary calcite and archaeological material is significant (e.g., radiocarbon dating of bioapatite in bones), and palaeoenvironmental studies in arid lands, where Bk horizon development is a function of past rainfall.

Keywords

Holocene; Calcic concretions~~Calcrete~~; North Africa; ~~Stable isotopes~~Cathodoluminescence microscopy; Radiocarbon dating; Pedogenesis.

1 Introduction

Calcic and petrocalcic soil horizons, and pPedogenic calcretes refers toare the results of a near-surface terrestrial accumulation of predominantly calcium carbonate, resulting from the introduction and cementation of calcium carbonate into a soil profile in different forms, i.e. powdery, nodular, laminar, or massive (Gile et al., 1965; Machette, 1985; Wright and Tucker, 1991; Wright, 2007; Durand et al., 2010);. they are present in present-day soils (WRB, 2006) as much as in paleosols (Mack et al., 1993; Retallack et al., 1993; Nettleton et al., 2000). These pedogenic bodiesIt often occurs in areas, where vadose and shallow phreatic groundwater is saturated with respect of calcium carbonate. This general definition is applied to a large variety of calcitic horizons at different stages of development, abundantly occurring worldwide, at different latitudes, within different geological contexts, and under different pedoclimate settings (Gile et al., 1966; Machette, 1985; McFadden and Tinsley, 1985; Alonso-Zarza and Wright, 2010). However, the most evident examples of calcitic soil horizons (Bk) developed in arid and semi-arid regions (Gile et al., 1966; Adamson et al., 1982; Machette, 1985). General assumption is that calcrete develops in soils, characterized by a net moisture deficit, in which the circulating fluids (vadose and shallow phreatic groundwater) are saturated in calcium carbonate. Calcite accumulation is promoted by several physical-chemical processes as well as by biological-mediated processes (Wright et al., 1988; Verrecchia and Verrecchia, 1994; Cailleau et al., 2011), which, in turn, are influenced by climatic conditions, in particular rainfall amount. As a consequence, calcrete is not generally the result of a single pedogenetic phase, but it corresponds to subsequent events, eventually separated by a long time span, during which previously precipitated carbonates undergo a partial or complete new dissolution and then re-precipitation. Calcic horizon and Ccalcrete development, therefore, consists of several, superimposed generations of micritic and/or sparitic calcium carbonate crystals. For this reason, and considering also that a continuous opening of the system hampers the possibility to date calcite with U/Th and ^{14}C, it is hard to define accurately the time and steps of calcrete pedogenesis.

Almost thirty-five years ago, ~~(~~Adamson et al.~~,~~ (1982) have carried out a huge campaign of radiocarbon dating of calcitic nodules in soils from Central Sudan, highlighting the occurrence of reworked carbonates and subsequent recrystallizations. For that reason and for the the large occurrence of carbonate pedofeatures, soils/paleosoils of arid Sudan are an exceptional case study to investigate the chronological development of carbonatic concretions. Therefore, ~~In~~ in this research~~,~~ a multi-analytical approach, consisting in mineralogical, micromorphological, geochemical, and geochronological analyses, is applied to the study of calcitic pedogenic ~~calcrete~~ features from Central Sudan, in order to contribute towards the understanding of dynamics and timing of ~~its~~ their formation and development. Carbonate-bearing soil horizons~~Calcrete~~ analysed in this study formed in a localised area along the left bank of the White Nile, few km south of the Khartoum-Omdurman urban system (Fig. 1), where a large, multiphase archaeological site (Al-Khiday, currently under excavation) is in tight relation with the ~~calcrete~~carbonate concretions. In fact, part of the vestiges of the site is embedded in the calcitic crust (Fig. ~~1a~~2a), whereas other features are clearly cut in the pre-existing carbonate-bearing horizon (Fig. ~~1b~~ 2b and ~~1c~~2c). Detailed studies on the local physiographic and palaeoenvironmental aspects (Zerboni, 2011; Williams et al., 2015), as well as on the anthropic activities, considering the wide span of time covered by the archaeological evidence (almost the whole Holocene) (Usai and Salvatori, 2002; Usai, 2003; Usai and Salvatori, 2005; Salvatori and Usai, 2009; Usai et al., 2010; Salvatori et al., 2011; Salvatori, 2012; Dal Sasso et al., 2014a; Jakob, 2014; Salvatori et al., 2014; Dal Sasso et al., 2014b; Usai et al., 2014; Dal Sasso et al., 2016; Iacumin et al., 2016; Usai et al., 2017; Maritan et al., 2018), supply important information to reconstruct the timing and steps of calcrete formation. In our study, results from the minero-petrographic and pedogenetic study of ~~calcrete~~ soil samples, coupled with additional archaeological and palaeoenvironmental information, allowed a more complete understanding of the processes involved in calcitic horizons and calcrete formation, recycling, and development. Moreover, since these processes are strongly dependent on water availability, which, in turn, depends on climatic conditions, our results are discussed taking into account the regional Holocene variations in water availability, as reconstructed by several palaeoenvironmental studies.

2 Study area, palaeoenvironmental settings, and archaeological background

A complex calcrete horizon has been found during the archaeological survey and excavation of several archaeological sites (16-D-3, 16-D-4, 16-D-4b, 16-D-5, 16-D-6) and the geomorphological survey of the region carried out since 2006 within the "El Salha ~~archaeological~~ Archaeological ~~project~~Project" (Usai and Salvatori, 2002; Usai, 2003; Usai and Salvatori, 2005; Salvatori and Usai, 2009; Usai et al., 2010; Salvatori et al., 2011; Salvatori, 2012). The archaeological sites are located on the western bank of the White Nile, near the Al Khiday village (Central Sudan), at 3.5 km from the present-day river course and about 22 Km south of its confluence with the Blue Nile (Fig. ~~2a~~1a). They are set on fluvial sandy ridges, corresponding to the remnants of late Pleistocene longitudinal river bars, at the limit of alluvial sediments deposited during the very late Quaternary flooding of the White Nile (Zerboni, 2011; Williams et al., 2015). These fluvial ridges and the surrounding flat areas are weakly weathered by Holocene pedogenesis, despite the intense accumulation of pedogenic calcium carbonate (Zerboni, 2011), thus the poorly developed local soils can be defined as aridisols (Buursink, 1971).

The archaeological excavation and geomorphological investigation (Usai et al., 2010; Salvatori et al., 2011; Zerboni, 2011) revealed a complex stratigraphy at these archaeological sites, resulting from anthropic activities, sedimentary, erosional, and pedogenic processes occurring along a wide span of time. The area had been inhabited several times along almost the entire Holocene. Focusing on the 16-D-4 site (Fig. ~~2b~~1b), a Mesolithic specialised use of the area was defined by the numerous pits (more than 100) that have been excavated, characterized by different types of filling material and presumably with different functions (Zerboni, 2011), and radiocarbon dated to 8650-8250 cal. BP (Salvatori et al., 2011). In addition, the site was used several times as a burial ground: at least three different burial phases have been identified. The most ancient one, named pre-Mesolithic, is characterized by individuals (at least 90) buried in a prone and elongated position. The chronology of this burial phase is uncertain but constrained by the Mesolithic use of the area, as a number of skeletons (16) were found to be cut by radiocarbon-dated Mesolithic pits (Salvatori et al., 2011), which indicate that the pre-Mesolithic burial phase is unambiguously older than 8650 cal. BP. The site was subsequently used as a cemetery during the Neolithic period (38 graves; 6500-6200 cal. BP), and later on during the Meroitic period (43 graves, 2100-1800 cal. BP) (Usai et al., 2010; Salvatori et al., 2011).

Soils in Central Sudan can be classified as Vertisols, Entisols, Aridisols, and Alfisols (Buursink, 1971) in the study region, the first three categories are the most represented and Aridisols are those most recurrent at Al Khiday. In the whole region, pedogenic processes lead to the accumulation of calcic pedofeatures, which have been described previously by several authors (Blokhius et al., 1968; Williams, 1968; Buursink, 1971; Adamson et al., 1982). ~~(~~Buursink~~,~~ (1971) in his classification of soil of Central Sudan describes several petrocalcic horizons, rich in $CaCO_3$ nodules and/or concretions, similar to the K horizons defined by ~~(~~Gile et al.~~,~~ (1966). The same pedofeatures have been reported by ~~(~~Blokhius et al., (1964) and~~;~~ Blokhius et al.~~,~~(1968), who also described the properties and distribution of pedogenic carbonate in Vertisols. Soils and paleosoils with common to abundant $CaCO_3$ concretions have been reported also by ~~(~~Williams~~,~~ (1968) along the White Nile.

Today, the climate of the region is arid, with mean annual temperature ranging from 22°C to 33°C and average rainfall of ca. 130 mm (El-Tom, 1975; Elagib and Mansell, 2000). However, climatic conditions were significantly different in the past and substantial climatic changes occurred at local and regional levels (Williams and Adamson, 1980; Gasse, 2000; Nicoll, 2001; Nicoll, 2004; Williams, 2009; Williams and Jacobsen, 2011; Zerboni, 2013; Gatto and Zerboni, 2015) during the wide time span of the site use (from the early Holocene to the beginning of the 1st millennium AD). In the early Holocene (11500-8000 cal. BP) the precipitation rate, and consequently also the environmental humidity, were substantially higher, as well as the flooding level of the White Nile, due to a northward expansion of the Indian monsoon domain (Gasse, 2000; Williams, 2009). The formation of seasonal swamps in the surrounding area of the Al Khiday sites during the Mesolithic occupation of the area is attested by geoarchaeological and geomorphological evidence (Williams and Jacobsen, 2011; Zerboni, 2011). Since the middle Holocene (8000-3600 cal. BP), the progressive weakening of monsoon intensity led to rainfall decrease and overall reduction of water availability. In the late Holocene (since ca. 3600 cal. BP), since the Meroitic period and later on, progressively drier environmental conditions occurred, up to the arid climate that now characterizes central Sudan; only short-timed wetter events have been occasionally recorded (Mawson and Williams, 1984). In addition to this general trend, palaeoenvironmental records identified several periods of rapid climatic changes during the early Holocene wet phase, when several short arid periods occurred (Williams, 2009).

3 Materials and methods

The samples considered in this research come from a test trench, exposed in the sandy deposit at Al Khiday and representing the local substrate, brought to light during the excavation of a Mesolithic pit (pit number 151A). The section shows a soil profile with at least 70 cm0.7 m of fine to coarse sand (occasionally lenses of pebbles are present), deeply cemented by calcium carbonate (calcrete). Horizons description is in Tab. 1. Six oriented and undisturbed blocks were collect,sampling points, namely A1, A2, A3a, A3b, A3c, and A3d, were selected at different depths from the top to the bottom of the section (see Tab. 1 and Fig. 3 for detailsFig. 3). At each sampling point, samples were collected and prepared as required for the analytical techniques applied in this study.A total of 9 samples (one for each block and an additional sample for A2, A3a, and A3d blocks) covering the whole section were selected, Samples were embedded under vacuum in epoxy resin (Araldite 2020) and prepared in petrographic thin sections (3x5 cm). Micromorphological analyses were carried out on thin sections by petrographic optical microscopy (OM), cathodoluminescence microscopy (CL), and scanning electron microscopy (SEM).

OM analysis was ~~carried out~~performed with a petrographic microscope (Nikon Eclipse E660) under plane-polarized (PPL) and cross-polarized light (XPL). CL analysis was performed with a petrographic microscope (NIKON Labophot2-POL) equipped with a cold cathode stage (CL8200 MK3, Cambridge Image Technology Ltd) and operating at 15 kV and 200 mA. SEM analysis was ~~performed~~ carried out with a CamScan MX 2500 coupled to a detector for Energy dispersive X-ray spectroscopy (EDS), equipped with a LaB6 cathode and operating at 20 kV and 160 nA. Thin-sections were described following the terminology proposed by Bullock et al. (1985) and Stoops (2003), and the interpretation mostly followed the concepts discussed in Stoops et al. (2010).

Samples adjoining those prepared in thin sections were selected for chemical and stable isotopes analyses and radiocarbon dating. The chemical characterization of samples was performed measuring $CaCO_3$ equivalents, pH, humified carbon content, total organic carbon, total carbon content (TC) and nitrogen content (TN). Calcium carbonate equivalents were chemically performed using a Dietrich–Frühling calcimeter, which measures the volume of CO_2 developed by acid reacting with the bulk sample, which is proportional to the carbonate concentration. Humified organic carbon was identified by means of the Walkley and Black (1934) method, using chromic acid to measure the oxidizable organic carbon (titration). Total organic carbon was estimated by loss on ignition - LOI - (Heiri et al., 2001); samples were air-dried (at 105°C) and organic matter was oxidized at 500–550°C to carbon dioxide and ash, then the weight lost during the reaction was measured by weighing the samples before and after heating. The analysis of total carbon and total nitrogen were performed on dried soil samples with a Thermo Fisher Scientific Organic Elemental Analyzer (OEA-Flash 2000). Samples were weighed out into tin containers to the nearest 0.001mg on a Gibertini MICRO1000 electronic microbalance. Each sample was then flash-combusted at 1800°C in the OEA.

~~On the basis of micromorphological analysis of thin sectionssamples were gently disaggregated in an agate mortar; distinctive~~ After a gentle disaggregation in an agate mortar, distinctive calcitic pedofeatures, described by thin section micromorphological analyses, were identified on massive samples ~~along the calcrete section were~~ and accurately separated by hand-picking under the stereoscopic microscope~~,~~. Each pedofeature~~and~~ was then analysed for stable carbon and oxygen isotopes and radiocarbon dated.

Stable isotopes analyses were carried out with a Thermo Scientific Delta V Advantage Isotope Ratio Mass Spectrometer. CO_2 was developed at 70 °C by complete reaction with >99% crystalline H_3PO_4 in a Gasbench II device connected to the spectrometer. Results were calibrated with two internal standards (sieved Carrara marble and Millipore Suprapur carbonate), periodically calibrated against the international reference carbonates NBS 19, NBS 18 and L-SVEC. A control standard (sieved Monzoni marble) was also measured and reproduced with external errors of better than 0.1‰ (1σ) for both carbon and oxygen.

Radiocarbon dating by accelerated mass spectrometry (AMS-^{14}C) was carried out at the Center for Isotopic Research on the Cultural and Environmental heritage (CIRCE) laboratory (Terrasi et al., 2008) of the Second University of Naples. All AMS-^{14}C ages were calibrated according to the INTCAL13 dataset (Reimer et al., 2013) using the CalPal software (Weninger and Jöris, 2008). The method of multiple-group calibration was used to graphically represent and compare calibrated AMS-^{14}C ages (Weninger, 1986).

4 Results

4.1 Field description

The ~~calcrete~~soil profile, here studied, corresponds to the section of the wall of the pit 151A, an archaeological feature related to the Mesolithic use of the site (8650-8250 cal. BP (Salvatori et al., 2011; Salvatori, 2012)), excavated on top of a fluvial sand~~y~~ ridge. ~~Calcrete horizon is established at about 30 cm under the current surface level.~~ In the area of Al Khiday, pedosedimentary sequences generally correspond to poorly weathered soils interlayered to sandy to silty sediments, eventually disturbed by anthropic activities (Buursink, 1971); the sequences are interpreted as fluvial deposits related to an Upper Pleistocene higher level of the White Nile (Zerboni, 2011). The general aspect of a typical soil profile consists of a sandy to silty top horizon, enriched of calcium carbonate in form of nodules (Bk) horizon, lying on a BC horizon~~with no or very poor evidence for pedogenesis~~. An abrupt limit (possibly erosional) marks the transition to the following 2Bk horizon ~~(the calcrete)~~, which consists of medium to coarse sand, sometimes including lenses of coarser grains (very coarse sand to small pebbles), deeply cemented by calcium carbonate; this buried petrocalcic horizon can be interpreted as a former calcrete. Beneath, there is a sequence of fluvial to lacustrine fine sediments (silt and sand), with few $CaCO_3$ nodules in the upper part (for a complete description see Williams et al., 2015).

At the sampling point, the pedostratigraphy is ~~slightly more complex~~very clear (Fig. 3~~), ~~):~~since~~ two distinct calcium carbonate-rich~~calcrete~~ horizons, separated by a sandy layer, can be observed. ~~The calcitic horizon (Bk), up to 1 m thick, is nodular and can be interpreted as an early stage of calcrete development in soil profile (Machette, 1985; Wright, 2007), resulting from the illuvial concentration of calcium carbonate in a siliciclastic host material (quartz sand and silt). Two main concentrations of calcium carbonate were identified. ~~The uppermost Bk horizon~~ part of the section, namely block~~ (sampling point A1)~~,~~ is constituted by quartz sand slightly cemented by calcium carbonate; calcite concentration within the sediments is detected as coalescent irregular calcitic nodules of few centimetres in diameter. A weakly cemented sandy ~~lens~~BC horizon~~,~~ (sampling point ~~corresponding to block ~~A2)~~,~~ is interposed between the first ~~(A1)~~Bk horizon and ~~the ~~a second concentration of calcium carbonate, corresponding to the lower part of the section (~~namely~~ sampling points~~from~~ A3a, A3b, A3c and ~~to ~~A3d~~ blocks~~). This deepest calcitic horizon (2Bk), up to 0.7 m thick, is nodular and can be interpreted as an early stage of calcrete development in soil profile (Machette, 1985; Wright, 2007), resulting from the illuvial concentration of calcium carbonate in a siliciclastic host material (quartz sand and silt). It is formed by cemented quartz sand and carbonate concretions, where calcitic nodules can be distinguished. Abundance of carbonate concretions as well as cementation increases with depth. From the pedological point of view, this evidence ~~can be interpreted as a single calcrete, rather than~~represents a sequence of distinct calcitic horizons~~, since calcrete developed~~ on ~~the same~~distinct parent materials, probably resulting from a ~~long-lasting~~discontinuous pedogenetic process and alternated sedimentary events. ~~(Wright, 2007).~~ The ~~calcrete~~ Bk horizon, as observed in the archaeological area and in naturally exposed sections is at about ~~30~~20-50 cm depth from the current surface level. In correspondence of site 16-D-4 the close relationship between calcitic pedofeatures~~calcrete~~ and archaeological features of different ages can provide further evidence on the timing of calcium carbonate ~~calcrete~~ development. Calcitic concretions ~~Calcrete~~ partially embed~~s~~ human bones belonging to the pre-Mesolithic burial phase, the most ancient attested at the site (Fig. ~~1a~~2a), whereas Mesolithic pits (Fig. ~~1b~~2b) and Meroitic graves (Fig. ~~1c~~2c) are cut into it. Nevertheless, pre-Mesolithic and Neolithic bones were found to be permeated by secondary calcite, whereas the Meroitic bones, belonging to the most recent burial phase were not affected by pedogenetic precipitation of calcite (Dal Sasso et al., 2014b; Dal Sasso et al., 2016; Dal Sasso et al., 2018). In addition, the lower part of most of the Mesolithic pits is characterized by filling material cemented by calcium carbonate; in particular, some pits, used as fireplaces, present a significant amount of whitish and hard calcitic concretion encrusting the archaeological materials. The same evidence of calcitic concretions embedding human and animal remains in archaeological contexts has been described elsewhere in Sudan, as on the Singa calvaria (McDermott et al., 1996), at Abu Hugar (Whiteman, 1971), and elsewhere in the Gezira (Adamson et al., 1982). The origin of this calcitic cement can be associated to the processes involved in calcrete development; however, the rather high level of cementation must imply a contribution to the total amount of calcite coming from the recrystallization of the abundant remains of Ca-rich wood ash (Canti, 2003) originally constituting the upper part of the pit infilling (Zerboni, 2011).

4.2 Micromorphology of thin sections

Thin sections ~~of the blocks (A1 and A2)~~ from the upper part of the ~~calcrete (Bk horizon)~~soil profile (A1 and A2 samples) show a groundmass with abundant sand- and silt-sized quartz grains, sub-rounded to sub-angular in shape, with a bimodal grain-size distribution. The authigenic calcite is heterogeneously distributed (in shape of nodules, coatings, and infillings) among the sections giving to the slides a single- to double-spaced porphyric c/f (coarse/fine) related distribution, locally open porphyric or gefuric. In the uppermost Bk horizon, ~~A~~areas corresponding to typical calcitic nodules, macroscopically identified, show a micromass mainly constituted by micrite and microsparite (Fig. 4a), much more abundant with respect to that observed for other portions of the poorly cemented samples (Fig. 4c). Allochthonous, well-rounded calcitic pedorelicts (Fig. 4b, 5c, 5d), comparable in size with sandy quartz grains, are frequent. They are constituted by a micritic matrix stained by Mn and Fe oxides/hydroxides, and contain veins of sparitic to micro-sparitic calcite, generally occurring within this kind of pedofeatures (Fig. 5c, 5d).

Samples from the upper units also evidenced the occasional occurrence of wood ash (calcite pseudomorphs after calcium oxalate crystals (Canti, 2003)), fish bone fragments and small charcoals (Fig. 4d). Anthropogenic features were observed in small localised areas of the thin section (Fig. 4d), and possibly migrated from the infilling of the nearby Mesolithic pit, due to intense bioturbation (Zerboni, 2011). SEM analysis on calcitic nodules from the~~se units~~ Bk horizon revealed that the microsparitic groundmass is heterogeneous in terms of compositions and cementation degree: some areas are characterized by densely packed calcite crystals (Fig. 6a) with respect of other areas, where a loose calcite crystals distribution is observed (Fig. 6c). In other areas, calcite crystals occur within a clayey matrix (Fig. 6b). The great heterogeneity in terms of calcite crystals distribution is detected also by CL, where the microsparitic micromass appears with an orange luminescence, whose intensity is proportional to the density of calcite crystals (Fig. 5a). Poorly cemented areas are characterized by low luminescence due to scarcity or lack of calcite in the matrix (Fig 5b).

Thin sections from the lower 2Bk horizon (samples A3a, A3b, A3c, A3d) show areas characterized by slightly cemented quartz grains, sub-rounded to sub-angular in shape, and sand- and silt-sized, embedded into a micritic micromass (Fig. 4e). The distribution of mineral grains and calcite generally results in a single spaced to open porphyric, occasionally gefuric, c/f related distribution.

Conversely, highly carbonated areas (Fig. 4f, 4g), corresponding to older calcitic nodules embedded in the micritic micromass, are predominantly constituted by microsparitic calcite, and quartz sand grains are extremely rare. Different textural pedofeatures were identified within calcitic nodules: some portions are characterized by well-cemented calcite crystals forming hard nodules (hereafter called cemented nodules) of sub-rounded to sub-angular shape, identifiable by OM (Fig. 4f, 4g), CL (Fig. 5e) and SEM (Fig 6e, 6f) analyses. These features (Fig. 7) are embedded in a loose matrix mainly constituted by calcite crystals similar in size, but less packed than in the cemented nodules, sometimes associated to clay minerals. Towards the bottom of the ~~calcrete~~2Bk horizon, the dimension of ~~calcitic~~ calcitic-cemented nodules decrease and their margins, in contact with the surrounding matrix, are less defined (Fig. 5f). CL analysis indicates a significant, but not systematic, luminescence variations of calcite crystals along the section, both dispersed and well packed. In some cases, homogeneously luminescent crystals were observed (Fig. 5g), whereas in others the innermost part of crystals is less luminescent with respect to their margins and inter-grain cement (Fig. 5h). OM, CL, and especially SEM images show an overall increase of calcite crystal size from the upper to the lower Bk horizon. Allochthonous calcitic pedorelicts, sub-rounded in shape and permeated by Fe oxides/hydroxides (different from the Mn and Fe-bearing oxides/hydroxides permeating the rounded grains identified in the upper unit) were observed in unit A3c and, less frequently, in unit A3d. Both the two types of pedorelicts show a high concentration of oxides near their margins and a thin layer of clay minerals coating the outer surface (Fig. 4h, 6d).

4.3 Chemical and physical analyses

Tab. 1 and Fig. 3 illustrate the results of chemical analyses on soil samples. Calcium carbonate equivalent content and pH show similar trends, being the latter generally basic and buffered by the high content of carbonates; the B horizon is the less rich in carbonate. Humified organic carbon contents show trends antithetic of $CaCO_3$ content and the highest peak in organics (B horizon) corresponds to the less basic horizon. LOI result indicates a higher content of organics in the lowermost part, possibly suggesting a lower preservation of organic matter in the uppermost part of the sequence, where in fact humified carbon is more abundant. TC content is mainly ruled by the occurrence of calcium carbonate, whereas TN variations corresponds to the variation of the humified carbon, confirming that organic matter is the main source of nitrogen.

4.3 4 AMS-^{14}C dating

Due to the lack of well identifiable organics in the soil matrix, AMS-^{14}C radiocarbon dating was performed on different calcium carbonate-bearing pedofeatures, identified by micro-morphological analysis, and mechanically selected under the stereographic stereoscopic microscope. As for the uppermost Bk horizon (A1 sampling point, Fig. 3) units, calcitic nodules, constituted by micritic/microsparitic micromass (as shown in Fig. 4a) were identified in the massive sample as powdery aggregates, up to 1 cm in size. A fraction of micritic/microsparitic micromass was selected for radiocarbon dating (A1-mt samples). allochthonous Allochthonous pedorelicts (A1-pedorelict) and calcitic nodules (A1-mt) from unit A1 were also selected from the same sampling point (A1) and dated.

In As for the lower unit2Bk horizon, micromorphological analyses of calcitic nodules (up to 2 cm in size) showed the occurrence of different textural pedofeatures, previously addressed as cemented nodules and loose calcitic-rich matrix (as shown in Fig. 4f, 4g and 5e). In Fig. 7, OM photomicrographs and the segmented false-colour image show a representative example of the relationship between these pedofeatures. On the massive samples, cemented nodules identified in thin sections were found to be much more lithified than the surrounding loose calcitic-rich matrix, therefore, after a gentle disaggregation of the samples, these two adjoining pedofeatures were effectively separated by hand-picking under a stereoscopic microscope. and were supposed to be less prone to the re-opening of the carbon system. This sampling strategy was then applied to massive samples collected at A3a, A3c and A3d points (Fig.3), so that for each of them cemented nodules (labelled as A3a-cn, A3c-cn and A3d-cn) and calcitic-rich matrix (labelled as A3a-mt, A3c-mt and A3d-mt) samples were selected for radiocarbon dating. ~~Therefore, three samples of cemented nodules (A3a-cn, A3c-cn and A3d-cn) and three samples of calcitic-rich matrix (A3a-mt, A3c-mt and A3d-mt) from blocks A3a, A3c, and A3d, respectively, were selected and dated.~~ As expected, an old radiocarbon age, 29540 ± 440 cal. years BP, was obtained for the allochthonous pedorelicts (A1-pedorelict). The cemented nodules from ~~blocks~~ A3a, A3c and A3d sampling points show older ages (9620 ± 100, 9900 ± 580 and 11480 ± 240 cal. years BP for~~,~~ A3a-cn, A3c-cn and A3d-cn, respectively) with respect to the nearby loose calcitic-rich matrix (6340 ± 80, 7920 ± 100 and 7730 ± 80 cal. years BP for A3a-mt, A3c-mt and A3d-mt, respectively) and from the calcitic nodules ~~of~~ from A1 ~~block~~ sampling point (6080 ± 240 cal. years BP) (Tab. ~~1~~2, Fig. ~~7a~~8a, 9a).

Apart from a single radiocarbon age dating to the Upper Pleistocene (for the allochthonous pedorelict), the radiocarbon dates are Holocene in age and can be tentatively clustered to the Early and Middle-Holocene~~;~~ . ~~statistical~~ Statistical treatment of dating results can better delineate the distribution of radiocarbon ages on the ~~calcrete samples~~sampled calcitic horizons. The method of multiple-group calibration (Weninger, 1986; Weninger and Jöris, 2008) was used to represent radiocarbon ages, in order to discern if close radiocarbon ages might refer to the same or different pedogenetic phases as well as to ease the comparison with other regional radiocarbon age datasets. ~~More in detail,~~Our AMS-^{14}C ages on carbonates were compared (Fig. 7) with the ^{14}C ages obtained on calcium carbonate deposits in soils from Central Sudan (Adamson et al., 1982), and ~~, mostly obtained~~ on fossil shells (Williams, 2009; Williams et al., 2015)~~,~~ The latter ages ~~indicating~~ indicates the late Quaternary high flow levels of the White Nile, representing ~~(which is~~ a proxy for wetter climatic conditions.~~), and with~~ In Fig.7 the radiometric chronology of the Holocene human occupation of the Al Khiday archaeological sites (Salvatori et al., 2011) is also reported ~~(Fig. 7)~~. A further, indirect piece of the chronological puzzle of calcrete development at Al Khiday is represented by the radiometric dating of the archaeological structures cutting the carbonatic crusts; most of them belong to the Mesolithic phase and date to the 8650-8250 cal years BP.

4.~~4.~~5 Stable isotopes analysis

C and O stable isotope analyses were carried out on an aliquot from the same samples that were radiocarbon dated; moreover, ~~for each calcrete block along the section,~~ additional samples of calcitic nodules from A1 and ~~of the~~ cemented nodules (cn) and calcitic-rich ~~loose~~ matrix (mt) from A3a, A3b, A3c and A3d sampling points (Fig. 3) were separately selected and analysed (Tab. ~~1~~2). Overall $\delta^{18}O$ ranges between -8.27‰ and -1.85‰ (V-PDB) and $\delta^{13}C$ between -1.48‰ and 1.06‰ (V-PDB). $\delta^{13}C$ values show a narrow range of variation and no significant differences were observed between cemented nodule and matrix samples. Conversely, a wider range of variation was observed for $\delta^{18}O$, with matrix samples showing more negative values with respect to cemented nodules (Tab. ~~1~~2, Fig. ~~8~~9b, 9c). A good consistency was observed between results obtained from the same samples double-measured, in particular for those from the matrix samples.

5 Discussion

~~5.1 Origin of calcium carbonate and calcrete formation~~

The authigenic accumulation of calcium carbonate in siliciclastic host sediments, composed of quartz sand lacking in calcite, indicates an external source for calcium carbonate. Conceivable sources may be identified in the geological bedrock of the area, as the limited quantity of calcite, occurring in the local sandstone and shale~~s~~, is firstly dissolved, then mobilized and finally re-precipitated thanks to circulating pore water. Further significant sources of carbonate may be represented by alkaline atmospheric dust and calcium carbonate precipitated over a long period in the Pleistocene lake sediments identified in the region (Williams et al., 2015). Similar sources of carbonates have been claimed by ~~(~~Cremaschi et al.~~,~~ (2010) to explain the origin of spring calcareous tufa in a sandstone-bearing central Saharan massif. Less important contributions are likely those from the Nile overbank sediments, and from the anthropogenic calcitic ash related to the Mesolithic occupation of the site, the latter being available only after the onset of pedogenetic processes related to the formation of calcrete. Moreover, the dissolution and mobilization of calcium carbonate accumulated in pre-existent Pleistocene Fe-enriched paleosols, which are highly cemented and heavily affected by pedogenesis (Fig. ~~1d~~2d), may have contributed to the formation of the calcrete horizon at 16D4 site. However, the origin of calcium carbonate in these paleosols is not well-defined and its accumulation likely results from long-lasting processes of dissolution/reprecipitation of calcite, possibly mediated by biological activity. Evidence of this type of paleosols, widely outcropping in the region (Zerboni et al., 2016), can be also found few hundred meters west from the 16D4 site. These Pleistocene paleosols are also the most probable source of the pedorelicts identified in the calcrete section (those separated from ~~block~~ sample A1 and dated to the 29540 ± 440 cal. years BP). In fact, they probably derive from surface transportation, as suggested by their sub-rounded to rounded shape and by the occurrence of clayey material coating their external surface, which can be interpreted as a rolled pedofeature (Zerboni, 2011). Also Adamson et al. (1982) obtained Upper Pleistocene dating on rolled carbonates, suggesting their single or multistep reworking of older carbonate-impregnated clays and silts from former soils.

~~Calcrete~~ Calcitic nodules formed since the accumulation of microcrystalline calcite; the small size of crystals suggests a relatively fast precipitation of calcite, associated with high rates of evapotranspiration. In this case, the contribution of microbially induced calcite precipitation is assumed to be minimal, as micromorphological features characteristic of biological activity (Newman et al., 1997; Richter et al., 2008) are not observed. The upper Bk horizon is characterized by weak cementation and nodules are formed by microcrystalline calcite precipitated in the porosity between sand- and silt-sized quartz grains. The lower 2Bk horizon shows a significant increase in the accumulation of calcium carbonate and the formation of larger ~~nodules~~concretions. The occurrence of very few quartz grains much more dispersed in the microsparitic groundmass within nodules, with respect to those observed in less cemented portions of the sample, may indicates a displacive calcite crystal growth (Armenteros, 2010). Moreover, higher permeating cementation of sediments was observed in this unit~~.~~, thus ~~This may~~ representing ~~a~~ subsequent development stages of ~~calcrete~~ the calcitic horizon~~;~~. ~~however~~However, features characteristic of successive stages of calcite precipitation/recrystallization observed in ~~more~~ well-developed calcrete profiles (Wright, 2007) are lacking in our case study, thus suggesting an intermediate development stage for ~~this calcrete~~calcitic horizons. At Al Khiday, Bk and 2Bk horizons ~~It~~ can be described as ~~a~~ nodular calcitic horizons as suggested by Alonso-Zarza and Wright (Alonso-Zarza and Wright, 2010), or at least ~~and~~ comparable to a Stage III of calcrete development (Machette, 1985).

Cathodoluminescence of carbonates, in terms of colours and intensities, is mainly attributed to the occurrence of Mn^{2+} and Fe^{2+} ions in trace quantity in the calcite crystal structure, which, in turn, is related to geochemical conditions during precipitation. Therefore, even if only qualitatively, luminescence variations of calcite crystals observed in CL images indicates variations in the chemical composition and/or redox conditions during precipitation and subsequent recrystallization (Hiatt and Pufahl, 2014). These data, coupled with information on the diachronic interaction between calcrete horizon and archaeological records, indicate that calcrete formation and subsequent development is a long-lasting and discontinuous multi-step process, acting at least since the Early Holocene. Notwithstanding the evidence of ~~calcrete formation~~calcite accumulation ~~o~~in Late Pleistocene fluvial sediments, the widespread occurrence of calcium carbonate features in paleosols and sediments of the region, may suggest that environmental conditions suitable for calcite mobilization, redistribution and precipitation in soils ~~form of calcrete~~ may have occurred many times since the Pleistocene, as described also elsewhere in North Africa (Szabo et al., 1995; Brookes, 2010; Zerboni et al., 2011). Yet, Adamson et al. (1982) suggest multiple events of carbonate dissolution and precipitations in soil and sediments of Central Sudan since the Late Pleistocene and probably earlier.

On these bases, timing the formation and development of carbonate concretions in the soil profile by radiometric dating techniques requires an accurate sampling strategy and a careful evaluation of results.

~~**5.2 Timing of calcrete development**~~

Radiocarbon dating of calcrete and recrystallization-prone carbonates is not a routinely performed type of analysis, even if some studies are reported in literature (Wang et al., 1996; Geyh and Eitel, 1998; Deutz et al., 2002; Geyh and Thiedig, 2008; Vogel and Geyh, 2008; Achyuthan et al., 2010). In fact, AMS-^{14}C dating of calcite forming calcrete horizons might not lead to a straightforward interpretation of results. When calcite precipitates, its ^{14}C activity is in equilibrium to that of circulating pore water, which, in turn, may not be in equilibrium with atmospheric CO_2 due to the so defined "reservoir effect" (Geyh and Eitel, 1998). This can cause an overestimation of the actual age of calcium carbonate. Moreover, when dissolution and recrystallization occurs, ^{14}C activity of former calcite is then superimposed to that of the new-generated calcite, in equilibrium with pore water circulating at that time (Geyh and Eitel, 1998). Notwithstanding that, Adamson et al. (1982) conclude that Sudanese soil carbonates are fairly suitable materials for dating. They are also aware of the ineluctability of contamination from some of the older carbonates in some cases; we may confirm this and highlight also the possibility of contamination from younger calcite precipitated after the climate-driven re-opening of the system.

Despite these difficulties, in our case study, the well-defined geomorphological, palaeoenvironmental, and archaeological contexts provide valuable information to estimate the consistency of radiocarbon ages on calcrete samples. Moreover, some of these issues can be overcome by the very low amount (~ 10 mg) of sample required by AMS-^{14}C dating, enabling one to apply an accurate sampling strategy on small portions of the sample, thus separately analysing calcite precipitated in a single pedogenetic event. In this case, the reservoir effect is assumed to be minimal, since circulating pore water is more conceivably provided by the White Nile flooding and, during the Early Holocene, by rainwater rather than fossil groundwater (Dee et al., 2010). In addition to the superficial location of the ~~calcrete~~ calcitic horizons, the high values of $\delta^{13}C$, measured both on cemented nodule and matrix samples, suggest the predominant contribution of atmospheric CO_2 as a source of CO_2 to the groundwater, whereas the contribution of plant-sourced

CO_2 can be considered minimal, thus suggesting a sparse vegetation cover (Cerling, 1984; Burns and Matter, 1995; Deutz et al., 2001) during the phases of precipitation.

The main issue that has to be taken into account when dealing with radiocarbon dating on pedogenic calcite is the overprinting effect, which is not negligible (Deutz et al., 2002). Calcitic horizons and ~~C~~calcretes form~~s~~ over time as results of subsequent dissolution and reprecipitation processes (e.g., ~~(~~Machette, 1985), thus ^{14}C activity is time averaged and determination of the time of actual onset of calcite precipitation may be hazardous. As a matter of fact, soil carbonates~~calcrete~~ can be reasonably considered an open system, implying environmental conditions that promote loops of calcite dissolution and reprecipitation. However, when changes in environmental conditions (mostly humidity) lead to the interruption of carbonate accumulation~~calcrete development~~, the closed system can be hypothesised. Therefore, radiocarbon ages of calcrete samples reasonably indicate the last stage of calcite recrystallization; this may provide valuable information on the timing of ~~calcrete~~ Bk horizons development. For these reasons, radiocarbon ages cannot be used according to sample stratigraphy to determine a linear sequence of depositional events~~ leading to calcrete formation~~; this is also obvious considering the complexity of this nonlinear and multistep process (Wright, 2007). However, micro-sampling should minimize the artificial homogenization of different generations of calcite, and thus radiocarbon ages may provide reliable information on the long ~~calcrete~~ soil carbonates evolution, even if each sample may still be partially affected by time-averaging blurring effect.

~~Before discussing the significance of the most of radiocarbon ages available for Al Khiday carbonates on the basis of statistical analysis (Fig. 7), it is necessary to discuss the significance of the single result on allochthonous calcitic pedorelicts, radiocarbon dated to 29540 ± 440 cal. years BP. This sample can be interpreted as the reworked remnants of Pleistocene soil carbonates that were eroded and transported.~~

The considered sequence consists of superimposed calcitic soil horizons, which distinctly developed in phases of enhanced evapotranspiration; consequently, as suggested by Machete (1985), the development of calcitic horizons is a clue to their dissolution-precipitation history. According to the distribution of radiocarbon ages shown in Fig. 9a, the lower part of the sequence (2Bk horizons) may have been affected by old pedogenetic accumulation of calcium carbonate; then, after the burying of this soil and aggradation of the uppermost part of the pedosequence, a further phase of calcite accumulation took place. Its occurrence is recorded by the accumulation of calcitic pedofeatures in the uppermost Bk horizon and the recrystallization or freshly accumulation of calcite in the 2Bk horizon. The higher concentration of calcitic pedofeatures in the 2Bk horizon can be interpreted as the result of subsequent phases of precipitation and/or of a more intense initial accumulation.

As for authigenic calcite, in order to correlate the radiocarbon ages of different calcrete pedofeatures to the climatic conditions occurring in the area, radiocarbon dating results were compared with radiometric ages obtained by ~~(~~Adamson et al.~~,~~ (1982),~~;~~ Williams~~,~~ (2009), and~~;~~ Williams et al.~~,~~ (2015) in a cumulative graph of calibrated radiocarbon ages (Fig. ~~7~~8). Williams (2015) identified several Late Quaternary periods characterized by more humid climatic conditions, corresponding to higher flow level of the White Nile, Blue Nile, and main Nile ~~river~~River. These phases occurred at 14700–13100, 9700–9000, 7900–7600, ca. 6300, and 3200–2800 cal. years BP (Fig. ~~7b~~8c). On the bases of published data we may infer several phases of carbonates development at c. >30000, 26000–24200, 18200–13000, and 11000–9100 cal. years BP (Adamson et al., 1982); these ages were obtained on bulk carbonate samples, not separated between matrix and cemented nodules (Fig. 8b).

In this study, ~~T~~the oldest radiocarbon ages were obtained on cemented nodules from lower ~~blocks~~ sampling points A3d, A3c, and A3a (11480 ± 240, 9900 ± 580, and 9620 ± 100 cal. years BP, respectively), corresponding to dry climatic phases (Fig. ~~7~~8), according to palaeoenvironmental evidence provided by Williams (2009). These older ages have a quite good correspondence (Fig. 8b) with those obtained by Adamson et al. (1982). Younger radiocarbon ages, obtained from powdery calcitic-rich matrix ~~from~~ sampled at A3d and A3c ~~blocks~~ points (dated to 7730 ± 80 and

7920 ± 100 cal. years BP, respectively) as well as from calcitic-rich matrix ~~from~~ sampled at A3a ~~block~~ and from calcitic nodules ~~from~~ sampled at A1 ~~block~~ (dated to 6340 ± 80 and 6080 ± 240 cal. years BP, respectively), show a good agreement with two short periods characterized by more humid conditions, dated to 7900-7600 and about 6300 cal. BP (Williams, 2009; Williams et al., 2015), respectively (Fig. ~~7~~8).

Further evidence that cemented nodules and calcitic-rich matrix possibly formed under different conditions is provided by the stable isotope analysis, in particular by the significant variation of $\delta^{18}O$ values observed between cemented nodules and matrix samples (Fig. 9a, 9b). Variation in $\delta^{18}O$ values of calcrete samples generally reflects the variation in isotopic composition of meteoric water; however, the latter may not necessarily reflect a significant variation in $\delta^{18}O$ of rainfall. In fact, considering the available information on palaeoenvironmental conditions in this region, previously discussed, a $\delta^{18}O$ enrichment can also be due to evaporative enrichment due to high evapotranspiration rates (Cerling, 1984; Burns and Matter, 1995; Budd et al., 2002). Therefore, the higher $\delta^{18}O$ values measured on cemented nodules can indicate higher evapotranspiration rates related to drier environmental conditions during calcite precipitation. On the other hand, more negative $\delta^{18}O$ values, as those measured on matrix samples, can reflect the $\delta^{18}O$ signature of rainfall or at least a certain $\delta^{18}O$ depletion, triggered by higher rainfall intensity caused by a short-timed increase of monsoon intensity (Cerling, 1984; Burns and Matter, 1995; Andrews et al., 1998).

The consistency of these results suggests that during the Late Pleistocene and mostly initial Holocene a first onset of calcite precipitation occurred during dry climatic conditions, which is compatible with the formation of a thick calcitic horizon in the lower part of the sequence~~calcrete~~. The occurrence of a net moisture deficit in the vadose zone, as well as pore water saturated with respect to calcium carbonate, due to decreased precipitation and the reduction of the White Nile flow, possibly promoted the calcite precipitation. Subsequently, more humid climatic conditions in the Early and Middle Holocene led to partial dissolution of calcite, whereas a subsequent shift towards drier conditions caused the reprecipitation of calcite. Therefore, alternation of wet and dry periods triggered the partial dissolution and reprecipitation of calcite, leading to a progressive calcite accumulation. Cemented nodules may be interpreted as remnants of previously precipitated calcium carbonate, partially dissolved during subsequent humid periods and then reprecipitated as looser calcitic matrix. This hypothesis also suggests that ~~calcrete~~ carbonate pedogenesis occurred as a series of subsequent events of calcite dissolution and precipitation, discontinuously distributed along the Upper Pleistocene and Holocene, driven by local environmental conditions.

This interpretation is further supported by ~~the~~ archaeological evidence. Several burial phases were identified and attributed to different periods along the Holocene (Fig. ~~7~~8), whereas pits, dated to the Mesolithic period, were established after the pre-Mesolithic burial phase (the oldest one). Mesolithic pits were cut into the ~~calcrete~~ deeper calcitic horizon, whereas pre-Mesolithic and Neolithic human bones are permeated by secondary calcite. In the Meroitic bones, belonging to the most recent burial phase (dated to 2000-1700 cal. BP; (Usai et al., 2010)), pedogenetic calcite is absent, despite the fact that graves were cut within the calcrete horizon and placed deeper from the surface with respect to the older ones. On the basis of these evidence, the mobilization of calcite in the last 2000 years, a period characterized by semi-arid to arid climatic conditions (Gasse, 2000) and lower level of the White Nile (Williams, 2009), was negligible, indicating the occurrence of quiescent stages during calcrete development process under arid conditions, when the amount of circulating pore water is extremely limited.

6 Conclusions

In Central Sudan ~~calcrete~~, the formation of calcitic soil horizons was a long-lasting process and ~~its~~ their development ~~at the site 16D4~~ was significantly influenced by changes from humid to arid environmental conditions. Bk horizons ~~Calcrete was~~were characterized by alternate periods of growth due to dissolution and precipitation processes, and periods of quiescence or extremely slow growth rates. These events possibly occurred many times along the Quaternary, but the best~~-~~-preserved evidence is the one related to the Holocene. Despite the fact that radiocarbon dating of calcrete has severe limitations due to the uncertain determination of the contribution of ^{14}C by different sources, accurate sampling method coupled with additional information from a well-defined palaeoenvironmental context may provide a reliable interpretation of the sequence of events. A higher number of carefully selected radiocarbon-dated samples could supply a more statistically significant dataset for radiocarbon ages as well as highlight the variability of AMS-^{14}C determinations on this type of material. However, radiocarbon ages obtained in the present work confirm the general model for accumulation~~calcrete~~, formation and development of calcium carbonate in sediments/soil horizons established in previous studies (Gile et al., 1966; Machette, 1985; Khormali et al., 2006; Zhou and Chafetz, 2009), suggesting a progressive accumulation of calcium carbonate within sediments/soil horizons.

Specifically for this context, the interest in deciphering the relationship between ~~calcrete~~ carbonates pedogenesis and archaeological records concerns the evaluation of the interaction between secondary calcite and archaeological materials. In fact, the occurrence of secondary calcite in archaeological materials may represent a complex issue in all those cases in which calcite may alter conventional radiocarbon dates. An example can be, in the specific case, represented by the radiocarbon dating of archaeological bones performed on bioapatite (the mineral fraction of bone material) (Zazzo, 2014). Calcite is therefore a significant contaminant when measuring ^{14}C activity of bioapatite; despite the chemical removal of secondary calcite, the radiocarbon ages obtained (Dal Sasso, 2015) are in good agreement with those obtained on pedogenic calcite~~calcrete~~, thus resulting substantially younger than those hypothesized on the basis of archaeological and stratigraphic evidences (Fig. ~~7c~~8d). Since bioapatite is not a closed system with respect to the environment (Cherkinsky, 2009), carbonate exchange between calcite and bioapatite during burial may significantly affect the result when dating the archaeological bones. Therefore, the study of soil sediments and burial environment is fundamental in order to assess the reliability of radiocarbon ages. A further example of the importance of understanding the time and steps of calcrete genesis in archaeological context concerns the applicability of luminescence dating on archaeological material (pottery); in fact, the dose rate of Thermoluminescence (TL) is heavily tuned by environmental humidity and radiation, and the carbonate content of sediments may influence water mobilization and change the natural radiation due to the increase of uranium occasionally substituting calcium in calcite crystals. In TL dating, radiation is generally supposed to be constant over time, but irregular development of calcrete through time may consistently vary the environmental radioactivity after the burial of archaeological material (Wintle and Murray, 2006).

This study highlights the relevance of a multi-analytical approach to the study of ~~calcrete~~ carbonates pedogenesis. Specifically for this case, a comprehensive study on the interaction between the archaeological record and the calcrete formation and development supplies valuable information both on the processes and timing of ~~calcrete~~ carbonates pedogenesis and on the preservation state of archaeological materials.

Considering a wider perspective, the results of this study may represent a further step in the comprehension of ~~calcrete~~ calcitic horizons formation and in the definition of a reliable method to date ~~its~~ their formation. This may offer a significant tool in palaeoenvironmental studies in arid lands, where carbonatic ~~crust~~ concretions may represent the only archive for past climatic changes~~.~~; in fact, several authors had highlighted the correspondence (climofunction, *sensu* ~~(~~Jenny~~,~~ (1941) between depth of Bk horizons and precipitations (e.g., ~~(~~Yaalon, 1983; Mack and James, 1992; Caudill et al., 1996; Retallack, 2000; Retallack, 2005), being horizon's depth the results of the average amount of rainfall.

Acknowledgments

We are grateful to ~~Dr.~~ Sandro Salvatori, co-director of the "El Salha Archaeological Project", for the precious collaboration. We thank the Italian Ministry of Foreign Affairs and Centro Studi Sudanesi e sub-Sahariani (CSSeS) for funding the archaeological research. We thank the "National Corporation for Antiquities and Museums", Khartoum (Sudan), in particular the General Director

Abdelrahman Ali Mohamed for authorising the study of archaeological materials. We thank ~~prof.~~ Filippo Terrasi and ~~Dr.~~ Fabio Marzaioli (Second University of Naples) for their help for radiocarbon dating, ~~and~~ ~~prof.~~ Nereo Preto (University of Padua) for his help for stable isotope analyses, ~~.~~ Massimo Tiepolo and Enrico Cannaò (University of Milano) for their help with the OEA. Two anonymous reviewers and Associate Editor Frank McDermott are acknowledged for insightful comments on a preliminary version of the manuscript.

Conflict of Interest

The authors declare that they have no conflict of interest.

References

Achyuthan H., Flora O., Braida M., Shankar N. and Stenni B. (2010) Radiocarbon ages of pedogenic carbonate nodules from Coimbatore region, Tamil Nadu. *J. Geol. Soc. India* **75**, 791–798.

Adamson D. A., Gillespie R. and Williams M. A. J. (1982) Palaeogeography of the Gezira and of the lower Blue and White Nile valleys. In *A Land between Two Niles: Quaternary Geology and Biology of the Central Sudan* (eds. M. A. J. Williams and D. A. Adamson). Balkema, Rotterdam. pp. 165–219.

Alonso-Zarza A. M. and Wright V. P. (2010) Chapter 5 Calcretes. In *Developments in Sedimentology* (eds. A. M. Alonso-Zarza and L. H. Tanner). Elsevier B.V. pp. 225–267. Available at: http://linkinghub.elsevier.com/retrieve/pii/S0070457109061056.

Andrews J. E., Singhvi A. K., Kailath A. J., Kuhn R., Dennis P. F., Tandon S. K. and Dhir R. P. (1998) Do Stable Isotope Data from Calcrete Record Late Pleistocene Monsoonal Climate Variation in the Thar Desert of India? *Quat. Res.* **50**, 240–251. Available at: http://www.sciencedirect.com/science/article/B6WPN-45M3173-5/1/f846d4a9d1da466792c556c2d9b72dfa%5Cnhttp://linkinghub.elsevier.com/retrieve/pii/S0033589498920026.

Armenteros I. (2010) Diagenesis of Carbonates in Continental Settings. In *Developments in Sedimentology* (eds. A. M. Alonso-Zarza and L. H. Tanner). pp. 61–151. Available at: http://linkinghub.elsevier.com/retrieve/pii/S0070457109062025.

Blokhius W. A., Ochtman L. H. J. and Peters K. H. (1964) Vertisols in the Gezira and the Khashm el Girba clay pan. *Soil Sci.* **5**, 591–603.

Blokhius W. A., Pape T. and Slager S. (1968) Morphology and distribution of pedogenic carbonate in some Vertisols of the Sudan. *Geoderma* **2**, 173–200.

Brookes I. A. (2010) Spatially variable sedimentary responses to orbitally driven pluvial climate during Marine Oxygen Isotope Stage 5.1, Dakhla Oasis region, Egypt. *Quat. Res.* **74**, 252–264.

Available at: http://dx.doi.org/10.1016/j.yqres.2010.05.001.

Budd D. a, Pack S. M. and Fogel M. L. (2002) The destruction of paleoclimatic isotopic signals in Pleistocene carbonate soil nodules of Western Australia. *Palaeogeogr. Palaeoclimatol. Palaeoecol.* **188**, 249–273.

Bullock P., Fedoroff N., Jongerius A., Stoops G., Tursina T. and Babel U. (1985) *Handbook for Soil Thin Section Description*., Waine Research Publication, Albrighton.

Burns S. J. and Matter A. (1995) Geochemistry of Carbonate Cements in Surficial Alluvial Conglomerates and their Paleoclimatic Implications, Sultanate of Oman. *SEPM J. Sediment. Res.* **Vol. 65A**. Available at: http://jsedres.sepmonline.org/cgi/doi/10.1306/D426805E-2B26-11D7-8648000102C1865D.

Buursink J. (1971) Soils of the central Sudan. .

Cailleau G., Braissant O. and Verrecchia E. P. (2011) Turning sunlight into stone: The oxalate-carbonate pathway in a tropical tree ecosystem. *Biogeosciences* **8**, 1755–1767.

Canti M. G. (2003) Aspects of the chemical and microscopic characteristics of plant ashes found in archaeological soils. *Catena* **54**, 339–361.

Caudill M. R., Driese S. G. and Mora C. I. (1996) Preservation of a proto-Vertisol and an estimate of Late Mississippian paleoprecipitation. *J. Sediment. Res.* **A66**, 58–70.

Cerling T. E. (1984) The stable isotopic composition of modern soil carbonate and its relationship to climate. *Earth Planet. Sci. Lett.* **71**, 229–240. Available at: http://linkinghub.elsevier.com/retrieve/pii/0012821X8490089X.

Cherkinsky A. (2009) Can We Get a Good Radiocarbon Age from “Bad Bone”? Determining the Reliability of Radiocarbon Age from Bioapatite. *Radiocarbon* **51**, 647–655. Available at: https://www.cambridge.org/core/product/identifier/S0033822200055995/type/journal_article.

Cremaschi M., Zerboni A., Spötl C. and Felletti F. (2010) The calcareous tufa in the Tadrart Acacus Mt. (SW Fezzan, Libya). *Palaeogeogr. Palaeoclimatol. Palaeoecol.* **287**, 81–94. Available at: http://linkinghub.elsevier.com/retrieve/pii/S0031018210000313.

Dal Sasso G. (2015) Characterization of archaeological bones from the Al Khiday cemetery (Central Sudan): structure and microstructure of diagenetically altered bioapatite. Università degli Studi di Padova.

Dal Sasso G., Angelini I., Maritan L. and Artioli G. (2018) Raman hyperspectral imaging as an effective and highly informative tool to study the diagenetic alteration of fossil bones. *Talanta* **179**, 167–176. Available at: http://dx.doi.org/10.1016/j.talanta.2017.10.059.

Dal Sasso G., Lebon M., Angelini I., Maritan L., Usai D. and Artioli G. (2016) Bone diagenesis variability among multiple burial phases at Al Khiday (Sudan) investigated by ATR-FTIR spectroscopy. *Palaeogeogr. Palaeoclimatol. Palaeoecol.* **463**, 168–179. Available at: http://linkinghub.elsevier.com/retrieve/pii/S0031018216305569.

Dal Sasso G., Maritan L., Salvatori S., Mazzoli C. and Artioli G. (2014a) Discriminating pottery production by image analysis: A case study of Mesolithic and Neolithic pottery from Al Khiday (Khartoum, Sudan). *J. Archaeol. Sci.* **46**, 125–143. Available at: http://dx.doi.org/10.1016/j.jas.2014.03.004.

Dal Sasso G., Maritan L., Usai D., Angelini I. and Artioli G. (2014b) Bone diagenesis at the micro-scale: Bone alteration patterns during multiple burial phases at Al Khiday (Khartoum, Sudan) between the Early Holocene and the II century AD. *Palaeogeogr. Palaeoclimatol. Palaeoecol.* **416**, 30–42. Available at: http://dx.doi.org/10.1016/j.palaeo.2014.06.034.

Dee M. W., Brock F., Harris S. A., Ramsey C. B., Shortland A. J., Higham T. F. G. and Rowland J. M. (2010) Investigating the likelihood of a reservoir offset in the radiocarbon record for ancient Egypt. *J. Archaeol. Sci.* **37**, 687–693. Available at: http://dx.doi.org/10.1016/j.jas.2009.09.003.

Deutz P., Montanez I. P. and Monger H. C. (2002) Morphology and Stable and Radiogenic Isotope Composition of Pedogenic Carbonates in Late Quaternary Relict Soils, New Mexico, U.S.A.: An Integrated Record of Pedogenic Overprinting. *J. Sediment. Res.* **72**, 809–822. Available at: http://jsedres.sepmonline.org/cgi/doi/10.1306/040102720809.

Deutz P., Montañez I. P., Monger H. C. and Morrison J. (2001) Morphology and isotope heterogeneity of Late Quaternary pedogenic carbonates: Implications for paleosol carbonates as paleoenvironmental proxies. *Palaeogeogr. Palaeoclimatol. Palaeoecol.* **166**, 293–317.

Durand N., Monger C. H. and Canti M. G. (2010) Calcium Carbonate Features. In *Interpretation of Micromorphological Features of Soils and Regoliths* (eds. G. Stoops, V. Marcelino, and F. Mees). Elsevier B.V. pp. 149–194. Available at: http://dx.doi.org/10.1016/B978-0-444-53156-8.00009-X.

El-Tom M. A. (1975) *The rains od the Sudan*., Khartoum University Press, Khartoum.

Elagib N. A. and Mansell M. G. (2000) Recent trends and anomalies in mean seasonal and annual temperatures over Sudan. *J. Arid Environ.* **45**, 263–288. Available at: http://www.idealibrary.com.

Gaballo V. (2009) Studio di reperti osteologici provenienti dalla necropoli 16-D-4 (Sudan) attraverso analisi spettroscopiche e spettrochimiche. Università degli Studi di Parma.

Gasse F. (2000) Hydrological changes in the African tropics since the Last Glacial Maximum. *Quat. Sci. Rev.* **19**, 189–211.

Gatto M. C. and Zerboni A. (2015) Holocene Supra-Regional Environmental Changes as Trigger for Major Socio-Cultural Processes in Northeastern Africa and the Sahara. *African Archaeol. Rev.* **32**, 301–333. Available at: http://link.springer.com/10.1007/s10437-015-9191-x.

Geyh M. A. and Eitel B. (1998) Radiometric dating of young and old calcrete. *Radiocarbon* **40**, 795–802.

Geyh M. A. and Thiedig F. (2008) The Middle Pleistocene Al Mahrúqah Formation in the Murzuq Basin, northern Sahara, Libya evidence for orbitally-forced humid episodes during the last 500,000 years. *Palaeogeogr. Palaeoclimatol. Palaeoecol.* **257**, 1–21.

Gile L. H., Peterson F. F. and Grossman R. B. (1966) Morphological and Genetic Sequences of Carbonate Accumulation in Desert Soils. *Soil Sci.* **101**, 347–360.

Gile L. H., Peterson F. F. and Grossman R. B. (1965) The K horizon: a master soil horizon of carbonate accumulation. *Soil Sci.* **99**, 74–82.

Heiri O., Lotter A. F. and Lemcke G. (2001) Loss on ignition as a method for estimating organic and carbonate content in sediments: Reproducibility and comparability of results. *J. Paleolimnol.* **25**, 101–110. Available at: http://link.springer.com/10.1023/A:1008119611481.

Hiatt E. E. and Pufahl P. K. (2014) Cathodoluminescence petrography of carbonate rocks: a review of applications for understanding diagenesis, reservoir quality, and pore system evolution. In *Cathodoluminescence and its application to geoscience* (ed. I. M. Coulson). Mineralogical Association of Canada short course, Fredericton NB. pp. 75–96.

Iacumin P., Di Matteo A., Usai D., Salvatori S. and Venturelli G. (2016) Stable isotope study on ancient populations of central sudan: Insights on their diet and environment. *Am. J. Phys. Anthropol.* **160**, 498–518.

Jakob T. (2014) A Bioarchaeological Appraisal of the Human Skeletal Remains from e l-Khiday 2, Central Sudan. In *The Fourth Cataract and Beyond. Proceedings of the 12th International Conference for Nubian Studies* (eds. J. R. Anderson and D. A. Welsby). Peeters Publishers, Leuven. pp. 271–277.

Jenny H. J. (1941) *Factors of soil formation*., McGraw-Hill, New York.

Khormali F., Abtahi A. and Stoops G. (2006) Micromorphology of calcitic features in highly calcareous soils of Fars Province, Southern Iran. *Geoderma* **132**, 31–46.

Machette M. N. (1985) Calcitic soils of the southwestern United States. *Geol. Soc. Am. Spec. Pap.* **203**, 1–22.

Mack G. H. and James W. C. (1992) Calcic paleosols of the Plio-Pleistocene Camp Rice and Palomas Formations, southern Rio Grande rift, USA. *Sediment. Geol.* **77**, 89–109. Available at: http://linkinghub.elsevier.com/retrieve/pii/003707389290105Z.

Mack G. H., James W. C. and Monger H. C. (1993) Classification of paleosols. *Geol. Soc. Am. Bull.* **105**, 129–136. Available at: https://pubs.geoscienceworld.org/gsabulletin/article/105/2/129-136/182768.

Maritan L., Iacumin P., Zerboni A., Venturelli G., Dal Sasso G., Linseele V., Talamo S., Salvatori S. and Usai D. (2018) Fish and salt: The successful recipe of White Nile Mesolithic hunter-gatherer-fishers. *J. Archaeol. Sci.* **92**, 48–62. Available at: http://linkinghub.elsevier.com/retrieve/pii/S0305440318300426.

Mawson R. and Williams M. A. J. (1984) A wetter climate in eastern Sudan 2,000 years ago? *Nature* **309**, 49–51. Available at: http://www.nature.com/doifinder/10.1038/309049a0.

McDermott F., Stringer C., Grün R., Williams C. T., Din V. K. and Hawkesworth C. J. (1996) New Late-Pleistocene uranium–thorium and ESR dates for the Singa hominid (Sudan). *J. Hum. Evol.* **31**, 507–516. Available at: http://linkinghub.elsevier.com/retrieve/pii/S0047248496900767.

McFadden L. D. and Tinsley J. C. (1985) Rate and depth of pedogenic-carbonate accumulation in soils: Formulation and testing of a compartment model. In pp. 23–42. Available at: https://pubs.geoscienceworld.org/books/book/339/chapter/3796184/.

Nettleton W. ., Olson C. . and Wysocki D. . (2000) Paleosol classification: Problems and solutions. *CATENA* **41**, 61–92. Available at: http://linkinghub.elsevier.com/retrieve/pii/S0341816200001090.

Newman B. D., Campbell A. R., Norman D. I. and Ringelberg D. B. (1997) A model for microbially induced precipitation of vadose-zone calcites in fractures at Los Alamos, New Mexico, USA. *Geochim. Cosmochim. Acta* **61**, 1783–1792. Available at: http://www.sciencedirect.com/science/article/pii/S0016703797000252.

Nicoll K. (2001) Radiocarbon chronologies for prehistoric human occupation and hydroclimatic change in Egypt and Northern Sudan. *Geoarchaeology* **16**, 47–64. Available at: http://doi.wiley.com/10.1002/1520-6548%28200101%2916%3A1%3C47%3A%3AAID-GEA5%3E3.0.CO%3B2-P.

Nicoll K. (2004) Recent environmental change and prehistoric human activity in Egypt and Northern Sudan. *Quat. Sci. Rev.* **23**, 561–580.

Reimer P. J., Bard E., Bayliss A., Beck J. W., Blackwell P. G., Bronk C., Caitlin R., Hai E. B. and Edwards R. L. (2013) Intcal13 and marine13 radiocarbon age calibration curves 0 – 50,000 years cal CP. *Radiocarbon* **55**, 1869–1887.

Retallack G. J. (2000) Depth to pedogenic carbonate horizon as a paleoprecipitation indicator?: Comment and Reply. *Geology* **28**, 572. Available at: https://pubs.geoscienceworld.org/geology/article/28/6/572/185736.

Retallack G. J. (2005) Pedogenic carbonate proxies for amount and seasonality of precipitation in paleosols. *Geology* **33**, 333. Available at: https://pubs.geoscienceworld.org/geology/article/33/4/333-336/29600.

Retallack G. J., James W. C., Mack G. H. and Monger H. C. (1993) Classification of paleosols: Discussion and reply. *Geol. Soc. Am. Bull.* **105**, 1635–1637. Available at: https://pubs.geoscienceworld.org/gsabulletin/article/105/12/1635-1637/182783.

Richter D. K., Immenhauser A. and Neuser R. D. (2008) Electron backscatter diffraction documents randomly orientated c-axes in moonmilk calcite fibres: Evidence for biologically induced precipitation. *Sedimentology* **55**, 487–497.

Salvatori S. (2012) Disclosing Archaeological Complexity of the Khartoum Mesolithic: New Data at the Site and Regional Level. *African Archaeol. Rev.* **29**, 399–472.

Salvatori S. and Usai D. (2009) El Salha Project 2005: New Khartoum Mesolithic sites from central Sudan. *Kush* **19**, 87–96.

Salvatori S., Usai D., Abdelrahman M. F., Di Matteo A., Iacumin P., Linseele V. and Magzoub M. K. (2014) Archaeological evidence at Al Khiday. New insight on the prehistory and History of Central Sudan. In *The Fourth Cataract and Beyond. Proceedings of the 12th International Conference of Nubian Studies* (eds. J. R. Anderson and D. A. Welsby). Peeters Publishers, Leuven. pp. 243–258.

Salvatori S., Usai D. and Zerboni A. (2011) Mesolithic Site Formation and Palaeoenvironment Along the White Nile (Central Sudan). *African Archaeol. Rev.* **28**, 177–211.

Stoops G. (2003) *Guidelines for analysis and description of soil and regolith thin sections*., Soil Science Society of America, Madison, WI.

Stoops G., Marcellino V. and Mees F. (2010) *Interpretation of micromorphological features of soil and regoliths*., Elsevier, Amsterdam.

Szabo B. J., Haynes C. V. and Maxwell T. a. (1995) Ages of Quaternary pluvial episodes determined by uranium-series and radiocarbon dating of lacustrine deposits of Eastern Sahara. *Palaeogeogr. Palaeoclimatol. Palaeoecol.* **113**, 227–242.

Terrasi F., De Cesare N., D'Onofrio A., Lubritto C., Marzaioli F., Passariello I., Rogalla D., Sabbarese C., Borriello G., Casa G. and Palmieri A. (2008) High precision 14C AMS at CIRCE. *Nucl. Instruments Methods Phys. Res. Sect. B Beam Interact. with Mater. Atoms* **266**, 2221–2224.

Usai D. (2003) The Is.I.A.O. El Salha project. *Kush* **18**, 173–182.

Usai D., Maritan L., Dal Sasso G., Artioli G., Salvatori S., Jakob T. and Salviato T. (2017) Late Pleistocene/Early Holocene Evidence of Prostatic Stones at Al Khiday Cemetery, Central Sudan. *PLoS One* **12**, e0169524. Available at: http://dx.plos.org/10.1371/journal.pone.0169524.

Usai D. and Salvatori S. (2002) The Is.I.A.O. El Salha archaeological project. *Sudan & Nubia* **6**, 67–72.

Usai D. and Salvatori S. (2005) The IsIAO archaeological project in the El Salha area (Omdurman South, Sudan): results and perspectives. *Africa (Lond).* **60**, 474–493.

Usai D., Salvatori S., Iacumin P., Di Matteo A., Jakob T. and Zerboni A. (2010) Excavating a unique pre-Mesolithic cemetery in central Sudan. *Antiquity* **84**, 16–18. Available at: http://www.antiquity.ac.uk/projgall/usai323/.

Usai D., Salvatori S., Jakob T. and David R. (2014) The Al Khiday Cemetery in Central Sudan and its "Classic/Late Meroitic" Period Graves. *J. African Archaeol.* **12**, 183–204. Available at: http://booksandjournals.brillonline.com/content/journals/10.3213/2191-5784-10254.

Verrecchia E. P. and Verrecchia K. E. (1994) Needle-fiber Calcite: A Critical Review and a Proposed Classification. *J. Sediment. Res.* **64**, 650–664. Available at: https://pubs.geoscienceworld.org/jsedres/article/64/3a/650-664/98618.

Vogel J. C. and Geyh M. A. (2008) Radiometric dating of hillslope calcrete in the Negev Desert, Israel. *S. Afr. J. Sci.* **104**, 493–495.

Walkley A. and Black I. A. (1934) An examination of Degtjareff method for determining soil organic matter and a proposed modification of the chromic acid titration method. *Soil Sci.* **37**, 29–38.

Wang Y., McDonald E., Amundson R., McFadden L. and Chadwick O. (1996) An isotopic study of soils in chronological sequences of alluvial deposits, Providence Mountains, California. *Bull. Geol. Soc. Am.* **108**, 379–391.

Weninger B. (1986) High-precision calibration of archaeological radiocarbon dates. *Acta Interdiscip. Archaeol.* **4**, 11–53.

Weninger B. and Jöris O. (2008) A 14C age calibration curve for the last 60 ka: the Greenland-Hulu U/Th timescale and its impact on understanding the Middle to Upper Paleolithic transition in Western Eurasia. *J. Hum. Evol.* **55**, 772–781.

Whiteman A. J. (1971) *The Geology of the Sudan Republic*., Oxford University Press, Oxford.

Williams M. A. J. (1968) A DUNE CATENA ON THE CLAY PLAINS OF THE WEST CENTRAL GEZIRA, REPUBLIC OF THE SUDAN. *J. Soil Sci.* **19**, 367–378. Available at: http://doi.wiley.com/10.1111/j.1365-2389.1968.tb01547.x.

Williams M. A. J. (2009) Late Pleistocene and Holocene environments in the Nile basin. *Glob. Planet. Change* **69**, 1–15. Available at: http://dx.doi.org/10.1016/j.gloplacha.2009.07.005.

Williams M. A. J. and Adamson D. (1980) Late Quaternary depositional history of the Blue and White Nile rivers in central Sudan. In *The Sahara and the Nile: Quaternary environments and prehistoric occupation in northern Africa* (eds. M. A. J. Williams and H. Faure). A. A. Balkema, Rotterdam. pp. 281–304.

Williams M. A. J. and Jacobsen G. E. (2011) A wetter climate in the desert of northern Sudan 9900-7600 years ago. *Sahara* **22**, 7–14.

Williams M. A. J., Usai D., Salvatori S., Williams F. M., Zerboni A., Maritan L. and Linseele V. (2015) Late Quaternary environments and prehistoric occupation in the lower White Nile valley, central Sudan. *Quat. Sci. Rev.* **130**, 72–88. Available at: http://dx.doi.org/10.1016/j.quascirev.2015.03.007.

Wintle A. G. and Murray A. S. (2006) A review of quartz optically stimulated luminescence characteristics and their relevance in single-aliquot regeneration dating protocols. *Radiat. Meas.* **41**, 369–391.

WRB (2006) *World reference base for soil resources 2006.* World Soil. ed. FAO, Rome.

Wright V. P. (2007) Calcrete. In *Geochemical Sediments and Landscapes* (eds. D. J. Nash and S. J. McLaren). Wiley-Blackwell. pp. 10–45.

Wright V. P., Platt N. H. and Wimbledon W. A. (1988) Biogenic laminar calcretes: evidence of calcified root-mat horizons in paleosols. *Sedimentology* **35**, 603–620. Available at: http://doi.wiley.com/10.1111/j.1365-3091.1988.tb01239.x.

Wright V. P. and Tucker M. E. (1991) Calcretes: an introduction. In *Calcretes* (eds. V. P. Wright and M. E. Tucker). Blackwell, Oxford. pp. 1–22.

Yaalon D. H. (1983) Climate, time and soil development. In *Pedogenesis and Soil Taxonomy. 1. Concepts and Interactions* (eds. L. P. Wilding, N. E. Smeck, and G. P. Hall). Elsevier, Amsterdam. pp. 233–251.

Zazzo A. (2014) Bone and enamel carbonate diagenesis: A radiocarbon prospective. *Palaeogeogr. Palaeoclimatol. Palaeoecol.* **416**, 168–178. Available at: http://dx.doi.org/10.1016/j.palaeo.2014.05.006.

Zerboni A. (2013) Early Holocene palaeoclimate in North Africa: an overview. In *Neolithisation of Northeastern Africa, Studies in Early Near Eastern Production, Subsistence, and Environment* (ed. N. Shirai). Ex Oriente, Berlin. pp. 65–82.

Zerboni A. (2011) Micromorphology reveals in situ Mesolithic living floors and archaeological features in multiphase sites in central Sudan. *Geoarchaeology* **26**, 365–391.

Zerboni A., Trombino L. and Cremaschi M. (2011) Micromorphological approach to polycyclic pedogenesis on the Messak Settafet plateau (central Sahara): Formative processes and palaeoenvironmental significance. *Geomorphology* **125**, 319–335. Available at: http://dx.doi.org/10.1016/j.geomorph.2010.10.015.

Zerboni A., Usai D. and Meyer M. (2016) The Middle Palaeolithic / Middle Stone Age site of Al Jamrab in central Sudan. *Antiq. Proj. Gall.*, 4–7. Available at: http://antiquity.ac.uk/projgall/zerboni351.

Zhou J. and Chafetz H. S. (2009) The genesis of late Quaternary caliche nodules in Mission Bay, Texas: Stable isotopic compositions and palaeoenvironmental interpretation. *Sedimentology* **56**, 1392–1410.

List of figures

~~**Figure 1. a.** Carbonate concretions partially embed pre-Mesolithic bones (grave 152); **b.** Mesolithic pit cut into the calcrete horizon; **c.** Meroitic grave cut into the calcrete horizon; **d**. Early (?) Pleistocene paleosol, highly cemented by calcium carbonate outcropping in the area surrounding 16D4 site.~~

Figure ~~2~~1. a. Location of archaeological sites at Al Khiday, Khartoum, Sudan (from Google Earth™, version 7.1.8.3036; 15°27'10.37"N, 32°24'25.73"E, alt 112.8 Km, Image Landsat/Copernicus, [12/05/2017]; **b.** Oblique aerial picture of the 16D4 site during the 2015 archaeological campaign (photo by Yves Guichard, CSSeS); a white arrow shows the location of the soil profile analysed in this study (pit 151A).

Figure ~~1~~2. a. Carbonate concretions partially embed pre-Mesolithic bones (grave 152); **b.** Mesolithic pit cut into the ~~calcrete~~calcium carbonate-rich horizon; **c.** Meroitic grave cut into the calcium carbonate-rich~~calcrete~~ horizon; **d**. Early (?) Pleistocene paleosol, highly cemented by calcium carbonate outcropping in the area surrounding 16D4 site.

Figure 3. Field photograph of exposed calcrete section sampled for this study (pit 151A). ~~A model representing upper and lower units identified within the section~~A schematic sketch of the studied profile and the location of ~~calcrete blocks sampled~~sampling points and results of physico-chemical analyses (carbonate and humified carbon content, pH, LOI, total carbon and total nitrogen content) are shown. 1: Quartz sand slightly cemented by calcium carbonate, coalescent irregular calcitic nodules occur (~~A1~~Bk); 2: Sandy lens weakly cemented by calcium carbonate (~~A2~~BC); 3: Quartz sand cemented by calcium carbonate and carbonate concretions (~~A3a – A3d~~2Bk).

Figure 4. Photomicrographs ~~of the~~from the ~~upper~~ Bk, BC (a–d) and ~~lower~~ 2Bk (e–h) ~~units sections~~horizons. **a.** Micritic micromass cementing quartz sand grains, corresponding to a calcitic nodule (A1 – XPL); **b.** Well-rounded allochthonous calcitic pedorelict stained by Mn and Fe oxides (A1 - XPL, top-right); **c.** Quartz grains in a porphyric c/f related distribution, poorly cemented by authigenic calcite (A1 - XPL); **d.** calcite recrystallized after wood ash, as confirmed by the

occurrence of microcharcoals (arrows); this calcite derives from the infilling material of the Mesolithic pit (A2 - PPL). **e.** Micritic micromass slightly cementing sand- and silt-sized quartz grains (A3a – XPL); **f.**, **g.** High concentration of calcium carbonate, corresponding to calcitic nodules predominantly constituted by microsparitic calcite. Cemented nodules formed by well-cemented calcite crystals with sub-rounded to sub-angular shape, are shown (A3a – XPL); **h.** Allochthonous calcitic pedorelict sub-rounded in shape and stained by Fe oxides (A3c – PPL).

Figure 5. CL photomicrographs of: **a.** Micritic micromass (orange) cementing quartz sand grains (dark blue) within calcitic nodule from the ~~upper unit~~BK horizon (A1); **b.** Poorly cemented area characterized by low luminescence due to the scarcity of calcite (A1); **c., d.** Well-rounded calcitic pedorelict constituted a by micritic matrix stained by Mn and Fe oxides-hydroxides and containing veins of sparitic and microsparitic calcite (A1, PPL and CL); **e.** Highly carbonated areas corresponding to a calcitic nodule from the ~~lower unit~~2Bk horizon, predominantly constituted by microsparitic calcite (A3a); cemented nodules formed by well-cemented calcite crystals, sub-rounded to sub-angular in shape, are shown; **f.** Cemented nodules characterized by lower size and less defined margins (A3d). **g., h.** Luminescence variations of calcite crystals forming cemented nodules from A3d and A3a ~~blocks~~sampling points.

Figure 6. SEM-BSE images of different portions of calcitic nodules from the ~~upper unit~~Bk (a-c) and 2Bk (d-f) horizons ~~(A1)~~ showing: **a.** Densely packed calcite crystals (light grey) and part of a quartz sand grain (dark grey); **b.** Calcite crystals associated to a clayey matrix; **c.** Sparse distribution of calcite crystals. SEM-BSE images of calcitic nodules from the lower unit showing: **d.** The outermost part of allochthonous calcitic pedorelict characterized by clay minerals coating its outer surface (A3c); **e.**, **f.** part of a cemented nodule, formed by well-cemented calcite crystals, embedded in a matrix characterized by less packed calcite crystals (A3a).

Figure 7. a., b. Photomicrographs of a calcitic nodule predominantly constituted by microsparitic calcite in which cemented nodules are well-distinguishable from the surrounding calcitic-rich

matrix (2Bk horizon, A3a sampling point – PPL, XPL); **c.** Segmented false-colour image obtained from Fig. 7a, 7b highlights the spatial distribution of these two pedofeatures.

Figure ~~7~~8. Cumulative calibrated dating probability of radiocarbon ages obtained from: **a.** ~~Calcrete~~ Calcium carbonate samples (8) from the section analysed in this study; **b.** Calcitic nodules from soils sampled in Central Sudan (Adamson et al., 1982) **c.** Freshwater shells (33) indicating higher flooding level of the White Nile (Williams, 2009; Williams et al., 2015). **~~c~~d.** Bioapatite fraction of archaeological bones (19) from graves found at 16D4 site (Gaballo, 2009; Zazzo, 2014; Dal Sasso, 2015). More humid periods characterized by higher flow of the White Nile (~~dark grey~~light-blue bars) and the chronology established for the anthropic use of the site at Al Khiday (Salvatori et al., 2011) (~~light grey~~orange bars – Mesolithic, Neolithic and Meroitic periods) are reported.

Figure ~~8~~9. a. AMS-^{14}C ages obtained for cemented nodules and calcitic-rich matrix at each sampling point. The sketch of the studied profile, shown in Fig. 3, is also reported; **b., c.** C and O ~~S~~stable isotope data ~~of~~ for cemented nodules and and calcitic-rich matrix samples.

Table 1

Soil horizon	Depth (m)	Sampling point	Sample depth (m)	Field properties	$CaCO_3$ equiv. (%)	pH	Humified C (g/Kg)	LOI (%)	TC (%)	TN (%)
-	0-0.2	-	-	Disturbed layer	-	-	-	-	-	-
Bk	0.2–0.35	A1	0.27	Sandy to sandy–loamy matrix (mostly quartz grains), almost deprived of finer components; locally it showed small lenses of pebbles; common to abundant, large calcium carbonate nodules and concretions; dominant color is 2.5Y 5/4 (light olive brown), scarce mottles 10YR 6/8 (brownish yellow); scares centimetre scale burrows, filled by brownish yellow sand are common; abrupt transition to the following horizon.	14.77	8.9	0.33	1.95	1.684	0.008
BC	0.35–0.46	A2	0.40	Sandy to sandy–loamy matrix (mostly quartz grains), almost deprived of finer components; scarce, small calcium carbonate nodules and coatings; dominant color is 10YR 6/6 (brownish yellow), scarce mottles 10YR 6/3 (pale brown); few burrows, filled by brownish yellow sand; abrupt limit to the following horizon.	3.76	8.7	1.12	1.64	0.727	0.014
2Bk	>0.46	A3a	0.51	Sandy to sandy–loamy matrix (mostly quartz grains); few, small lenses of pebbles; abundant calcium carbonate concretions; dominant color is 2.5Y 7/4 (pale yellow), scarce mottles in the uppermost part 2.5Y 5/4 (light olive brown); scares centimetre scale burrows in the uppermost part, filled by brownish yellow sand are common; limit of the horizon not reached.	8.42	8.7	1.04	2.63	1.29	0.019
		A3b	0.61		28.58	8.9	0.35	3.81	3.499	0.015
		A3c	0.73		26.34	8.8	0.61	4.95	3.067	0.016
		A3d	0.84		37.28	8.9	0.37	5.56	4.682	0.015

Table 1. Field properties (color according to Munsell®, 1994) and results of physical and chemical analyses on collected samples.

Table 2

Soil horizon	Depth (m)	Sample name	Sample	^{14}C age	2σ cal. BP	δ^{18}O‰ (V-PDB)	δ^{13}C‰ (V-PDB)
Bk	0.27-	A1-p	Pedorelict	25439 ± 153	29540 ± 440		
			Pedorelict				
Bk	0.27	A1-mt	Calcitic-rich matrix	5290 ±102	6080 ± 240	-6.25 (0.02)	0.10 (0.01)
			Calcitic-rich matrix			-8.27 (0.04)	0.23 (0.03)
2Bk	0.51	A3a-mt	Calcitic-rich matrix	5536 ±29	6340 ± 80	-6.70 (0.04)	0.59 (0.02)
			Calcitic-rich matrix			-4.12 (0.06)	0.42 (0.05)
2Bk	0.51	A3a-cn	Cemented nodules	8663 ±40	9620 ± 100	-4.66 (0.07)	-0.05 (0.06)
			Cemented nodules			-8.03(0.05)	0.58 (0.02)
2Bk	0.61	A3b-mt	Calcitic-rich matrix			-7.72 (0.07)	1.06 (0.05)
2Bk	0.61	A3b-cn	Cemented nodules			-4.98 (0.06)	0.07 (0.02)
2Bk	0.73	A3c-mt	Calcitic-rich matrix	7104 ±42	7920 ± 100	-7.71 (0.04)	0.75 (0.03)
			Calcitic-rich matrix			-7.60 (0.07)	0.79 (0.04)
2Bk	0.73	A3c-cn	Cemented nodules	8823 ±242	9900 ± 580	-5.43 (0.04)	-0.18(0.05)
			Cemented nodules			-4.15 (0.04)	0.03 (0.05)
			Cemented nodules			-2.30 (0.08)	-0.66 (0.05)
2Bk	0.84	A3d-mt	Calcitic-rich matrix	6891 ±31	7730 ± 80	-6.26 (0.03)	0.44 (0.01)
			Calcitic-rich matrix			-6.60 (0.04)	0.21 (0.02)
2Bk	0.84	A3d-cn	Cemented nodules	10005 ±41	11480 ± 240	-3.32 (0.04)	-1.48 (0.03)
			Cemented nodules			-1.85 (0.05)	-0.75 (0.03)

Table 2. ^{14}C ages, calibrated ages, δ^{18}O and δ^{13}C values and their standard deviation obtained on selected calcitic pedofeatures (p: Pedorelict; mt: Calcitic-rich matrix; cn: Cemented nodules).

Figure 1

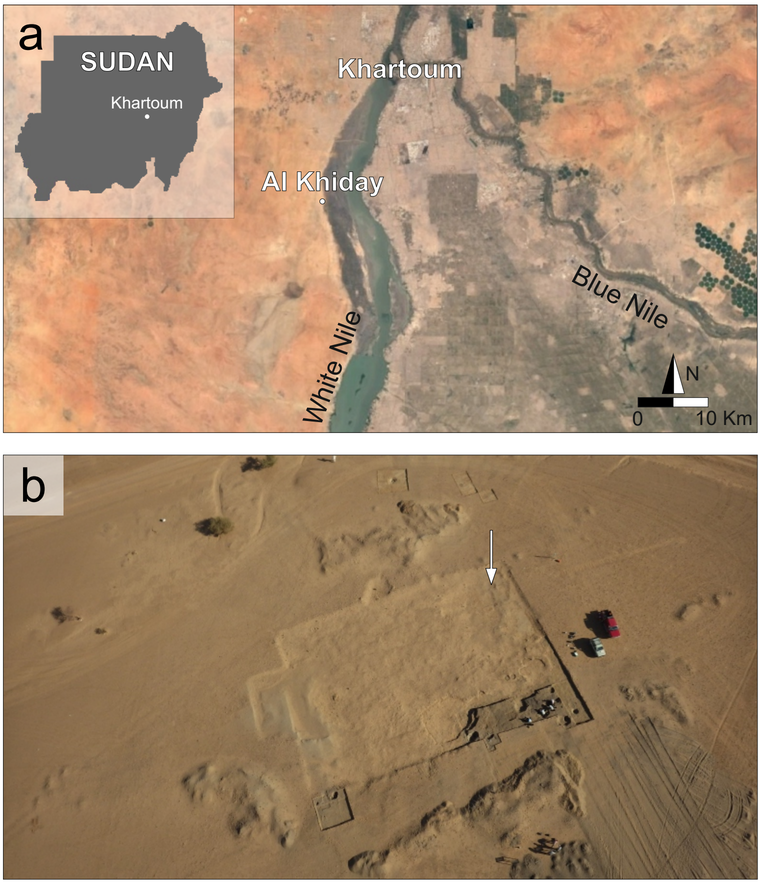
a
SUDAN
Khartoum
Khartoum
Al Khiday
White Nile
Blue Nile
N
0
10 Km
b

Figure 2

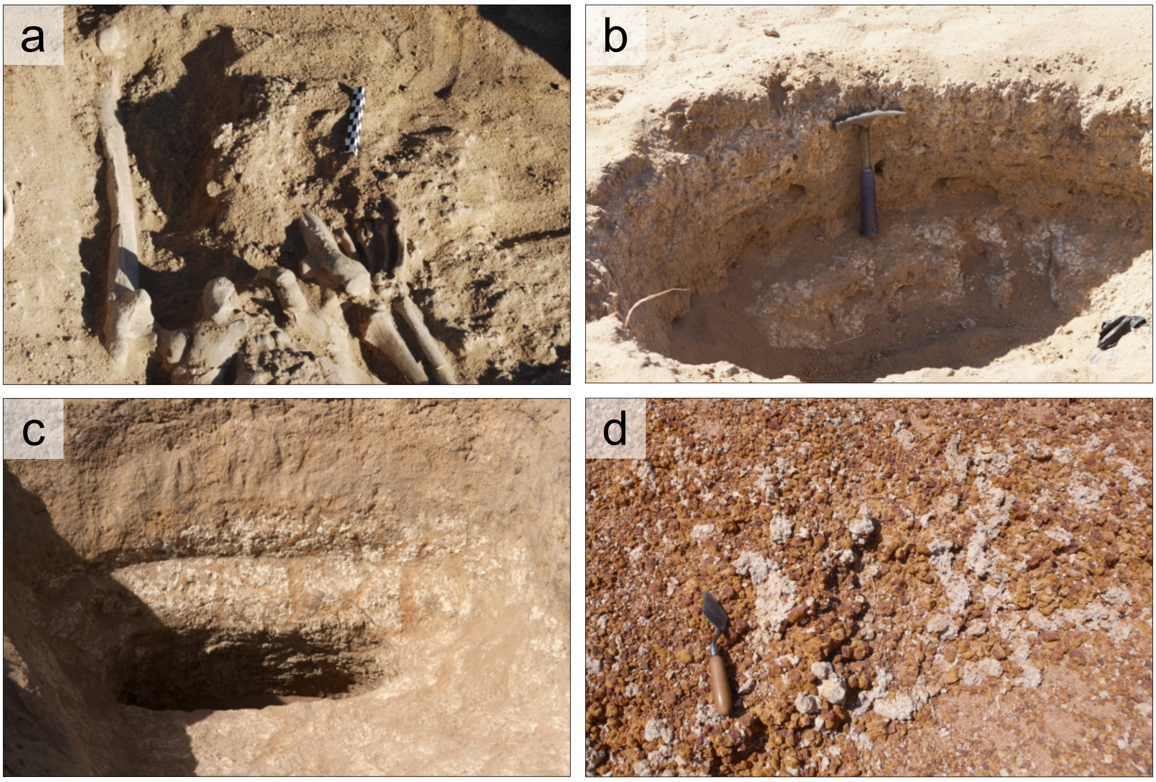

Figure 3

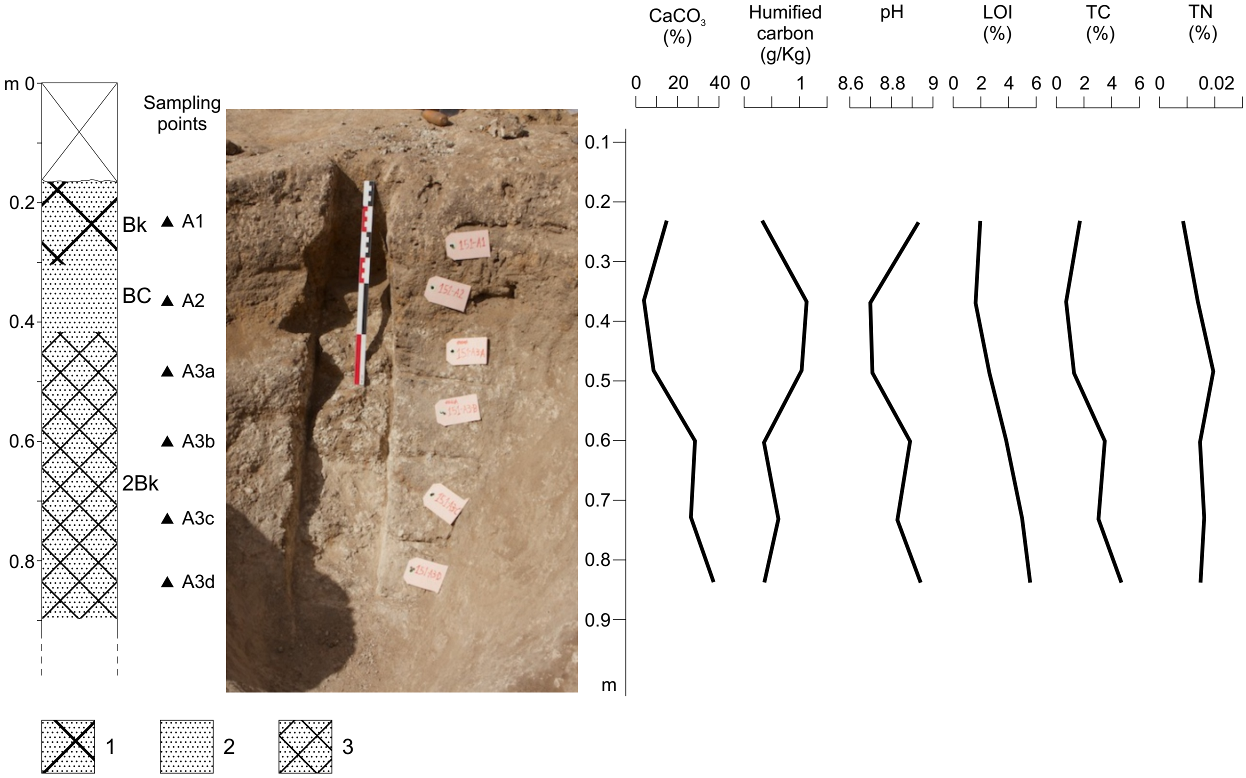

m 0
0.2
0.4
0.6
0.8
Bk
BC
2Bk
Sampling points
▲ A1
▲ A2
▲ A3a
▲ A3b
▲ A3c
▲ A3d
0.1
0.2
0.3
0.4
0.5
0.6
0.7
0.8
0.9
m
CaCO3 (%)
0 20 40
Humified carbon (g/Kg)
0 1
pH
8.6 8.8 9
LOI (%)
0 2 4 6
TC (%)
0 2 4 6
TN (%)
0 0.02
1
2
3

Figure 4

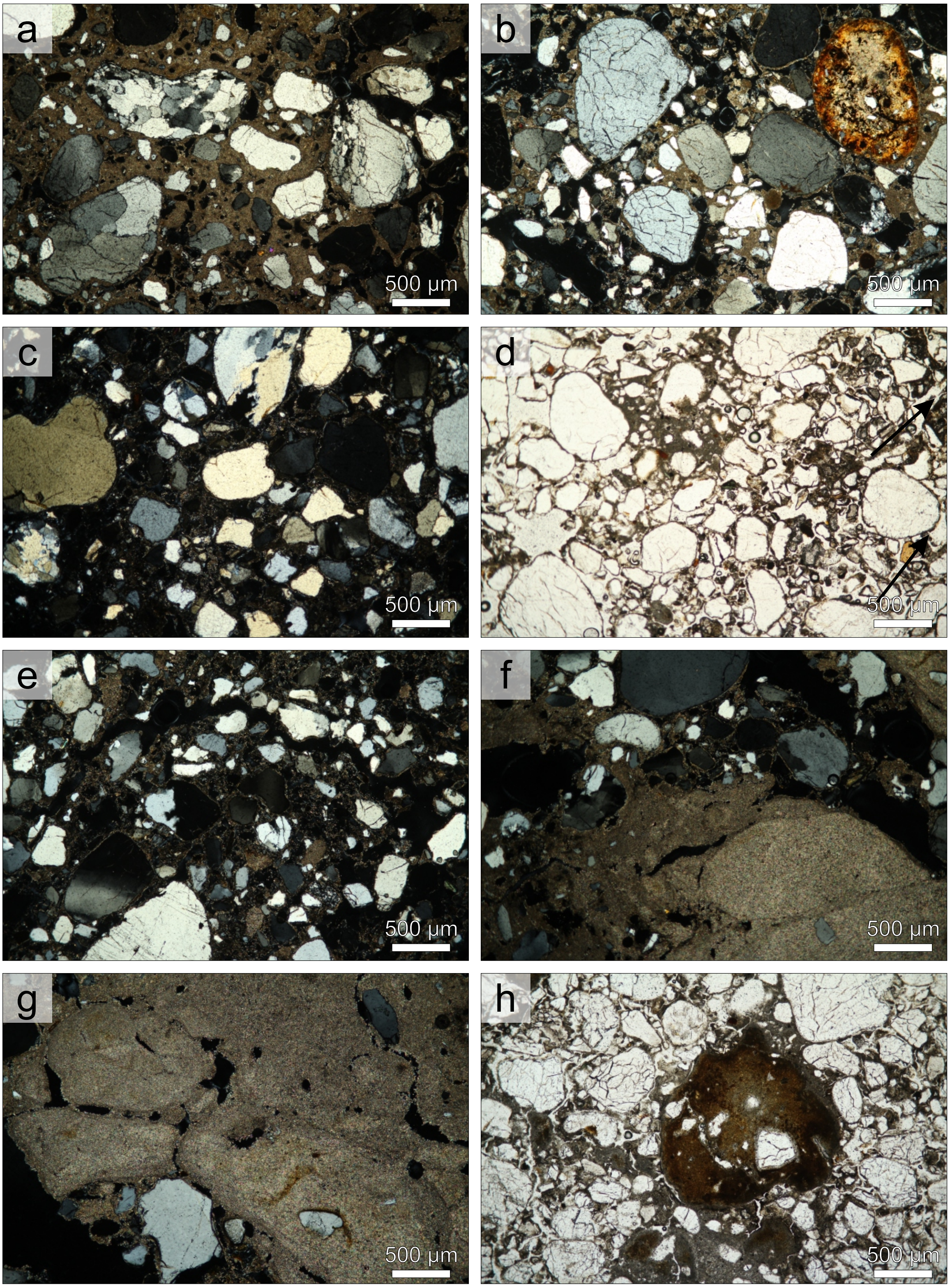

Figure 5

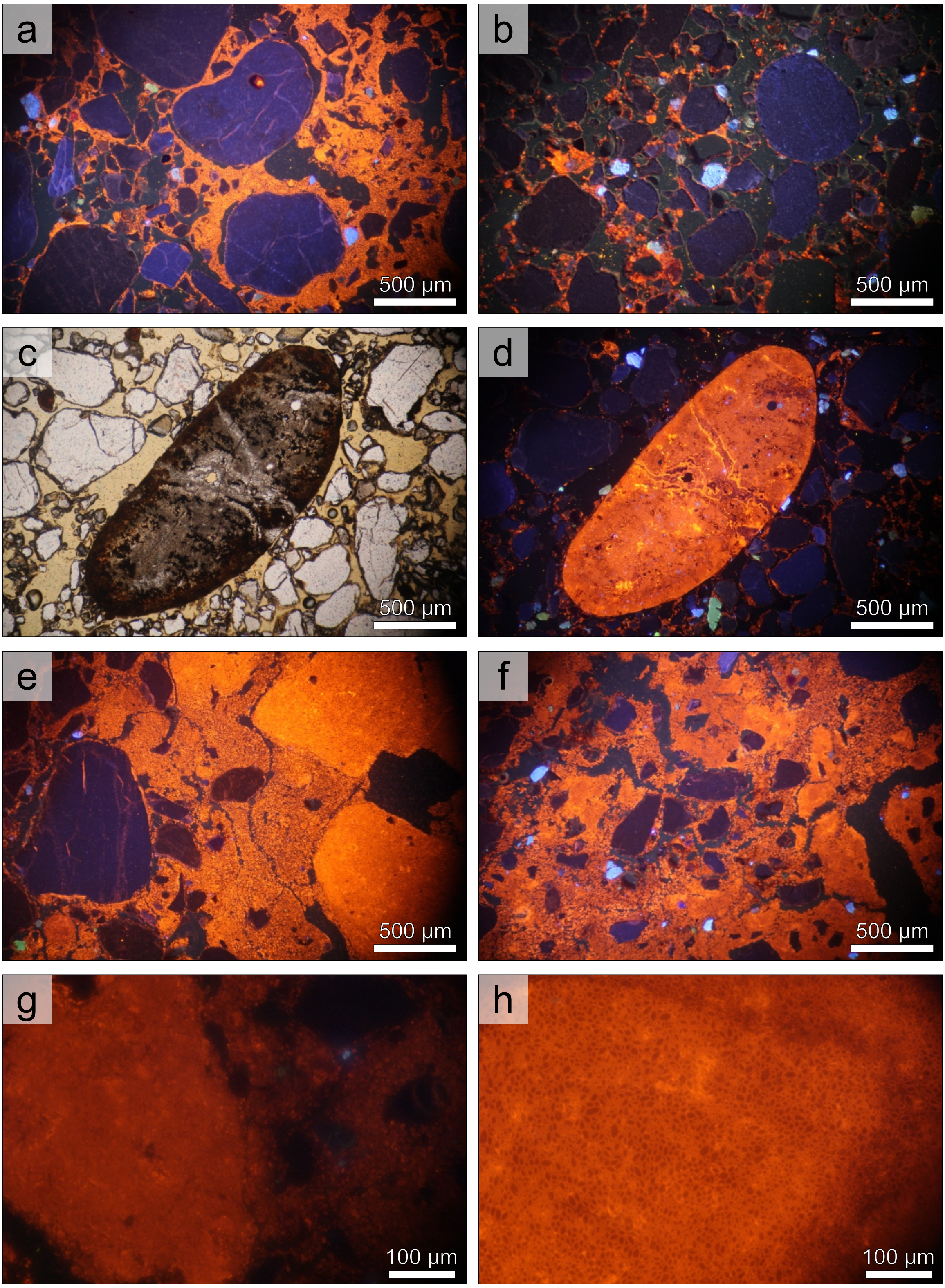

Figure 6

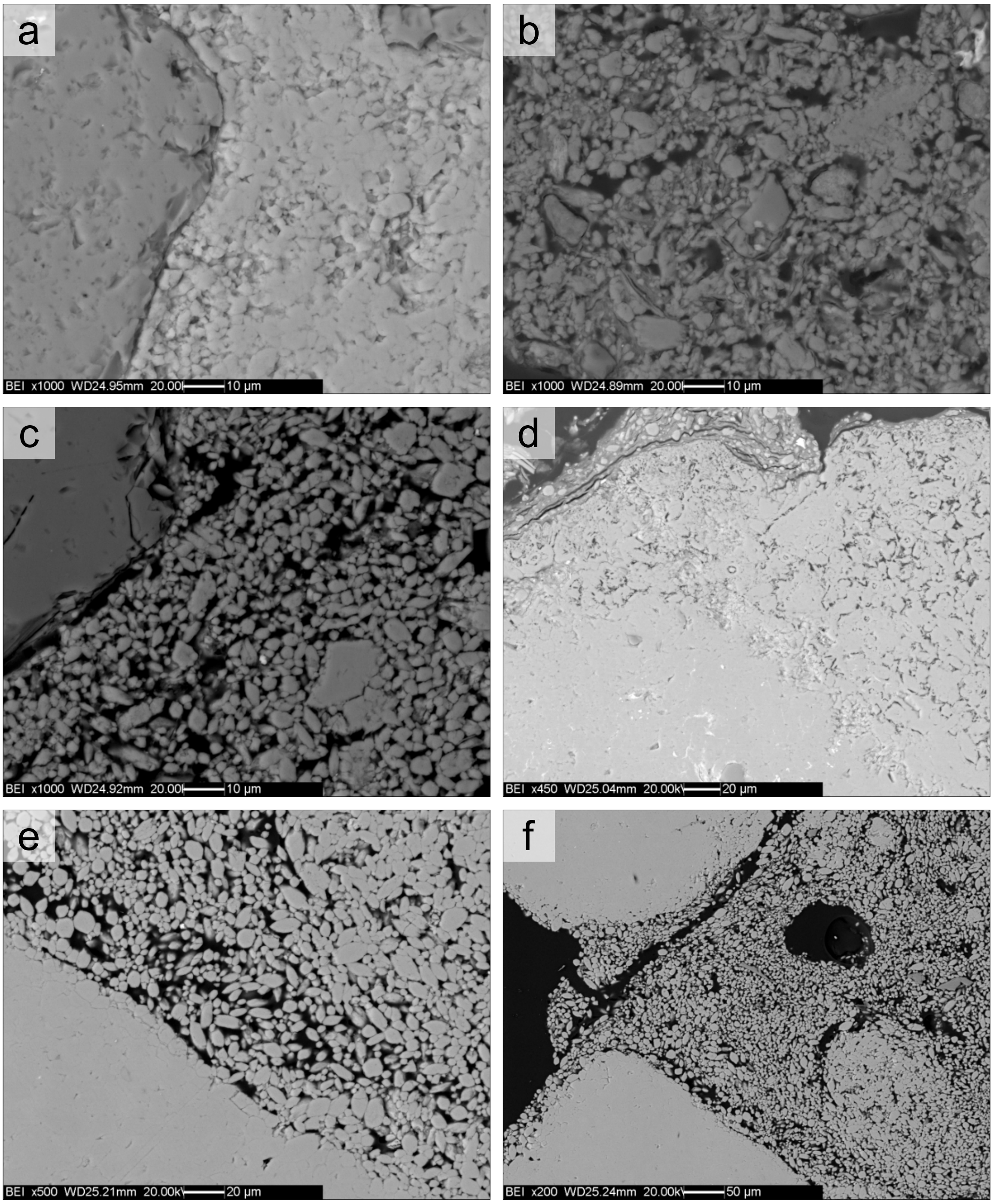
a
BEI x1000 WD24.95mm 20.00k 10 µm
b
BEI x1000 WD24.89mm 20.00k 10 µm
c
BEI x1000 WD24.92mm 20.00k 10 µm
d
BEI x450 WD25.04mm 20.00kV 20 µm
e
BEI x500 WD25.21mm 20.00kV 20 µm
f
BEI x200 WD25.24mm 20.00kV 50 µm

Figure 7

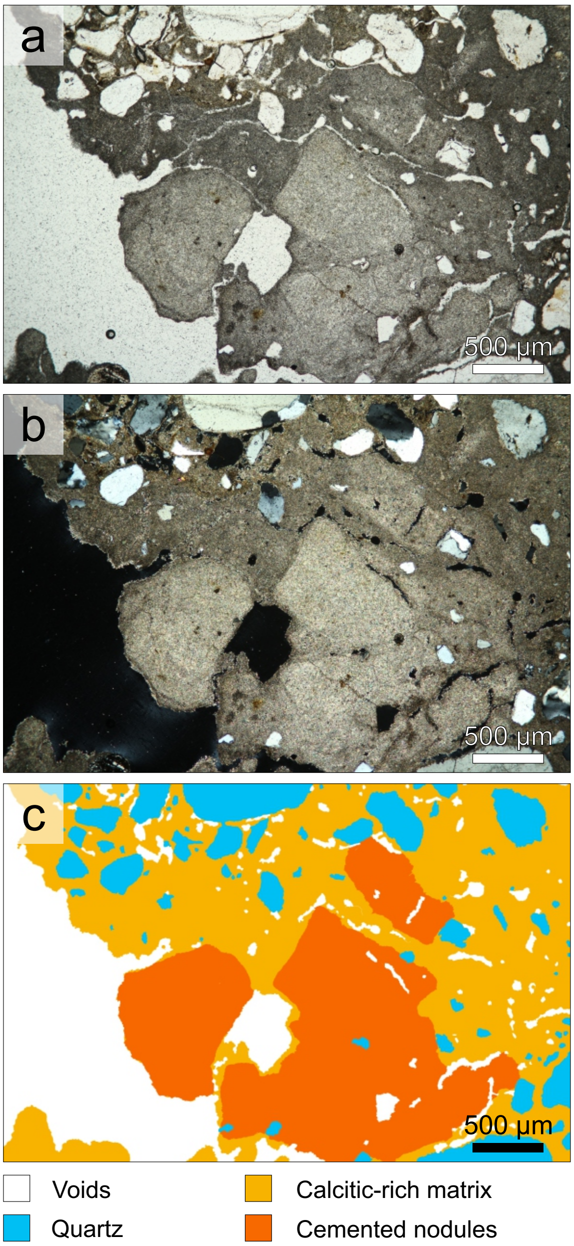

a
500 µm
b
500 µm
c
500 µm
Voids
Quartz
Calcitic-rich matrix
Cemented nodules

Figure 8

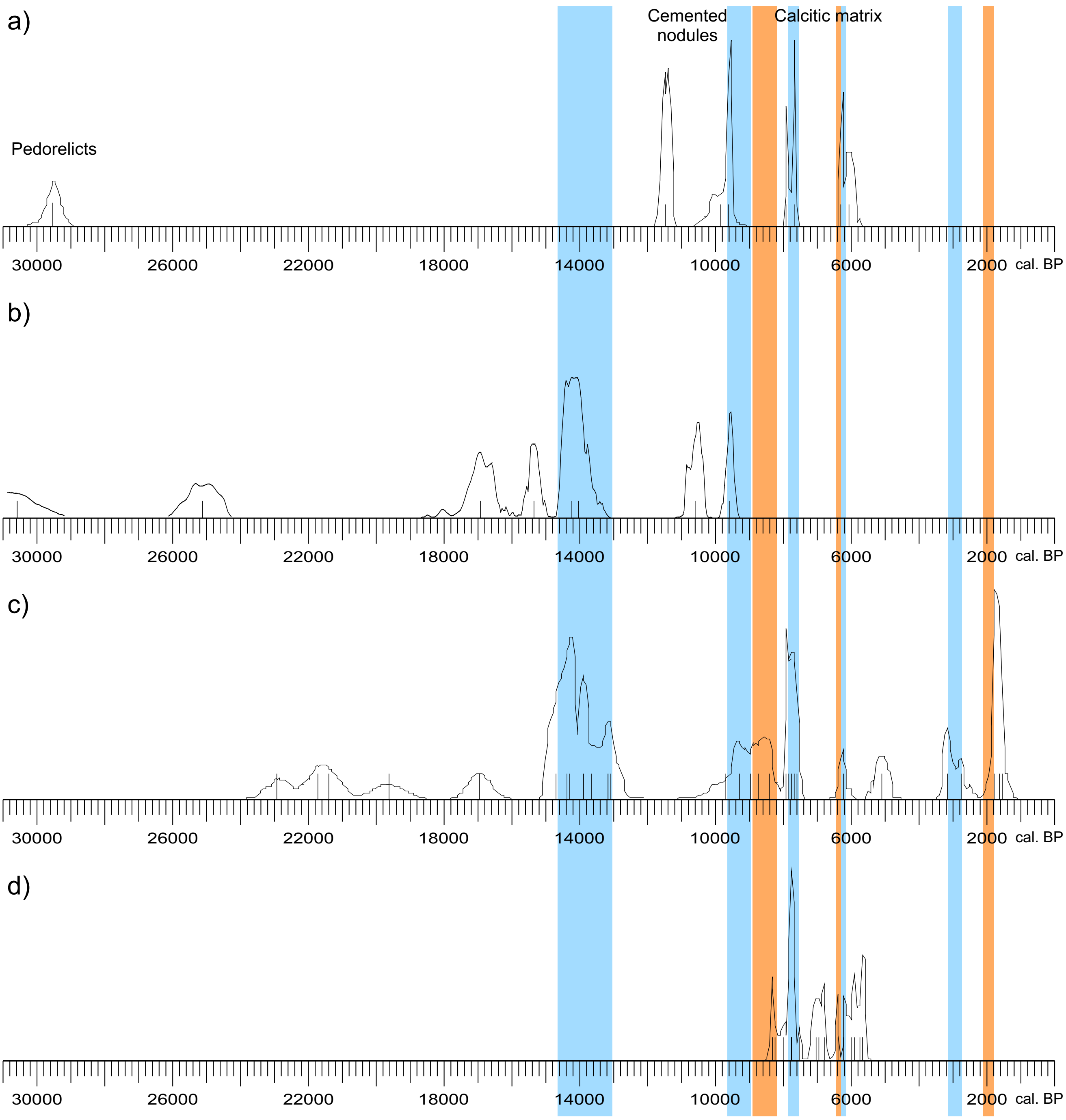
a)
Pedorelicts
Cemented
nodules
Calcitic matrix
30000
26000
22000
18000
14000
10000
6000
2000
cal. BP
b)
c)
d)

Figure 9

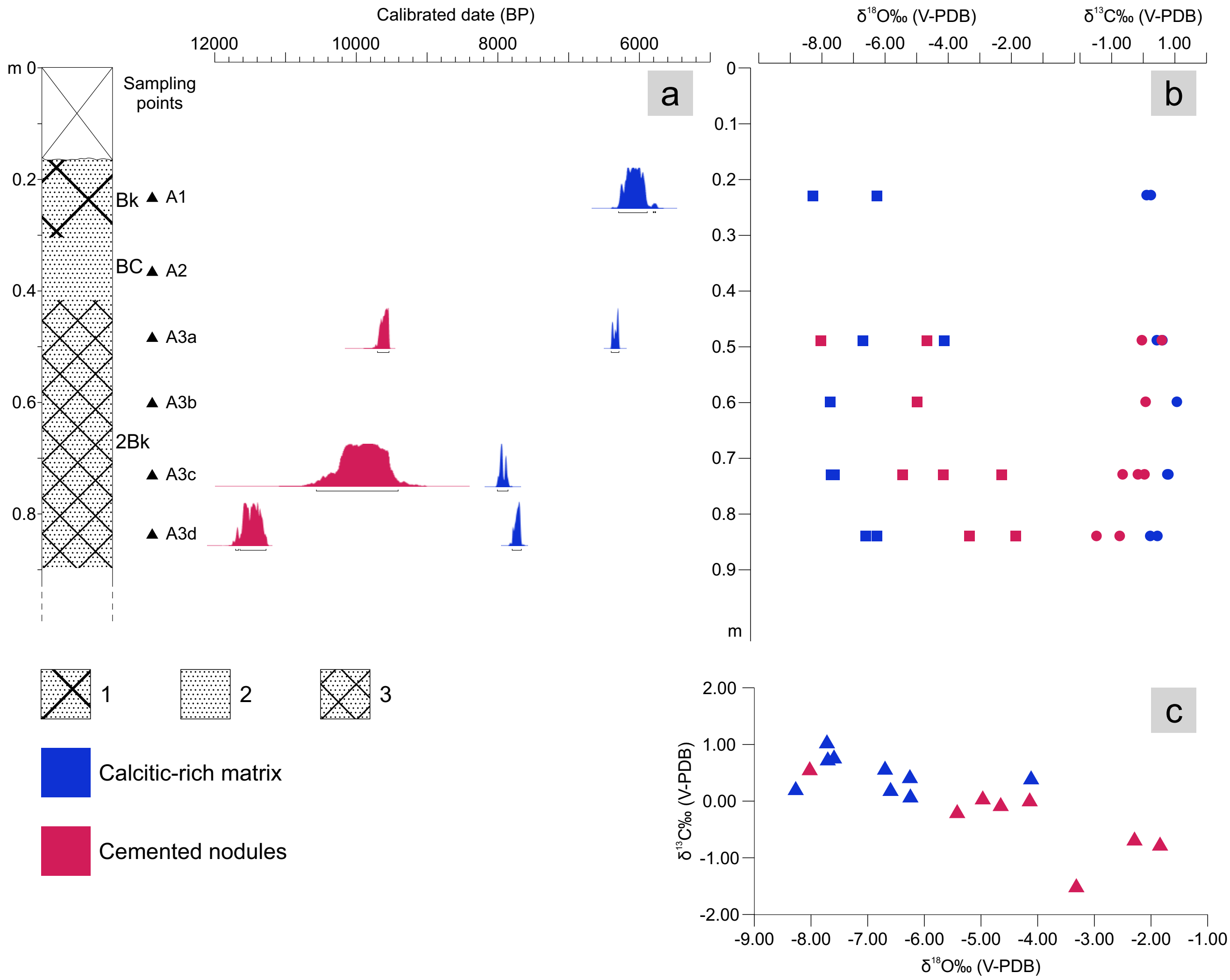

Calibrated date (BP)
12000
10000
8000
6000
a
δ18O‰ (V-PDB)
-8.00
-6.00
-4.00
-2.00
δ13C‰ (V-PDB)
-1.00
1.00
b
m 0
0.2
0.4
0.6
0.8
Sampling points
Bk
BC
2Bk
A1
A2
A3a
A3b
A3c
A3d
0
0.1
0.2
0.3
0.4
0.5
0.6
0.7
0.8
0.9
m
1
2
3
Calcitic-rich matrix
Cemented nodules
c
2.00
1.00
0.00
-1.00
-2.00
δ13C‰ (V-PDB)
-9.00
-8.00
-7.00
-6.00
-5.00
-4.00
-3.00
-2.00
-1.00
δ18O‰ (V-PDB)

Interactive Map file (.kml or .kmz)

Click here to download Interactive Map file (.kml or .kmz): 16D4.kmz